NASA CR-114570

DESIGN INTEGRATION AND NOISE STUDIES FOR JET STOL AIRCRAFT

Task VIIA

AUGMENTOR WING CRUISE BLOWING VALVELESS SYSTEM

Volume II—Design Exploration

April 1973

Prepared under Contract NAS2-6344 by
BOEING COMMERCIAL AIRPLANE COMPANY
P.O. Box 3707
Seattle, Washington 98124

for

Ames Research Center

NATIONAL AERONAUTICS AND SPACE ADMINISTRATION

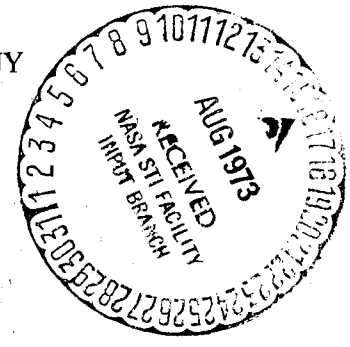

1. Report No.	2. Government Accession No.	3. Recipient's Catalog No.
NASA CR-114570		

4. Title and Subtitle	5. Report Date
DESIGN INTEGRATION AND NOISE STUDIES FOR JET STOL AIRCRAFT– TASK VIIA, AUGMENTOR WING CRUISE BLOWING VALVELESS SYSTEM, Volume II, Design Exploration	October 1972
	6. Performing Organization Code
7. Author(s)	8. Performing Organization Report No. D6-40829
	10. Work Unit No.
9. Performing Organization Name and Address BOEING COMMERCIAL AIRPLANE COMPANY P.O. Box 3707 Seattle, Washington 98124	11. Contract or Grant No. NAS2-6344
	13. Type of Report and Period Covered
12. Sponsoring Agency Name and Address NATIONAL AERONAUTICS AND SPACE ADMINISTRATION Ames Research Center	14. Sponsoring Agency Code

15. Supplementary Notes

16. Abstract

A design integration study program was conducted by The Boeing Company to determine size and performance parameters of an augmentor wing cruise blowing (valveless) system in a 150-passenger STOL airplane for the purpose of defining size and configuration of static rig, flow duct, and wind tunnel test hardware. The studies encompassed blowing systems powered by low-pressure (single stage) and high-pressure (three and four stage) engine fans. A range of wing aspect ratios, wing thicknesses, and duct flow velocity effects were investigated to establish airplane characteristics which minimize takeoff gross weight while achieving desirable sideline noise requirements for an advanced commercial STOL airplane.

17. Key Words (Suggested by Author(s))		18. Distribution Statement
Installed thrust	Aircraft noise	
Duct flow analysis	Blowing engine	
Augmentor wing	Thrust lapse	
Cruise blowing	Aspect ratio	
Valveless augmentor	Wing thickness	

19. Security Classif. (of this report)	20. Security Classif. (of this page)	21. No. of Pages	22. Price*
Unclassified	Unclassified	127	

*For sale by the National Technical Information Service, Springfield, Virginia 22151

CONTENTS

Page

1.0 SUMMARY 1

2.0 INTRODUCTION 9

3.0 SYMBOLS AND ABBREVIATIONS 10

4.0 SYSTEM DESIGN INTEGRATION 14
- 4.1 Duct Systems 14
  - 4.1.1 Expandable Duct Systems 14
  - 4.1.2 Rigid Duct Systems 16
- 4.2 Engine Cycle Studies 26
  - 4.2.1 Cycle Definition and Assumptions 26
  - 4.2.2 Engine Cycle Performance 28
  - 4.2.3 Performance Comparisons 28
- 4.3 Engine Installations 44
  - 4.3.1 High-Pressure Installations 44
  - 4.3.2 Low Pressure 46
  - 4.3.3 Thrust Vectored Nacelle 46
- 4.4 Duct Performance Evaluation 46
  - 4.4.1 Duct Performance Comparisons 46
  - 4.4.2 Computerized Performance Analysis 51
- 4.5 Augmentor System Design Integration 61
  - 4.5.1 Augmentor Performance 61
  - 4.5.2 Noise 75
- 4.6 Airplane Integration 79
  - 4.6.1 Airplane/System Parameters 79
    - 4.6.1.1 Engine Characteristics 81
    - 4.6.1.2 Augmentor System Characteristics 81
  - 4.6.2 Airplane Sizing 87
    - 4.6.2.1 Low-Pressure Systems 87
      - 4.6.2.1.1 Fan Pressure Ratio = 1.7 90
      - 4.6.2.1.2 Fan Pressure Ratio = 1.8 94
    - 4.6.2.2 High-Pressure Systems 98
      - 4.6.2.2.1 Fan Pressure Ratio = 3.2 98
      - 4.6.2.2.2 Fan Pressure Ratio = 3.75 101
  - 4.6.3 Effects of Varying System Parameters 101
    - 4.6.3.1 Wing Aspect Ratio Relationships 101
    - 4.6.3.2 System Pressure Ratio Effects 106
    - 4.6.3.3 Wing Thickness Effects 108
    - 4.6.3.4 Duct Flow Velocity Effects 108
  - 4.6.4 Airplane Integration Summary and Definition of Selected Configuration 116

CONTENTS–Concluded

Page

5.0 CONCLUSIONS 117

APPENDIX–Augmentor Wing Expandable Duct Concept Drawings 119

1.0 SUMMARY

Task VII of DNS Contract NAS2-6344 was implemented by The Boeing Company in March 1972 to define a cruise blowing, valveless augmentor wing system to be used in static performance and noise tests and small-scale model wind tunnel tests leading to a selected configuration and large-scale model evaluation in the Ames 40- by 80-ft wind tunnel.

Figure 1 illustrates the cruise blowing system concept in which flow diverter valves and separate cruise nozzles are eliminated. The fan air is directed to the wing ducts, with a portion used for leading edge and aileron boundary layer control. The major part of the air discharges from multielement lobed nozzles through acoustically lined flaps in the augmentor mode. In the cruise mode the flaps are retracted, and the air continues to blow over the flap upper surface.

This report covers the initial exploratory design studies resulting in blowing system configuration and sizing data for a projected commercial STOL transport airplane. These data have been used to establish a small-scale model for preliminary two-dimensional wind tunnel tests and to define the configuration used in the static performance and noise tests.

Ground rules for the study vehicle were as follows:

150-passenger airplane

2000-ft takeoff field length (FAR)

500-nmi STOL range

1500-nmi CTOL range

Mach 0.8 at 30 000-ft cruise altitude

90-PNdB maximum takeoff noise at 500-ft sideline objective

1978-80 initial production goal

To provide a consistent basis for the blowing system studies, engine cycle and size data were derived for fan pressure ratios of 1.7 (single-stage fan) to 3.7 (four-stage fan) assuming core engine characteristics of the P&WA STF-395D.

Various expandable duct schemes were examined in designs which projected substantial increases in blowing volume capability. However, these schemes tended toward increased complexity or were incompatible with cruise blowing operation due to out-of-contour panels and doors in the expanded position.

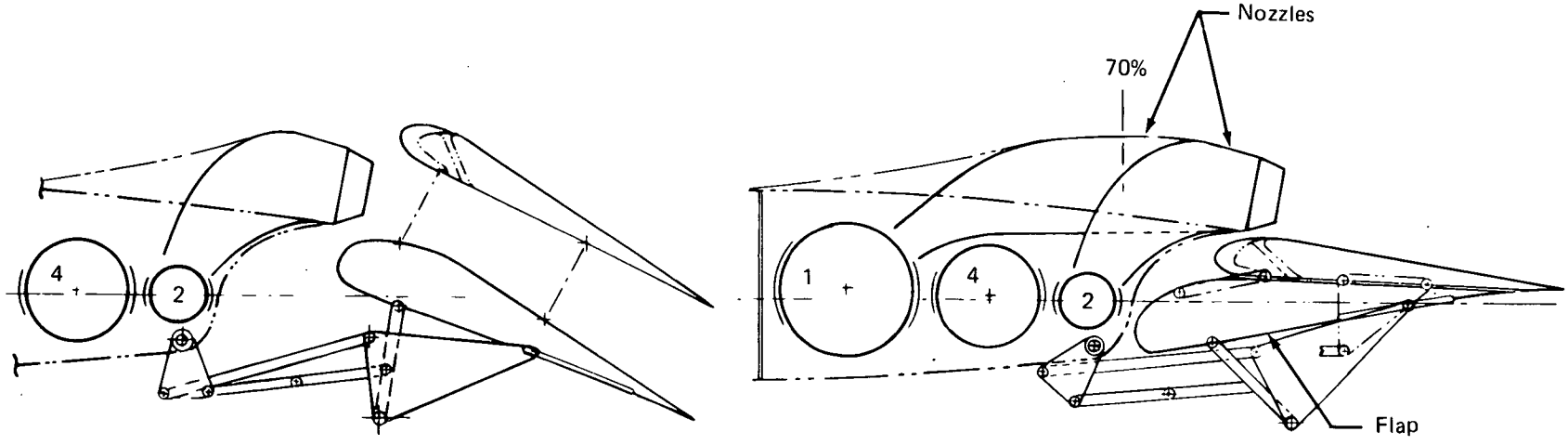

FIGURE 1.– AUGMENTOR WING CRUISE BLOWING FLAP CONCEPT

Fixed, rigid-wall duct systems (one concept having cross-body ducts located in the wing aft cavity as described in NAS2-6344, task III, CR-114472,* and another with cross ducts in the wing leading edge) were sized and analyses were conducted to evaluate flow loss characteristics and the resulting thrust capacities. A range of wing geometries was covered, including aspect ratios from 5.5 to 8.5 with thicknesses of 0.201 c at side of body to 0.157 c at 50% b/2, and 0.176 c at side of body to 0.132 c at 50% b/2. The thrust capacities, T/S (installed thrust per square foot of wing area), of these duct systems are shown in figure 2 as a function of wing aspect ratio for fan pressure ratios of 1.7 and 3.2.

As figure 2 indicates, the duct capacity is not sufficient to accept the large-volume flow of the low-pressure fan at acceptable wing loadings. The incompatibility was resolved by assuming 50% of the fan air directed through a conventional nozzle in the nacelle. In this design the axially discharged fan jet becomes the predominant noise source, and, at the expense of increased system weight, overwing engine installations were chosen in order to achieve wing shielding of the fan jet noise. Large penalties were incurred in engine size primarily due to the high cruise thrust lapse of the low-pressure engine cycle coupled with the basic relationship of blowing nozzle thrust to system pressure and duct loss illustrated in figure 3. Engine size was further adversely affected by reduction in powered lift and total thrust with 50% of the fan air to the wing as well as reduction in thrust augmentation ratio due to the large nozzle area required for low-pressure air.

A summary of the major airplane characteristics as a function of blowing system pressure is shown in figure 4.

The airplane low-pressure system is defined as follows:

Wing aspect ratio	= 6.5
Wing sweep angle (0.25 c)	= 25°
Wing thickness, t/c	= 0.201_{SOB}; $0.157_{outboard}$
Duct configuration	= Leading edge cross ducts
Wing loading	= 93 lb/sq ft
Static thrust augmentation	= 1.14
Fan pressure ratio	= 1.7
Fan air to wing	= 50%
Engine size	= 34 700 lb SLST (uninstalled)
TOGW (STOL)	= 232 100 lb
500-ft sideline peak noise (takeoff), PNdB	
Overall	= 103
Augmentor	= 96
Aft turbomachinery plus jet exhaust	= 103
Forward turbomachinery (inlet)	= 103**

With the higher pressure systems it was possible to direct all the fan air through the aft cross-duct system with higher wing aspect ratio. While the system with fan pressure ratio = 3.7 yielded the lowest TOGW (187 000 lb), it was felt that this did not offset the probable cost of adding the fourth fan stage and the potential risk of flutter problems in the 8.5 aspect ratio

*_Design Integration and Noise Studies for Jet STOL Aircraft,_ Final Report, Volume II, "System Design and Evaluation Studies." (Originally issued as CR-114284.)

**Adjusted to match aft turbomachinery noise floor.

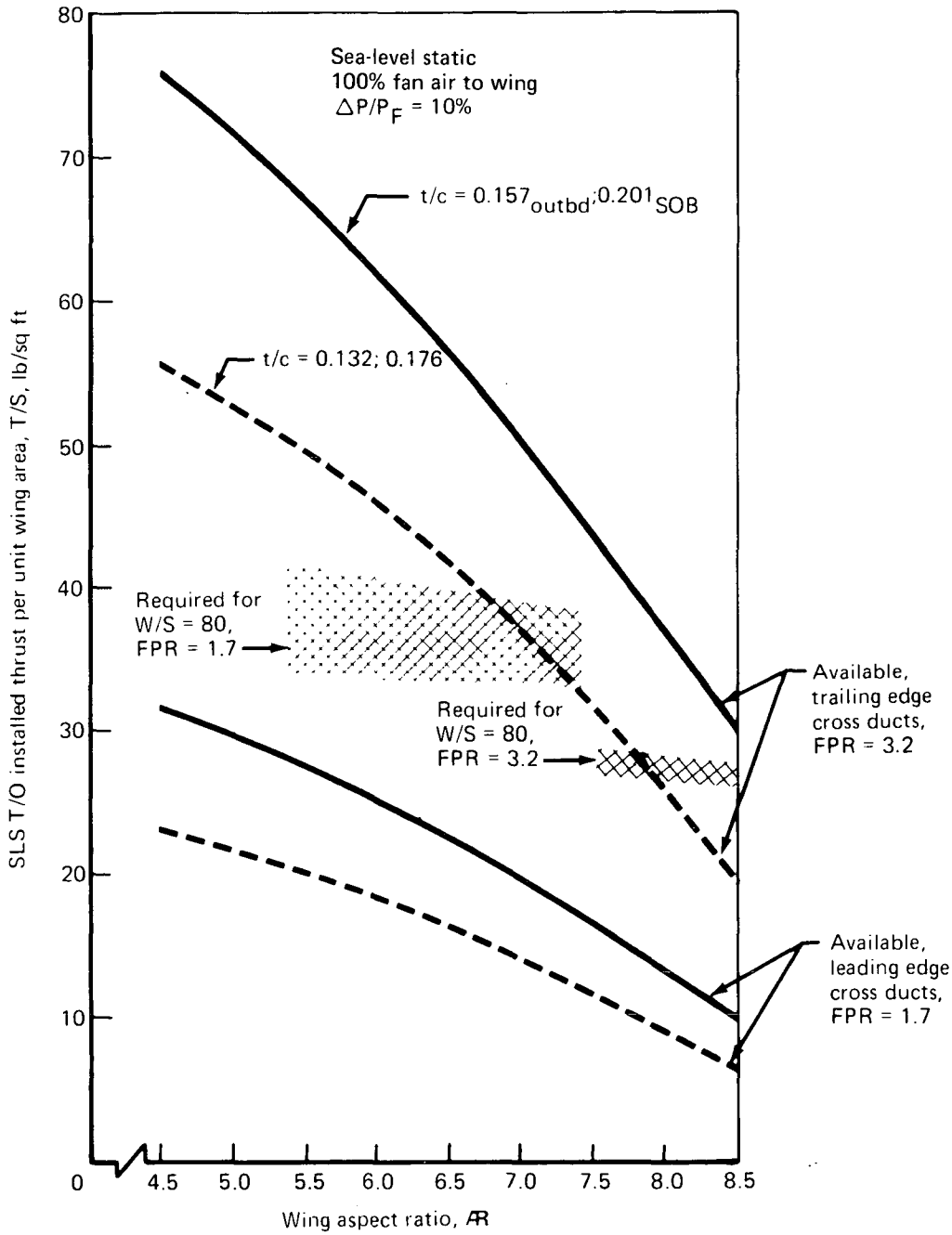

FIGURE 2.–EFFECT OF WING GEOMETRY AND SYSTEM PRESSURE ON INSTALLED THRUST CAPACITY FOR A VALVELESS AUGMENTOR WING CRUISE BLOWING SYSTEM

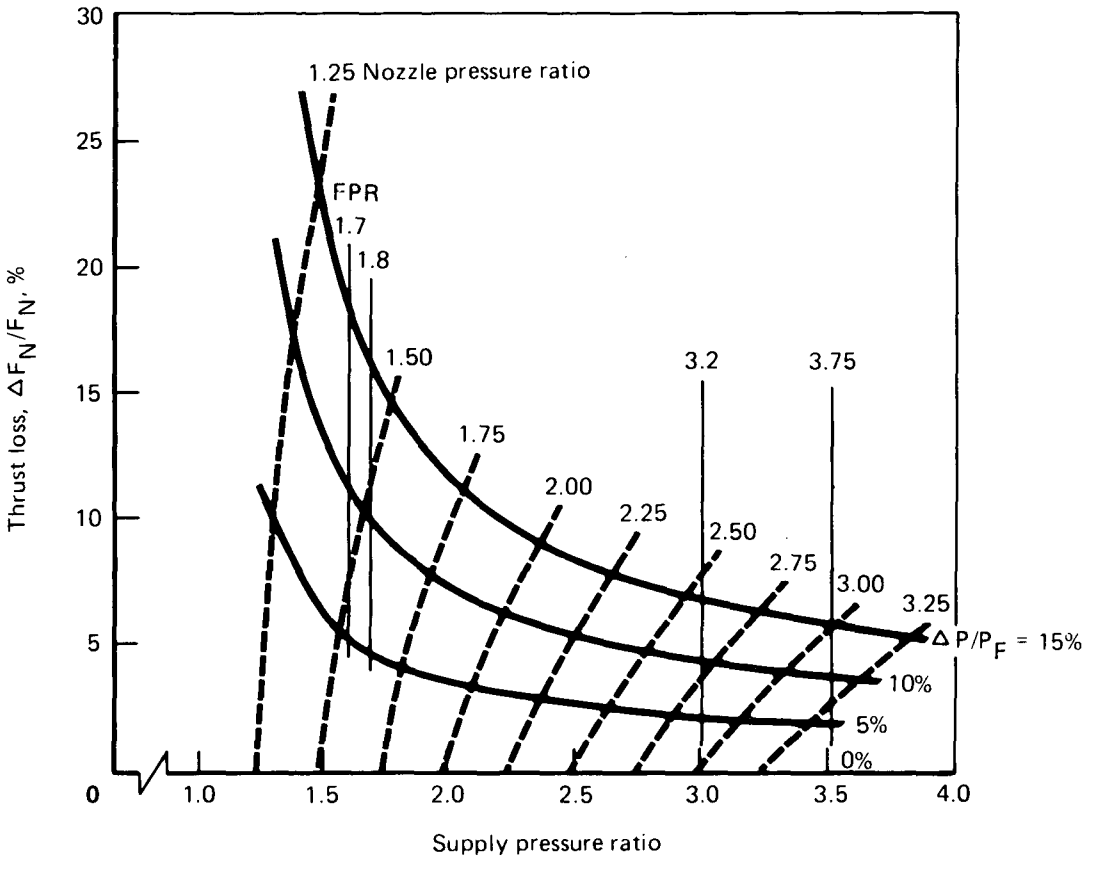

FIGURE 3.—DUCT PRESSURE LOSS-THRUST LOSS CORRELATION

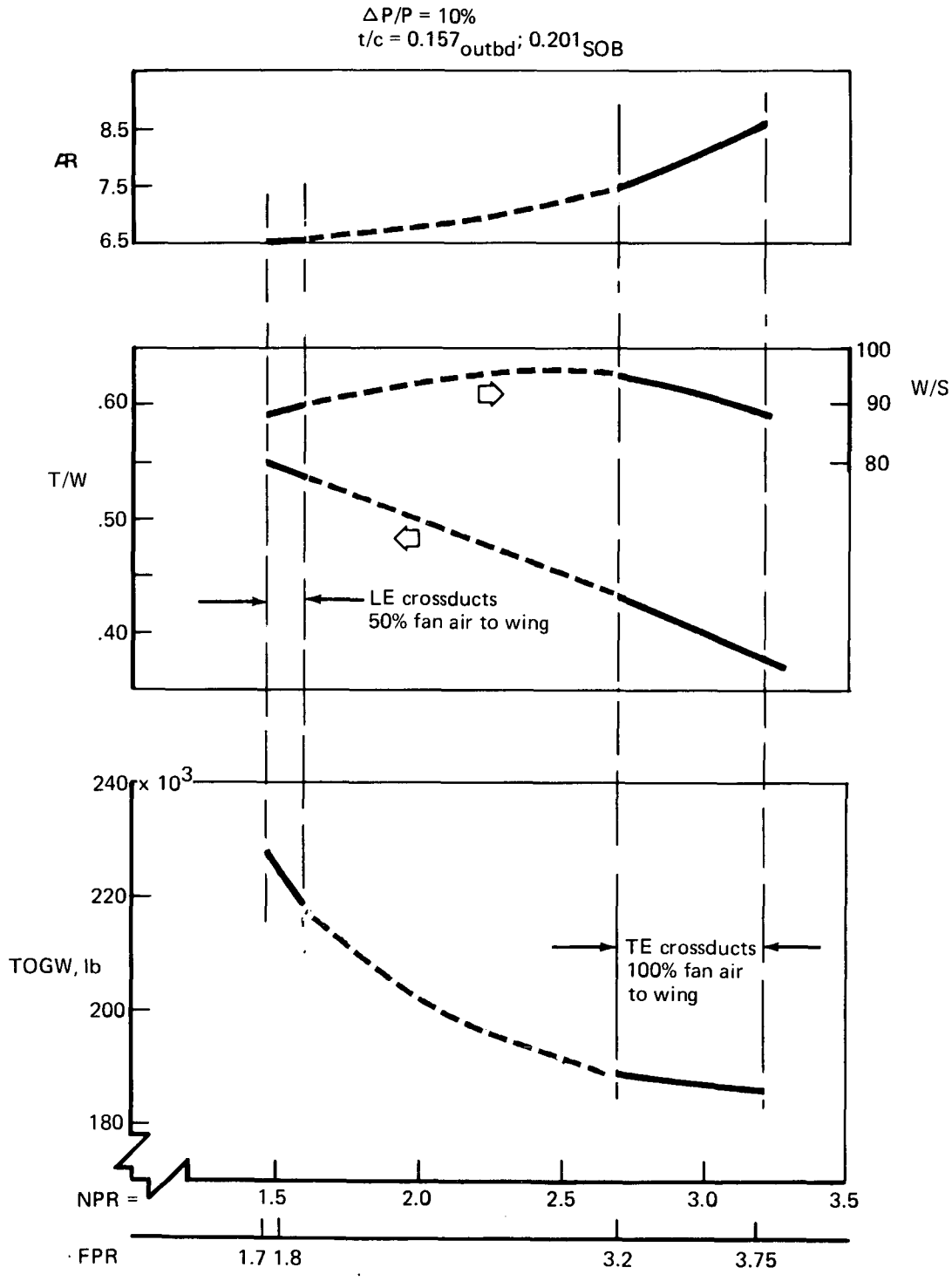

FIGURE 4.—EFFECT OF SYSTEM PRESSURE ON MAJOR AIRPLANE CHARACTERISTICS, AUGMENTOR WING CRUISE BLOWING SYSTEM

wing of that airplane. Therefore, the airplane characteristics chosen as the most appropriate are as follows:

Wing aspect ratio	= 7.5
Wing sweep angle (0.25 c)	= 25°
Wing thickness	= 0.176_{SOB}; $0.132_{outboard}$
Duct configuration	= Trailing edge cross ducts
Wing loading	= 84 lb/sq ft
Static thrust augmentation	= 1.38
Fan pressure ratio	= 3.2
Fan air to wing	= 100%
Engine size	= 18 300 lb SLST (uninstalled)
TOGW (STOL)	= 191 500 lb
500-ft sideline peak noise (takeoff), PNdB	
Overall	= 90
Augmentor	= 90
Aft turbomachinery plus jet exhaust	= 90
Forward turbomachinery (inlet)	= 90*

The sizing parameters for this airplane are shown in figure 5, which gives airplane weight as a function of wing and thrust loading with the limitations of duct volume, fuel volume, field length, and cruise thrust indicated.

*Adjusted to match aft noise floor.

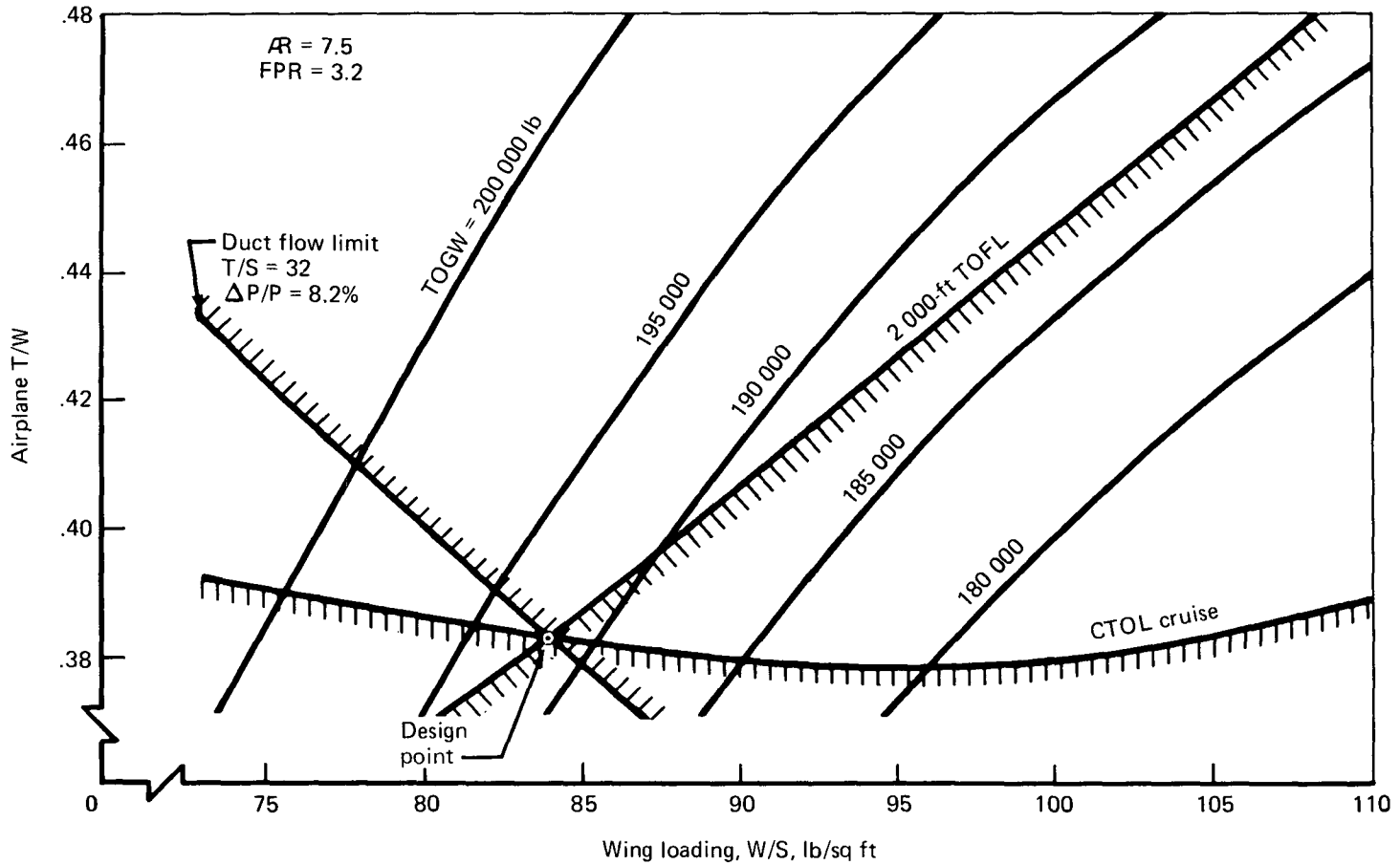

FIGURE 5.–AUGMENTOR WING CRUISE BLOWING SYSTEM AIRPLANE SIZING PARAMETERS

2.0 INTRODUCTION

Studies of the augmentor wing powered lift concept have shown that the inherent characteristics of an ejector-suppressor can result in a commercial STOL airplane with lower noise potential than other systems proposed.

The characteristics were verified through work completed by The Boeing Company in March 1972, under tasks I, II, and III of contract NAS2-6344, "Design Integration and Noise Studies for a Large STOL Augmentor Wing Transport." Pertinent results of that program are reported in NASA CR-114284.

Task VII of contract NAS2-6344 is directed toward large-scale model evaluation (NASA Ames 40- by 80-ft wind tunnel testing) of a concept which utilizes the noise suppression and powered lift advantages of the augmentor wing in the takeoff and landing approach modes, but which eliminates diverter valves and separate nozzles for the cruise mode. During cruise the augmentor flaps are stowed, and the wing nozzles blow over the upper surface.

This interim report on the task VII program covers exploratory system studies which were undertaken to establish design parameters for the testing portions of the program.

The studies were based on a 150-passenger airplane with 2000-ft FAR field length and 90-PNdB noise level objective at 500-ft sideline. The cruise requirement was 30 000-ft altitude at Mach 0.8 with a STOL range of 500 nmi and alternate mission CTOL range of 1500 nmi.

3.0 SYMBOLS AND ABBREVIATIONS

A*	blowing nozzle area at Mach 1.0, sq in.
A_A/S	augmentor nozzle area, square inches per square foot of wing area
A_N/S	total wing nozzle area, square inches per square foot of wing area
AAR	augmentor primary nozzle array area ratio, area enclosed by array/nozzle flow area
AR	airplane aspect ratio, b/c, or nozzle aspect ratio, $b_{aug}/h_{\overline{E}}$
ail	aileron
BLC	boundary layer control
BPR	bypass ratio, engine secondary airflow/engine primary airflow
b	span, ft or in.
C_D	drag coefficient or nozzle discharge coefficient (measured mean airflow/ideal airflow)
c_F, C_f	flap chord, percent wing chord
C_J	total blowing momentum coefficient, augmentor primary nozzle isentropic thrust/qS
C_L	lift coefficient
C_{LP}	design lift coefficient
C_V	nozzle velocity coefficient, $\left(\frac{\text{measured thrust}}{\text{measured mass flow x ideal velocity}}\right)$
C_j	sectional blowing momentum coefficient, augmentor primary nozzle isentropic thrust/q x sectional area
CTOL	conventional takeoff and landing
c	chord
D	drag
d	diameter, in.
dB	decibel

F	augmentor primary nozzle thrust, lb
F_W/A_N	wing thrust, pounds per square inch of wing nozzle area
FPR	fan pressure ratio
g	gravitational constant, ft/sec^2
H	nozzle height, in.
H_A	nozzle array height, in.
HP	high pressure or horsepower
HPX	shaft power extraction, horsepower
h	height, Y direction, in.
L	length, usually X direction; lift
LE	leading edge
LP	low pressure
M	Mach number
NPR	nozzle pressure ratio
OWE	operating weight empty, lb
P	total pressure, psi, or lobe or tube centerline pitch
PNdB	unit of perceived noise level
PNL	perceived noise level, PNdB
q	dynamic pressure (free or ducted stream)
RP	pressure ratio
S, S_W	wing area, sq ft
SFC	specific fuel consumption, lb/hr/lb thrust
SLS	sea level static
SOB	side of body
STOL	short takeoff and landing

shp	shaft horsepower
T	temperature, °R, or airplane net thrust, lb
$(T/A_N)_{in}$	engine installed thrust, lb per square inch of wing nozzle area
TE	trailing edge
Thumbprint	plot of airplane $(T/W)_{un}$ as a function of GW and W/S
TIT	high-pressure turbine inlet temperature at stator inlet, °R
T/O	takeoff power setting
TOFL	takeoff field length, ft
TOGW	takeoff gross weight, lb
T/S	wing thrust loading, airplane thrust/wing area ratio, lb/sq ft
T/W	airplane uninstalled thrust/weight ratio, lb/lb
t/c	wing thickness ratio, thickness/chord
T_4	turbine inlet temperature at rotor inlet, °R
V	velocity, ft/sec
W	weight or airplane weight, lb
W_N	lobe nozzle width, in
WCP	wing chord plane
W/S	wing loading, lb/sq ft
w	lobe width, in.
α	angle of attack, deg
$\Delta P/P_F$	fan air total pressure loss fraction relative to fan exit total pressure
δ_F	flap rotation angle with respect to WCP, deg
δ_N	augmentor primary nozzle deflection angle with respect to WCP, deg
δ_T	turning angle, deg ($\delta_T = \delta_F - \delta_N$)

Λ	airplane wing sweep of quarter chord, deg
λ	wavelength or wing chord taper ratio
ϕ	thrust augmentation; flaps on thrust/flaps off thrust

Subscripts:

app	approach
aug	augmentor
$\bar{E}$	equivalent slot nozzle area, sq in.
eff	thrust augmentation value that accounts for nozzle ventilation
eng	bare engine
F	fan exit total conditions
in	installed or inches
N	net or nozzle
MCR	maximum cruise rating
pri	primary
S	static
SLS	sea level static
SOB	side of body
STR	streamwise
sec	secondary engine stream, or induced flow regions of the augmentor
t	total (i.e., T_t, total temperature)
un	uninstalled
∞	ambient

4.0 SYSTEM DESIGN INTEGRATION

The process of selecting the configuration and size of augmentor to be represented in cruise blowing wind tunnel models included several logical steps, beginning with the layout and sizing of duct system concepts within the constraints of wing installation space and wing spanwise distribution requirements. Flow analysis of duct geometry together with engine performance data provided a definition of the installed thrust, thus establishing the size of the blowing nozzles with which the augmentor flaps were integrated.

Wing aspect ratios, wing thicknesses, and system pressures were varied for selected duct systems permitting parametric matching of the augmentor with airplane characteristics to establish STOL takeoff gross weights.

4.1 DUCT SYSTEMS

The objective of the duct design study was to simplify the previous arrangement reported in NASA CR-114284. Elimination of the fan air diverter valve in favor of continuous (cruise) blowing through the wing nozzles provides such an advantage and at the same time permits an engine-duct to wing-duct wye design with significant reduction in flow loss. Concurrent with studies of valveless systems, several alternate approaches were investigated in an effort to utilize expandable ducts and variable blowing nozzles to achieve the large duct volumes necessary to accommodate low fan pressure. A summary of the exploratory design drawings is given in table 1. Concept 1, the result of the studies reported in CR-114284, is shown as a reference. The factor A_N/S nozzle area in square inches per square foot of wing area, is given as a measure of relative duct volume (capacity) of the various systems. All valveless duct systems in this study were sized preliminarily for $\Delta P/P_F = 0.10$ except as noted.

4.1.1 Expandable Duct Systems

Concepts 4, 5, and 6 of table 1 incorporate expandable ducts and also retain diverter valves in order that the expansion panels may be returned to wing contour for cruise. Concept 7 eliminates diverter valves, but adds shutoff valves in the cross ducts. In the powered-lift mode a drop panel collects air from the cruise nozzle and diverts it to expandable ducts within the flap, while in the cruise mode the fan flow is split so that 36% exits through wing nozzles and 64% through the cruise nozzle.

Concept 8 provides a similar air split in the cruise mode with expandable drop panels at midchord and a diverter valve in the cruise nozzle duct.

In concept 9, all air exits through the wing nozzle. Ducts are sized for 15% flow loss in the augmentor mode and cross-duct shutoff valves are employed to reduce flow losses during cruise, but it is also necessary to introduce variable-area wing nozzles to accommodate the diverted flow. Large duct volume is achieved by the use of pressurized wing cavities and a compound duct-within-duct arrangement in a very thick lower flap. This results in an excessively thin upper shroud.

TABLE 1.– AUGMENTOR WING CRUISE BLOWING AND EXPANDABLE DUCT CONCEPT DRAWINGS

Concept	Description		Drawing	Wing t/c at SOB; 50% b/2	$(A_N/S)_{wing}$, sq in./sq ft			Duct loss, $\Delta P/P_F$, %
					4.0	5.5	7.5	
1	Diverter valves	Task III (reference) Rigid TE cross ducts Non-cruise blowing	LO-100 NASA CR 114284, pp. 61, 62, and 63	0.164; 0.120		0.76	0.45	14
2	Valveless	Rigid TE cross ducts Cruise blowing	LO-201, 202, and 222 LO-207 and 221	0.176; 0.132 0.201; 0.157		1.15* 1.55*	0.74* 1.01*	10 10
3	Valveless	Rigid LE cross ducts Cruise blowing	LO-201 LO-207, 208, and 216	0.176; 0.132 0.201; 0.157	2.5	1.52* 2.1 *	0.88* 1.24*	10 10
4	Diverter valves	LE cross ducts Retractable nozzles Expandable ducts Non-cruise blowing	LO-203	0.164; 0.120		1.1		10
5	Diverter valves	LE cross ducts Fixed nozzles Expandable ducts Non-cruise blowing	LO-213	0.164; 0.120		1.1		10
6	Diverter valves	Expandable cross ducts in flap Non-cruise blowing	LO-211	0.164; 0.120		2.3		10
7	Cross duct valves	Expandable cross ducts in flaps Drop panel and engine nozzle Cruise blowing	LO-204	0.164; 0.120		2.3		10
8	Diverter valves	Midchord drop panel Expandable cross ducts Cruise blowing	LO-210	0.201; 0.157		2.3		10
9	Cross duct valves	Rigid TE cross ducts Duct in duct in flap Pressurized aft cavity Variable area slot nozzle Cruise blowing	LO-212 LO-214	0.201; 0.17 0.176; 0.132		2.3	1.41	15
10	Valveless	Rigid TE cross ducts Duct in duct in flap Pressurized aft cavity Fixed slot nozzle Cruise blowing	LO-217	0.176; 0.132			1.41	10

*Based on duct flow analysis which supersedes applicable drawing.

The cross-duct valves and variable nozzles are eliminated in concept 10, thus satisfying the objective of valveless cruise blowing while retaining relatively large duct volume through the use of pressurized cavities and ducts-within-ducts.

Drawings of concepts 4 through 10 are provided in the appendix. Critical comments are included on each drawing, pointing out features which bear consideration in evaluating the various configurations.

Substantial increases in duct volume appear to be possible in many of these exploratory concepts, but with varying degrees of complexity which do not satisfy the basic objective of simplification. For that reason, attention was directed toward rigid duct systems and no further effort was devoted to expandable ducts.

4.1.2 Rigid Duct Systems

Layouts were analyzed to evaluate available duct volume for the cruise blowing configuration. The duct volume is increased from that of the reference diverter valve configuration, (CR-114472, originally issued as CR-114284) by locating the nozzle array above the wing, so that the ducts can occupy space formerly taken by the nozzle array. This is displayed in figure 6, which shows that the cruise blowing scheme, using a slightly thicker airfoil than that of the reference design, has about 50% more available duct volume.

Two types of rigid duct systems listed as concepts 2 and 3 in table 1 were investigated; the trailing edge crossover system, figure 7, which is similar in routing to that of the reference design, and the higher capacity leading edge crossover, figure 8. Because one goal of the cruise blowing system is to reduce complexity by eliminating diverter valves, the ailerons are fed from the outboard numbers 1 and 4 ducts. The aileron flow was increased to 9% (from 5% on the reference leading edge plenum) to allow for engine-out conditions. The leading edge BLC plenum airflow was reduced from 10% to 3%. This plenum duct is closed during cruise, and the 3% flow is routed through the augmentor nozzles. This gives an effective nozzle area reduction, which tends to improve cruise SFC (see section 4.2). A typical spanwise flow distribution is shown in figure 9.

The trailing edge crossover, figure 7, uses the rear spar chordwise location of the reference design. The rear spar varies from 50% chord at the fuselage and aileron to 45% chord at the outboard engine. The leading edge crossover concept (fig. 8) requires that the front spar be moved from 20% to 25% chord to allow the number 4 crossover duct to be routed along the leading edge. With this crossover duct in the leading edge, the augmentor ducts can be made larger and the rear spar can be kept at 50% chord. Although the leading edge crossover gives about a 38% increase in duct volume over the trailing edge crossover, it has disadvantages in a complex body crossover, increased weight, and aerodynamic drag associated with the pods which carry the crossover duct from the leading to the trailing edge. The leading edge crossover weight penalty is about 1500 lb OWE for a wing of $t/c = 0.132_{outbd}; 0.176_{SOB}$. Additional layouts were made to give duct volume scaling information from the t/c 0.132; 0.176, 5.5 aspect ratio wing of figures 7 and 8. These layouts are shown in figures 10 through 14, which investigate t/c values up to 0.157; 0.201 and aspect ratios up to 7.5. Figure 12 shows an extreme case to obtain large duct volume by using a thick wing, 4.0 aspect ratio, and leading edge ducts. Figure 14 shows a t/c = 0.132; 0.176, 7.5 aspect ratio, trailing edge duct layout representative of the high-pressure design point discussed in sections 4.6.2.2 and 4.6.4.

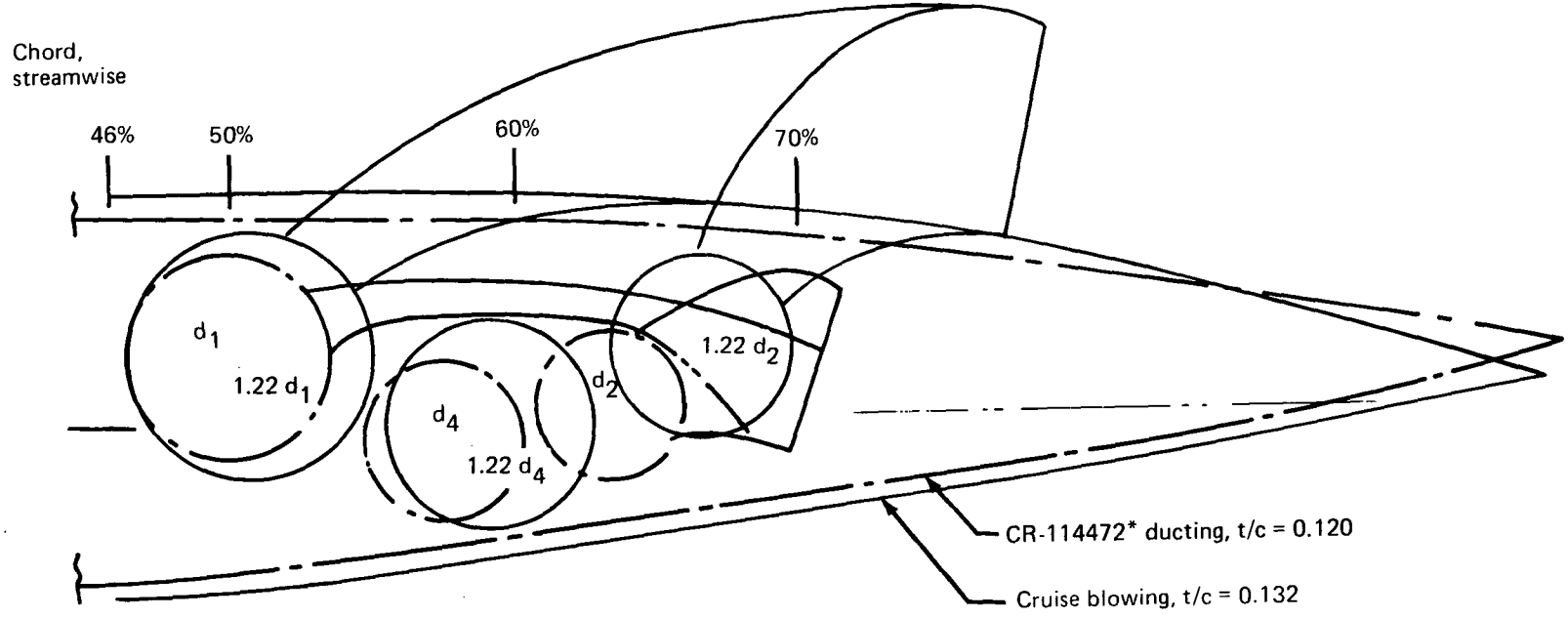

FIGURE 6.– COMPARISON OF AVAILABLE DUCT VOLUME (SECTION BETWEEN ENGINES, APPROXIMATELY 35% b/2)

* Originally issued as CR-114284.

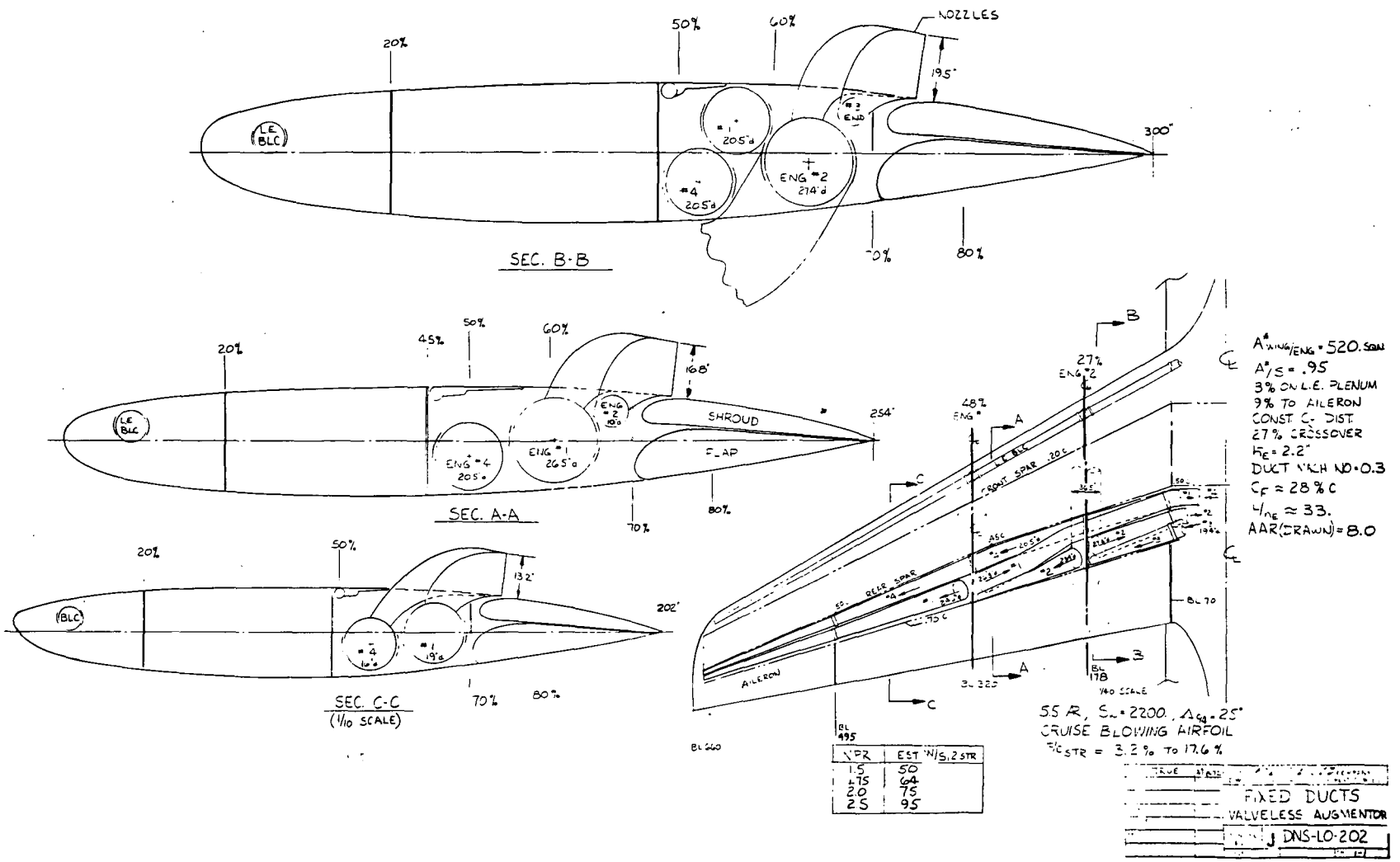

FIGURE 7.—LO-DNS-202, TRAILING EDGE CROSS DUCTS, AR = 5.5, t/c = 0.132$_{outbd}$; 0.176$_{SOB}$

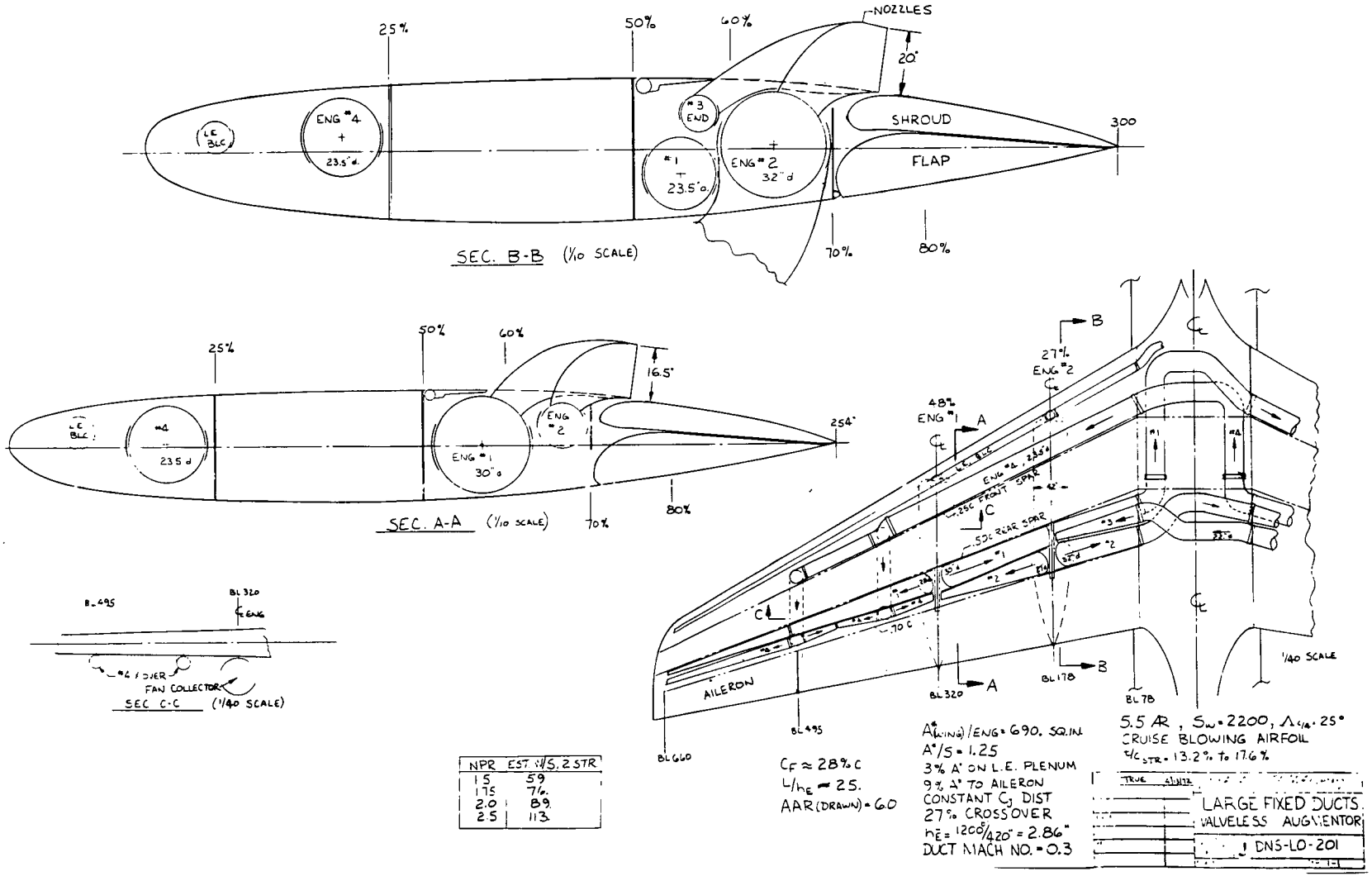

FIGURE 8.—LO-DNS-201, LEADING EDGE CROSS DUCTS, AR= 5.5, t/c = 0.132$_{outbd}$; 0.176$_{SOB}$

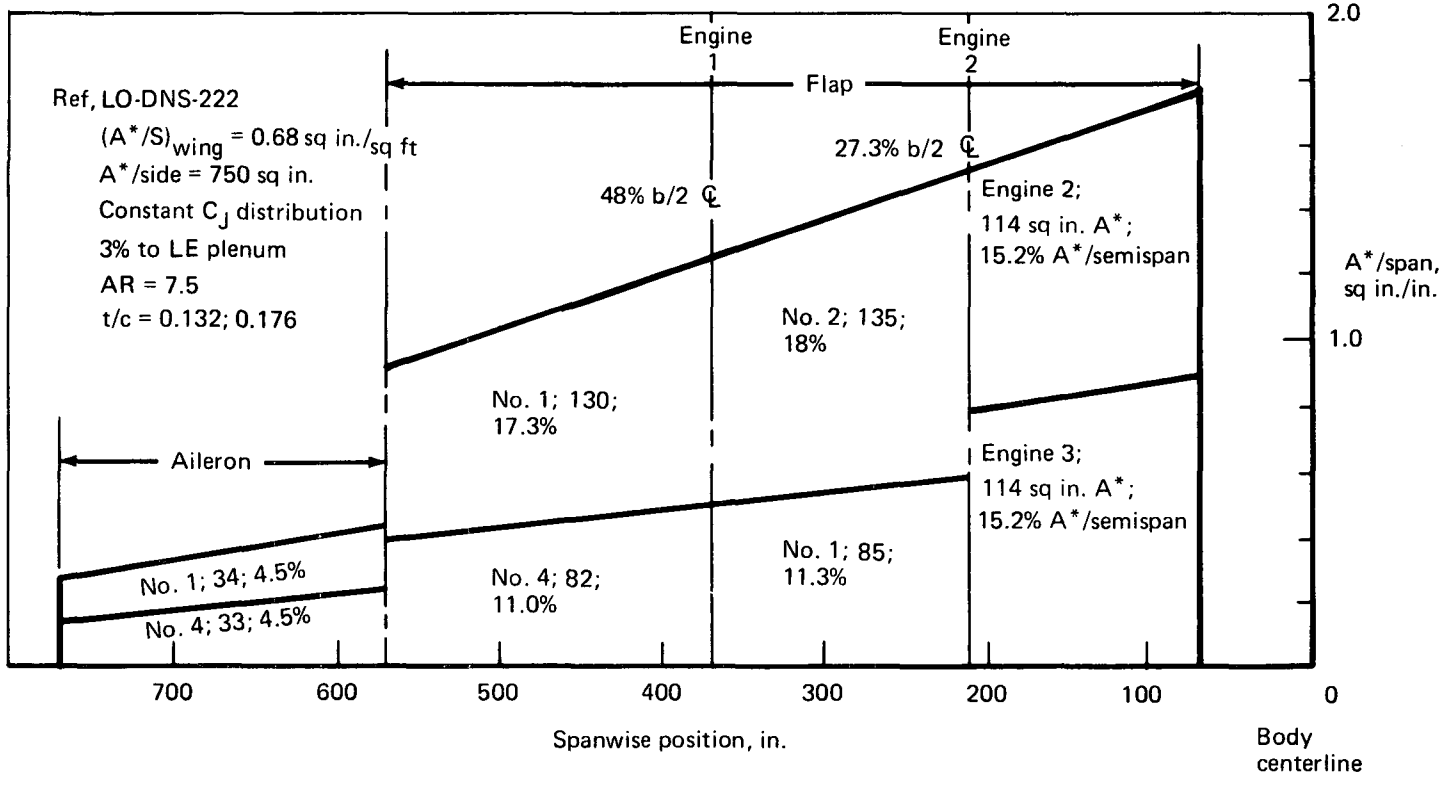

FIGURE 9.– TYPICAL NOZZLE AREA SPANWISE DISTRIBUTION

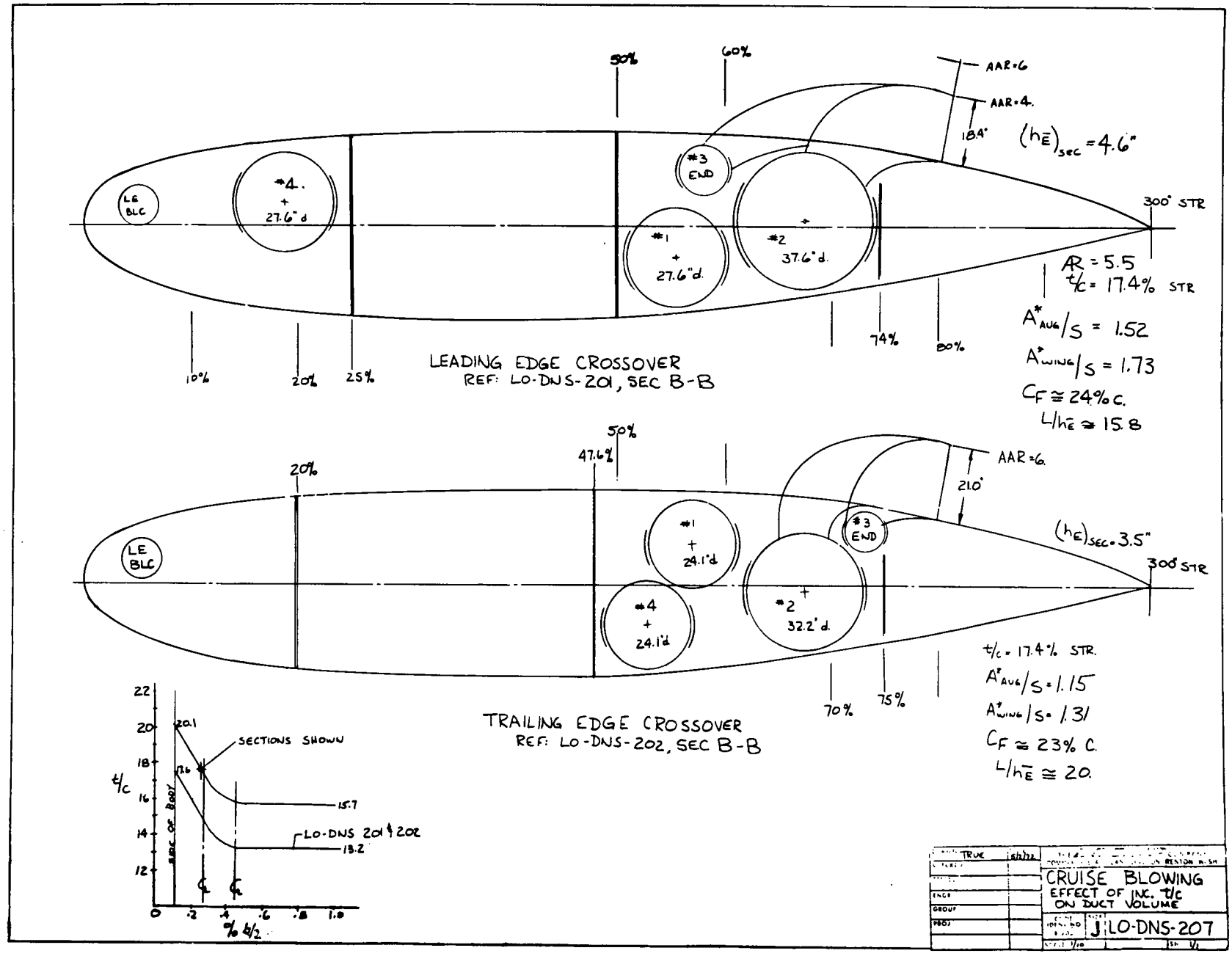

FIGURE 10.—LO-DNS-207, EFFECT OF INCREASING t/c ON DUCT VOLUME

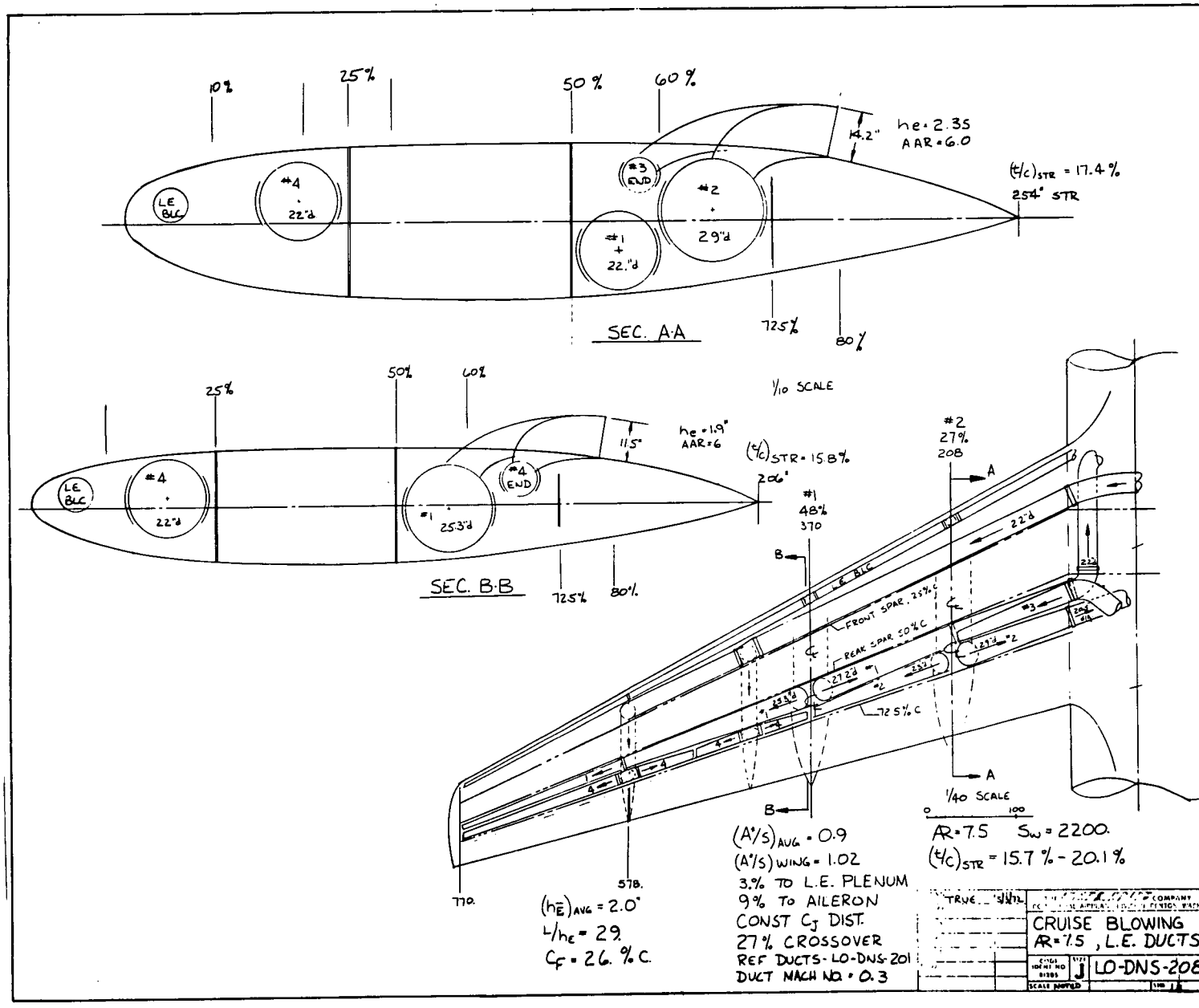

FIGURE 11.—LO-DNS-208, LEADING EDGE CROSS DUCTS, AR = 7.5, t/c = 0.157$_{outbd}$; 0.201$_{SOB}$

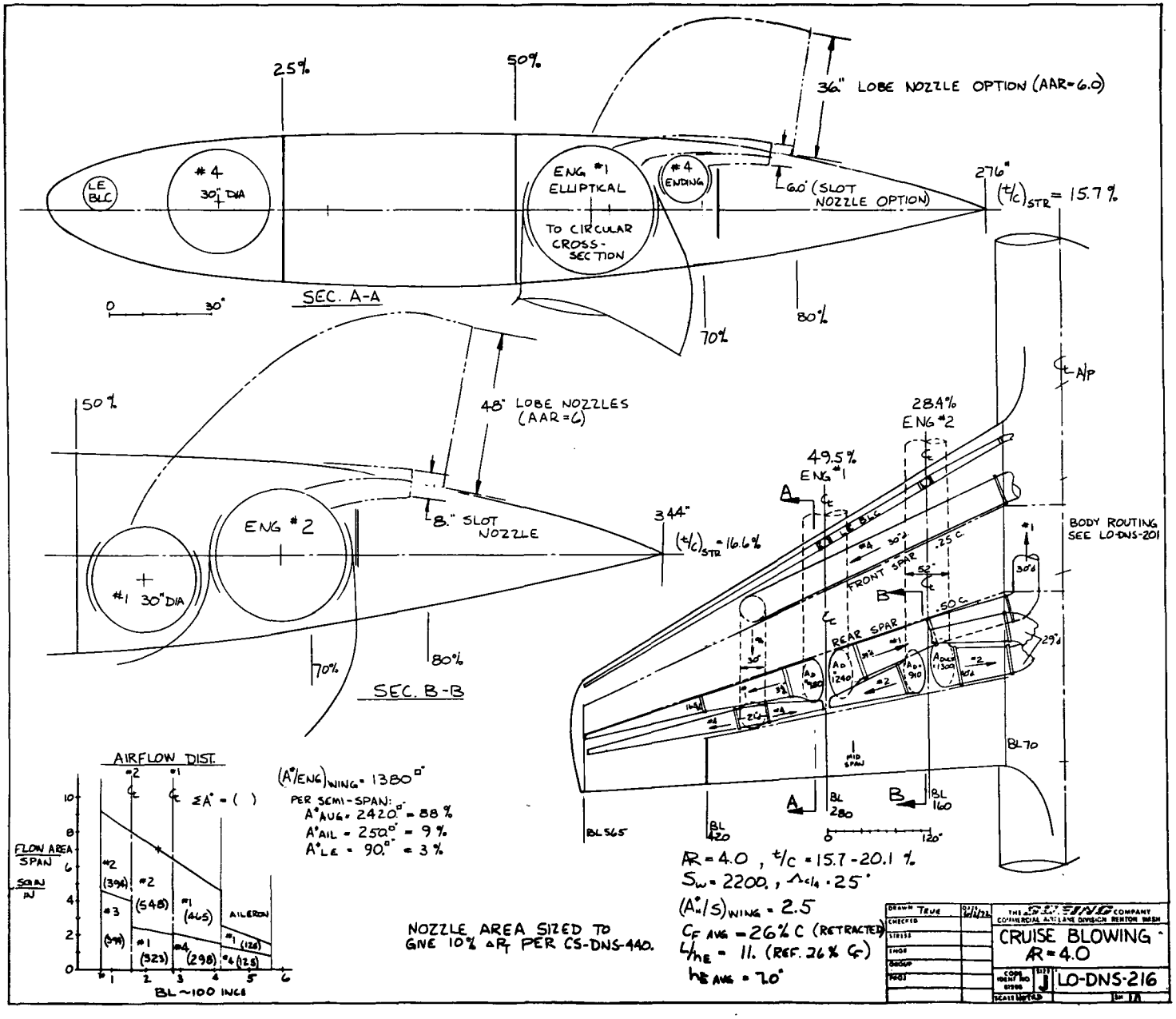

FIGURE 12.—LO-DNS-216, LEADING EDGE CROSS DUCTS, AR = 4.0, t/c = 0.157$_{outbd}$; 0.201$_{SOB}$

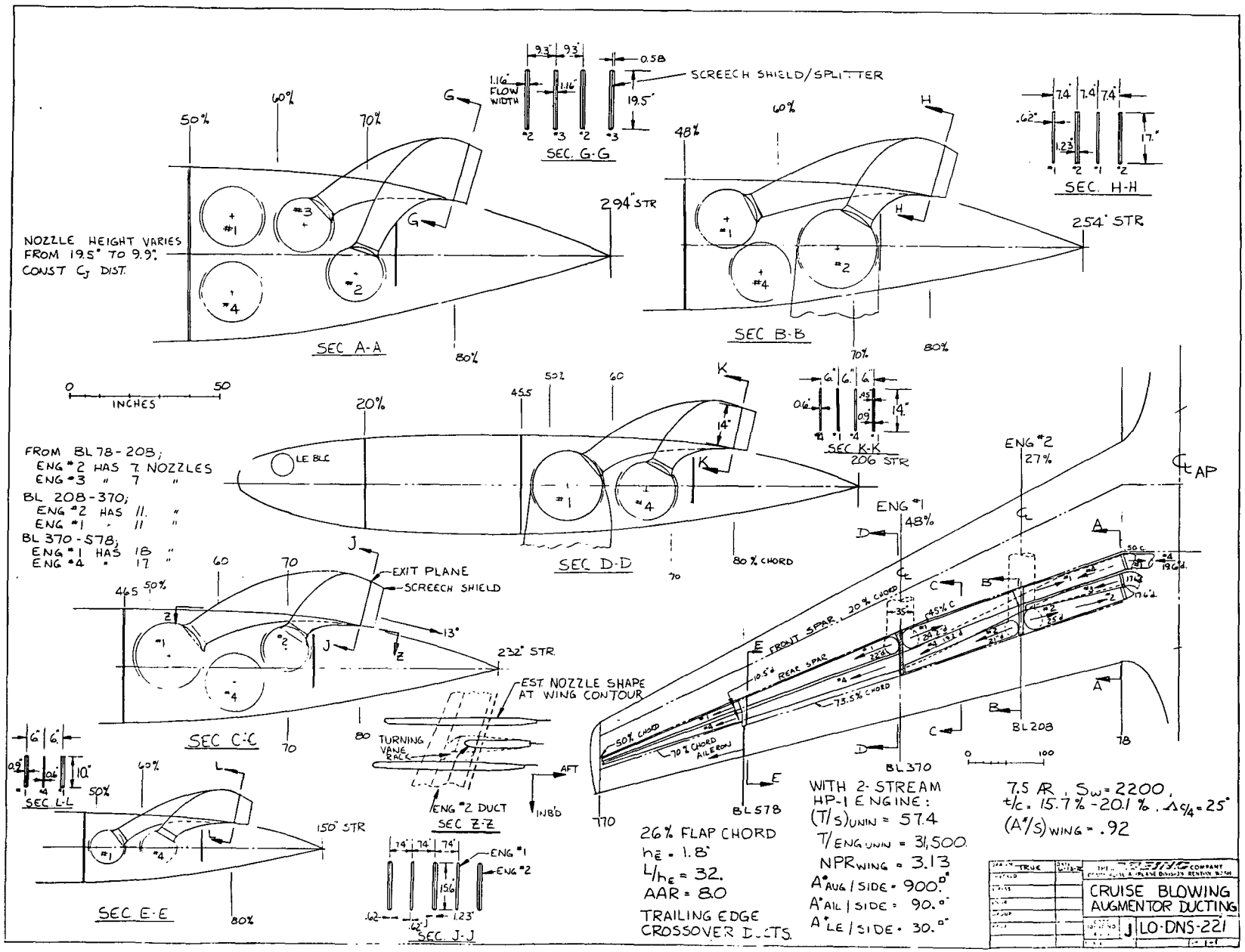

FIGURE 13.—LO-DNS-221, TRAILING EDGE CROSS DUCTS, AR = 7.5, t/c = 0.157$_{outbd}$; 0.201$_{SOB}$

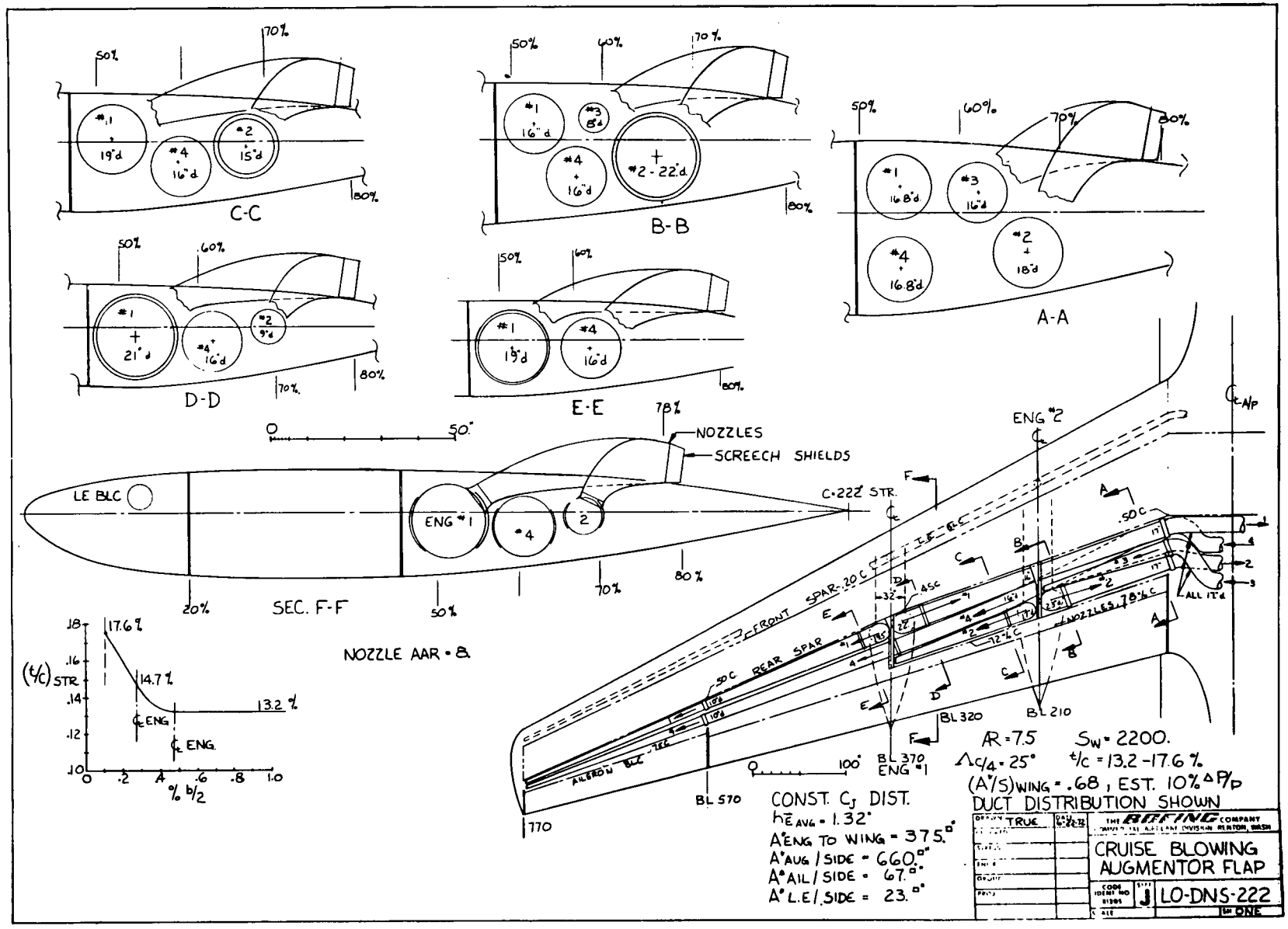

FIGURE 14.—LO-DNS-222, TRAILING EDGE CROSS DUCTS, AR = 7.5, t/c = 0.132$_{outbd}$; 0.176$_{SOB}$

The criterion used to evaluate available duct volume is the ratio of available nozzle area to wing area (A_N/S) in square inches per square foot. Since the available nozzle area of a given duct system is a strong function of the Mach number and pressure drop of the flow in the duct, A_N/S must, for comparison purposes, be related to pressure drop ($\Delta P/P_F$). Selected ducting layouts were analyzed for pressure drop, and the results are described in section 4.4. The A_N/S and $\Delta P/P_F$ shown in figures 7 through 14 are preliminary estimates made prior to the analysis and are superseded by those shown in figures 39 through 48.

Since nozzle array height, for a constant nozzle array area ratio, is proportional to the A_N/S, the nozzle height can be ratioed directly to the desired A_N/S. Figure 13 shows some typical nozzle exit dimensions. The nozzle widths (W_N) are determined by acoustic requirements and are nearly independent of moderate changes in A_N/S. The actual nozzle dimensions will be chosen following additional model testing and analysis. It should be noted that the duct sizing layouts provide nominal allowance for structural load paths and so should be considered as preliminary until verified by structure layouts.

4.2 ENGINE CYCLE STUDIES

To provide a consistent basis for augmentor system comparisons involving both low- and high-pressure systems, engine cycle analyses were performed for a range of engine fan pressure ratios. Cycles of proposed engines were established by adjusting the bypass ratio to obtain primary jet velocity and noise compatible with other noise sources. Approximate size and weight for these engines were calculated based on a P&WA advanced high-pressure spool. The study encompassed a range of engine fan pressure ratios from a single-stage fan, 1.7 FPR cycle to a four-stage fan, 3.75 FPR cycle.

4.2.1 Cycle Definition and Assumptions

The engines selected for augmentor wing system studies were two-stream cycles chosen to satisfy two main requirements, namely that: (1) the bypass ratio, together with the required fan pressure ratio, must give a cycle producing a primary jet noise of 90 PNdB or less, with four engines at 500-ft sideline, and (2) the cycle performance and technology should reflect that expected by the engine manufacturer for the 1978 to 1980 production time period.

The engine cycles are consistent with the technology of the P&WA STF-395D engine, which is based on an advanced high-pressure spool under development.

All engines in the study are two-stream, dual rotor, axial-flow turbofan engines with a variable primary exhaust nozzle. The two low-pressure cycles, designated LP-2 and LP-4, employ single-stage fans with SLS takeoff pressure ratios of 1.8 and 1.7, respectively. The two high-pressure cycles employ a three-stage fan, STF-395D (BM-2), and a four-stage fan, HP-1, with SLS takeoff pressure ratios of 3.2 and 3.75, respectively. The SLS takeoff thrust is flat-rated for all cycles to an ambient temperature of 90° F. Table 2 gives the principal cycle characteristics for the study engines.

The only significant difference between the STF-395D (BM-2) cycle and the STF-395D (BM-1) cycle used in the reference design is a 5% lower bare engine weight due to a more rigorous analysis of the (BM-2) engine weight.

The cycle performance data are based on the following assumptions:

- Uninstalled

  Inlet recovery factor = 1.0
  No external bleed or power extraction
  Fan duct total pressure loss, $\Delta P/P_F = 0.015$
  Primary duct total pressure loss, $\Delta P/P = 0.016$
  Fan nozzle $C_V = 1.0$
  Primary nozzle $C_V = 0.99$

- Installed

	Sea Level	Cruise
Inlet recovery factor	0.97	0.99
Power extraction, HP	225.	50.
Interstage bleed, lb/sec	0.93	0.72
Primary nozzle C_V	0.99	0.99

While the inlet recovery loss directly degrades the pressure of the fan stream, the power and air extracted from the core adversely affect fan speed and thus pressure ratio. The cumulative effect of these decrements is determined in the cycle analysis.

To account for the wing duct installation, an additional 10% pressure loss was applied to the secondary air ducted to the wing, from the 3/4 fan duct junction to the wing nozzle. Included in this 10% pressure loss is a wing nozzle $C_V = 0.96$, representing a simple lobe nozzle. An additional wing nozzle $C_V = 0.97$ was applied to the cruise performance to account for nozzle exit geometry. For the low-pressure systems only 50% of the secondary air was ducted to the wing. An additional 3% pressure loss was applied to the remaining fan nozzle airflow to account for acoustic splitters in the nacelle duct. These additional losses are summarized below.

	Sea Level	Cruise
Wing duct total pressure loss, $\Delta P/P$	0.10	0.10
Wing nozzle C_V	1.0**	0.97
Fan duct total pressure loss, $\Delta P/P_F$*	0.03	0.03
Fan nozzle C_V*	0.985	0.985

The bare engine weights for the study engines were determined by adding weight estimates for the fan, fan case, LP turbine, and rear frame to the weight of the basic high-pressure core. The weight of the high-pressure core, including engine accessories, was obtained from P&WA consistent with the STF-395D engine core. The component weight estimates were based on the technique of predicting weights for individual engine components by a weight-corrected airflow relationship derived by a statistical correlation of engine manufacturers' data.

*For low-pressure cycles with 50% airflow split.

**To account for the nozzles assumed in the vehicle, nozzle $c_v = 0.97$ was applied in airplane STOL calculations consistent with the cruise assumption.

4.2.2 Engine Cycle Performance

The principal uninstalled and installed engine cycle performance for takeoff and cruise is included in table 2. The uninstalled SLS takeoff thrust corresponds to that developed using the P&WA advanced core of unit size.

Curves of installed performance data for the study engines are presented in figures 15 through 26 for the takeoff, approach, and cruise conditions as detailed below.

Engine Cycle	Figures
LP-4, 1.7 FPR	15, 16, and 17
LP-2, 1.8 FPR	18, 19, and 20
STF-395D (BM-2), 3.2 FPR	21, 22, and 23
HP-1, 3.75 FPR	24, 25, and 26

4.2.3 Performance Comparisons

A comparison of the basic performance of the low-pressure LP-2 and LP-4 cycles with that of the high-pressure HP-1 and STF-395D (BM-2) cycles can be obtained from table 2. Performance is shown for installed engines, with 50% secondary airflow to the wing for the low-pressure cycles and 100% secondary airflow to the wing for the high-pressure cycles.

Figure 27 compares cruise thrust lapse as a function of design fan pressure ratio. The upper curve on figure 27 is the uninstalled thrust lapse for the LP-2, LP-4, STF-395D, STF-395D (BM-2), and HP-1 cycles. These cycles all have the same maximum cruise/SLS takeoff turbine inlet temperature ratio of 0.9. The lower curves are the installed maximum cruise/uninstalled SLS takeoff thrust. The "high-pressure" cycles were for installed engines with 100% secondary airflow to the wing. For comparison with the low-pressure cycles, the thrust lapse for the HP-1 and STF-395D (BM-2) is also shown for a 50% secondary airflow split.

The uninstalled thrust lapse and turbine inlet temperature ratio range for current high-bypass engine cycles is also shown in figure 27. This curve shows the relative increase in thrust lapse as the fan pressure ratio decreases. Also, by comparing the turbine-temperature-ratio to cruise-thrust-lapse relationship, the study engines are consistent with the current engines.

The difference between the uninstalled and installed thrust lapse is equal to the thrust loss due to installation effects. The installation thrust loss increases significantly for lower fan pressure ratio (higher bypass ratio) engines. This is due to the fact that these engines are more sensitive to installation losses primarily because of the high secondary-gross-thrust to total-net-thrust ratio and the basic relationship of blowing nozzle thrust with system pressure and duct flow loss which results in substantial penalties at low pressures.

The cruise thrust and SFC losses due to the installation effects are given in table 2. The sensitivity of the low-pressure systems can be readily seen. As an example of this sensitivity, figure 28 presents a breakdown of the installation losses at cruise for the LP-4 (1.7 FPR) and STF-395D (BM-2) (3.2 FPR) cycles. Both cycles are installed as detailed in section 4.2.1. The

TABLE 2.–PERFORMANCE CHARACTERISTICS, AUGMENTOR WING ENGINE CYCLES

Cycle	LP-4	LP-2	STF-395D (BM-2)	HP-1
Percentage of secondary airflow to wing	50%	50%	100%	100%
Uninstalled–SLS, standard day, takeoff				
Fan pressure ratio	1.7	1.8	3.2	3.74
Bypass ratio	5.26	4.67	2.11	1.73
Overall pressure ratio	24.0	24.0	25.6	30.0
Total thrust, lb	26 119	24 721	18 248	19 333
Total corrected airflow, lb/sec	859	777	441	450
Bare engine weight, lb	3862	3669	3185	3740
Thrust/weight, lb/lb	6.76	6.73	5.73	5.17
Thrust/airflow, lb/lb/sec	30.4	31.8	41.4	43.0
Bare engine length, in.	100	100	97.6	110
Fan tip diameter, in.	68.7	65.9	49.2	49.5
Installed–SLS, standard day, takeoff				
Total net thrust, lb	21 140	20 503	16 195	17 386
Thrust installation loss, %	15.7	14.8	11.2	10.1
Total actual airflow, lb/sec	815	738	418	427
Augmentor nozzle pressure ratio	1.44	1.52	2.67	3.13
Installed–100 kn, standard day, takeoff				
Primary nozzle ideal absolute jet velocity, fps	779	768	745	786
Fan nozzle ideal absolute jet velocity, fps	949	938	–	–
Augmentor nozzle ideal absolute jet velocity, fps	871	1011	1505	1640
Fan tip speed, fps	1540	1550	1440	1420
Installed–30 000 ft, Mach 0.8, maximum cruise, 60% primary nozzle area				
Total net thrust, lb	4962	4997	4703	5164
Thrust installation loss, %	18.0	14.7	11.7	10.1
Thrust lapse, $F_{n_{CR}}/F_{SLS_{un}}$	0.190	0.202	0.258	0.267
SFC, lb/hr/lb	0.765	0.762	0.829	0.820
SFC installation increase, %	18.0	14.3	7.7	6.4
SFC decrease for primary nozzle area change (100%–60%)	2.5	3.2	8.2	9.5
Max cruise TIT/sea level takeoff TIT	0.9	0.9	0.9	0.9

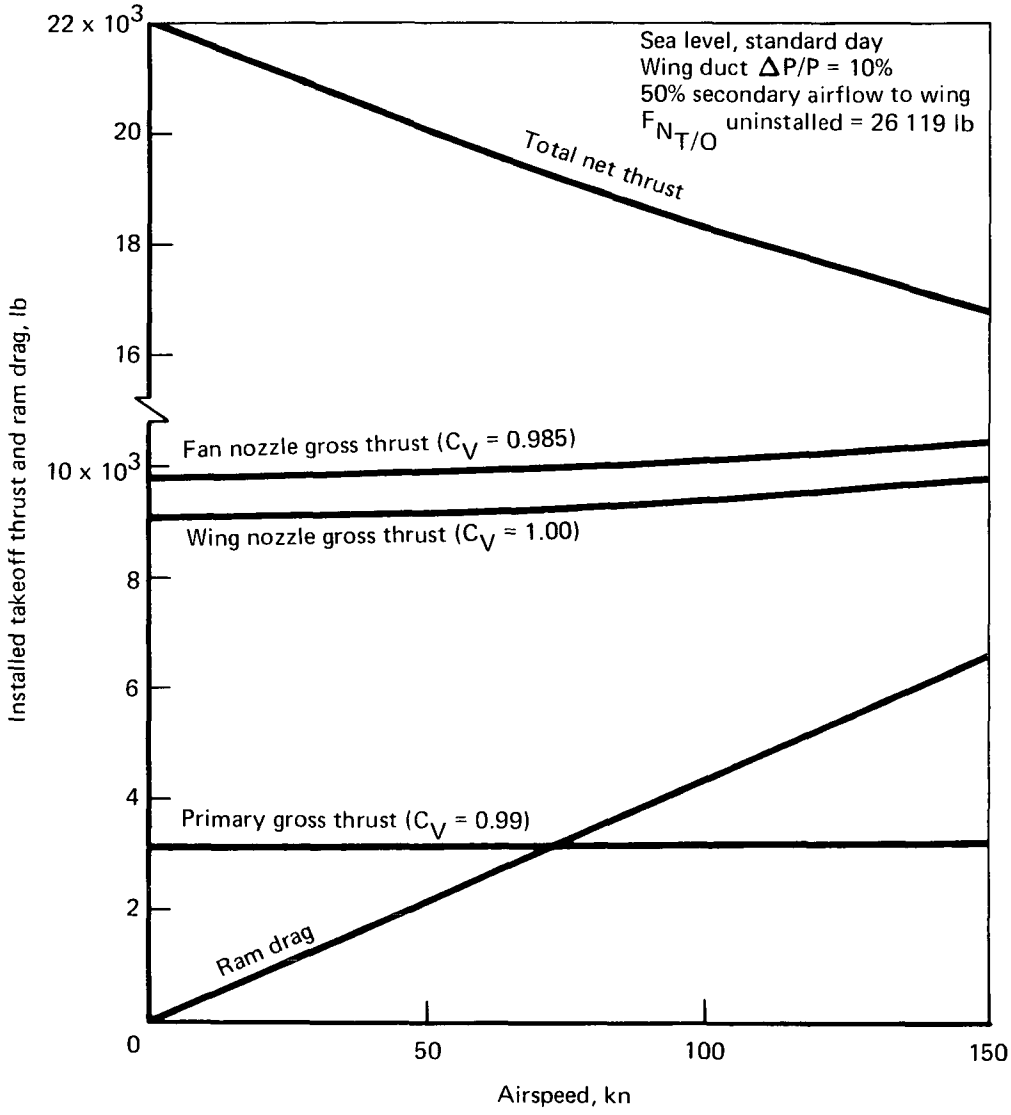

FIGURE 15.—TAKEOFF PERFORMANCE, INSTALLED—LP-4 CYCLE, FPR = 1.7

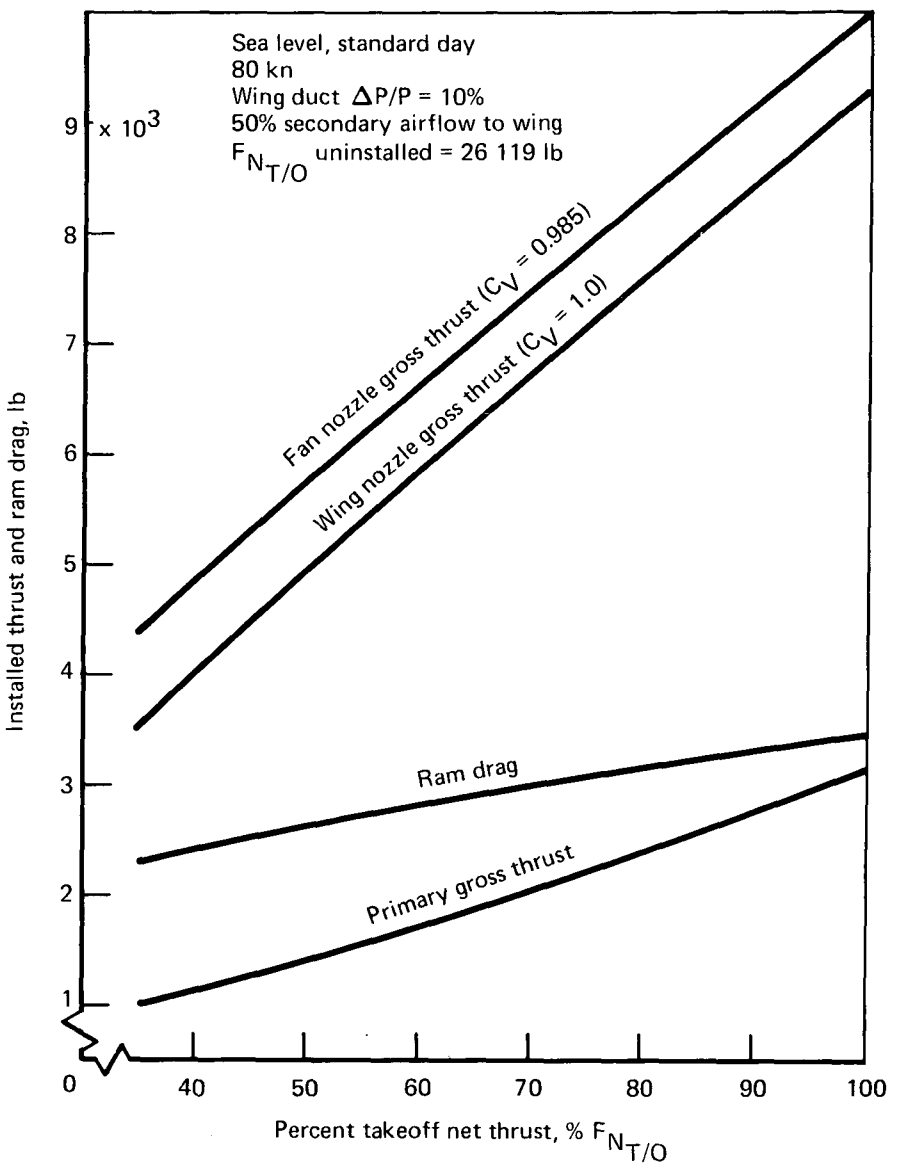

FIGURE 16.—APPROACH PERFORMANCE, INSTALLED—LP-4 CYCLE, FPR = 1.7

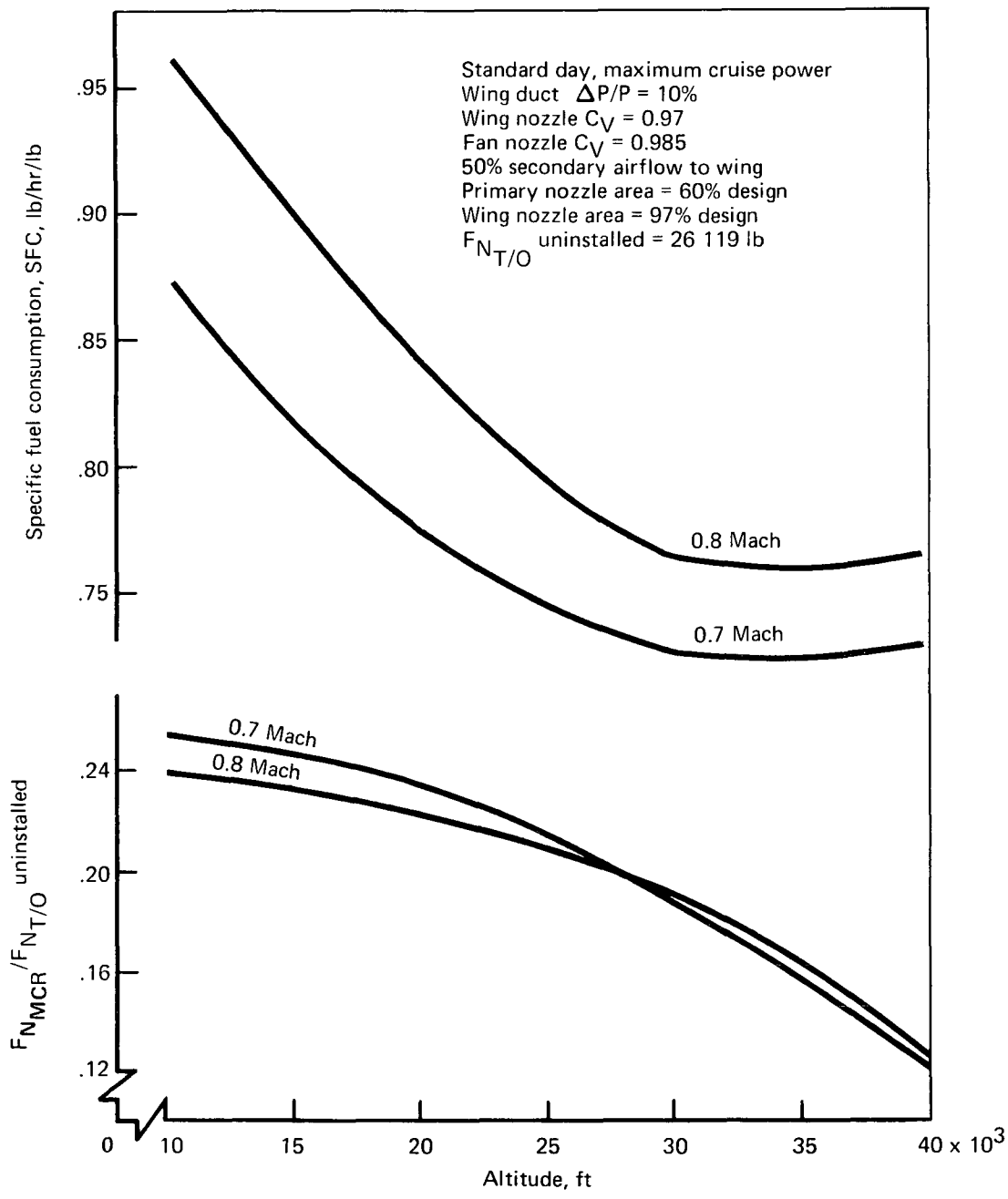

FIGURE 17.– CRUISE PERFORMANCE, INSTALLED–LP-4 CYCLE, FPR = 1.7

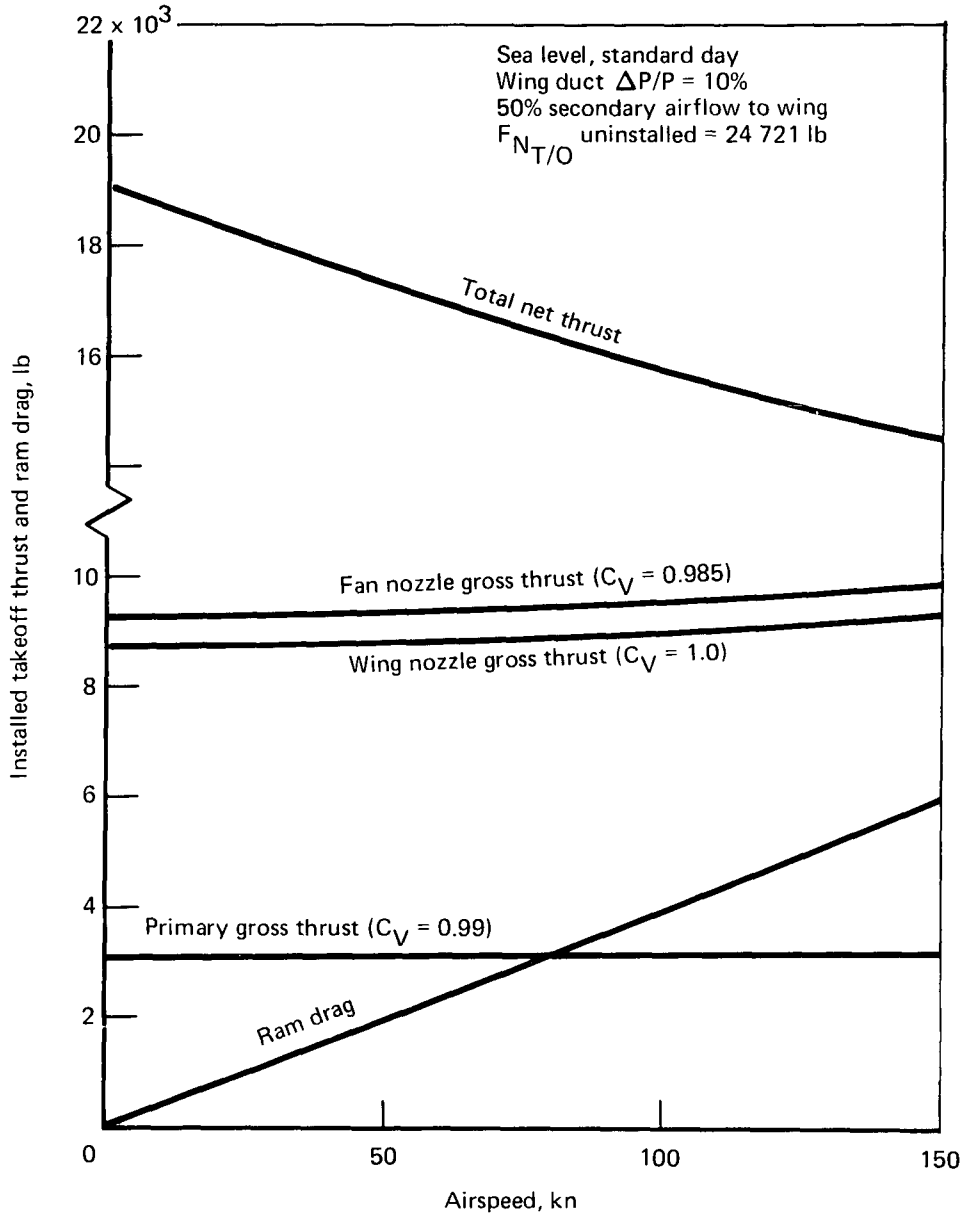

FIGURE 18.—TAKEOFF PERFORMANCE, INSTALLED—LP-2 CYCLE, FPR = 1.8

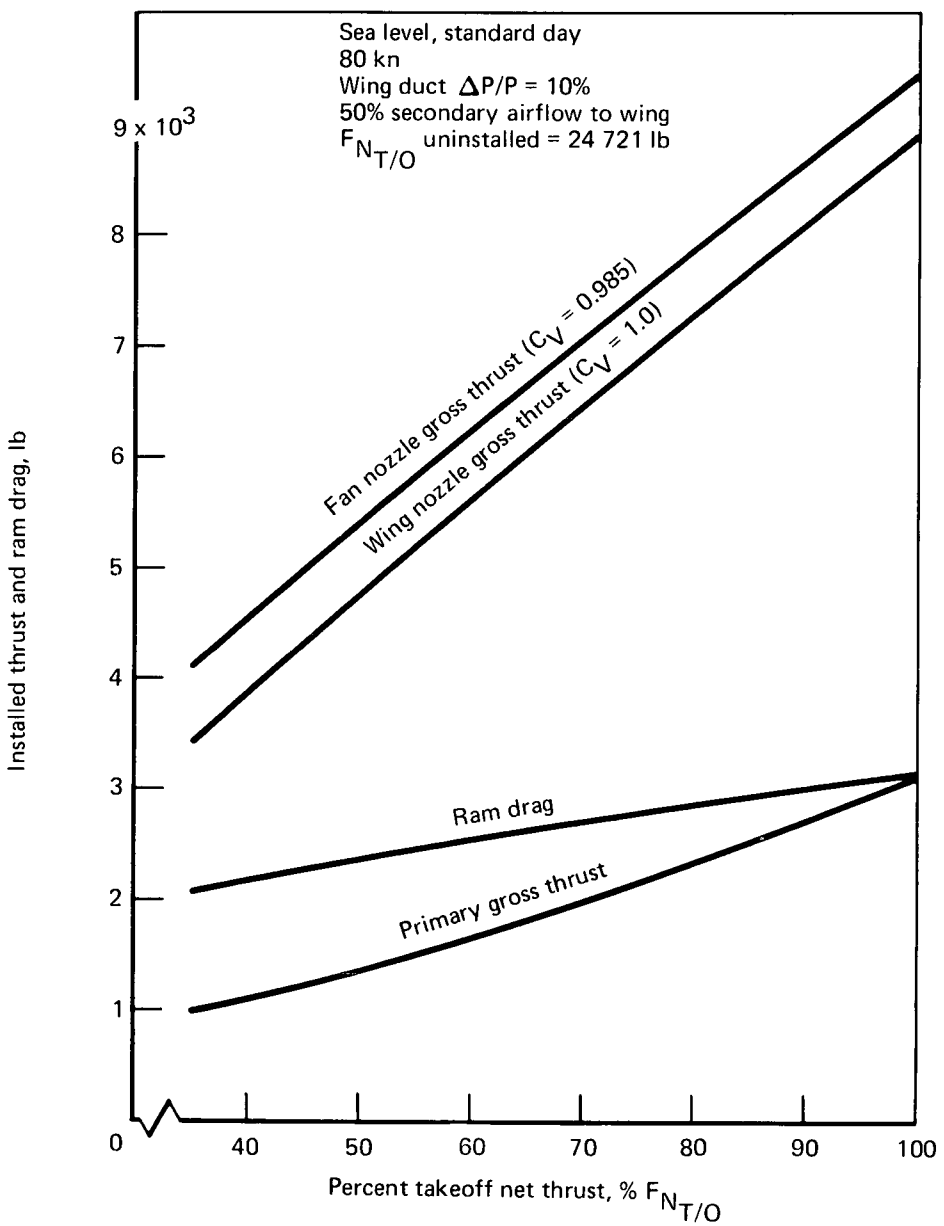

FIGURE 19.–APPROACH PERFORMANCE, INSTALLED–LP-2 CYCLE, FPR = 1.8

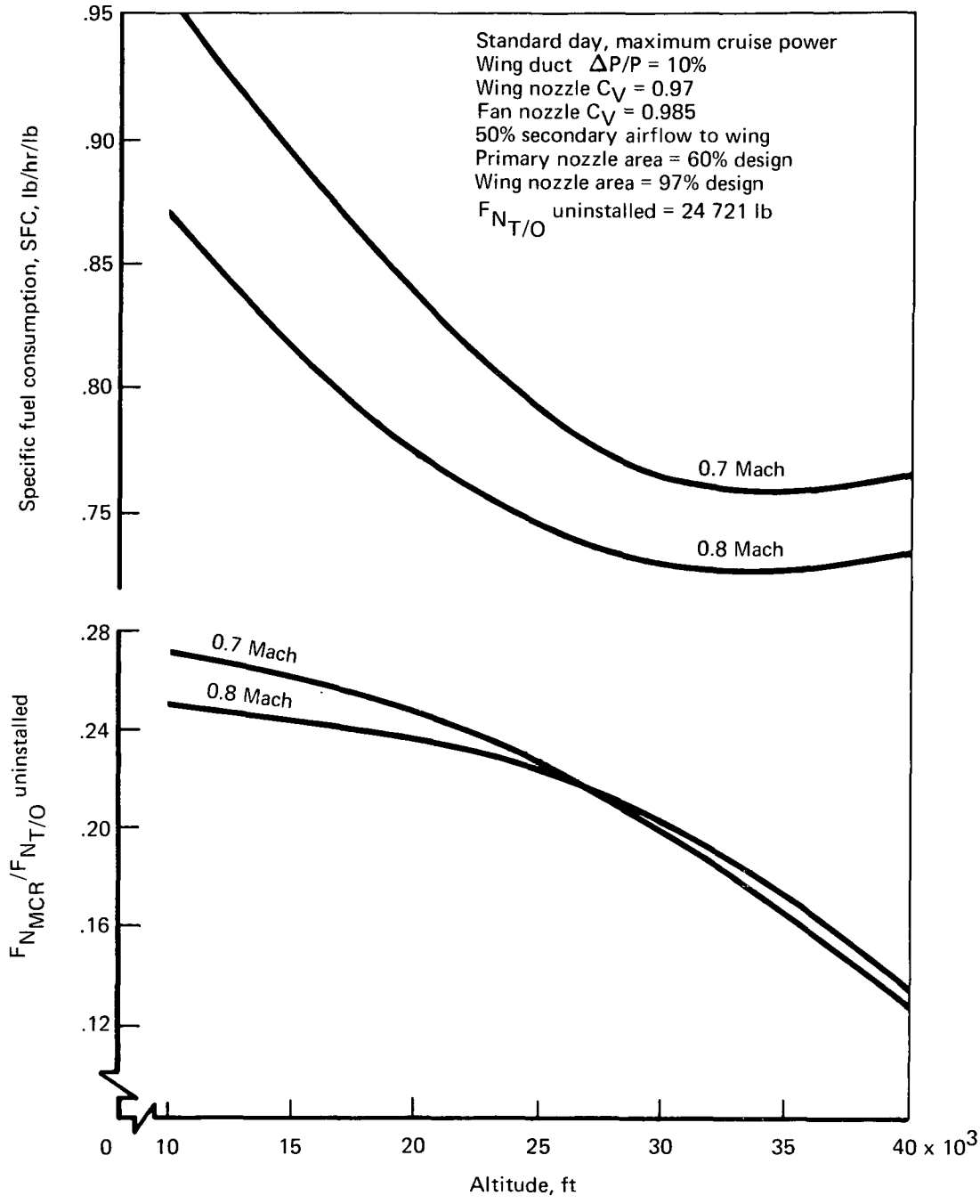

FIGURE 20.–CRUISE PERFORMANCE, INSTALLED–LP-2 CYCLE, FPR = 1.8

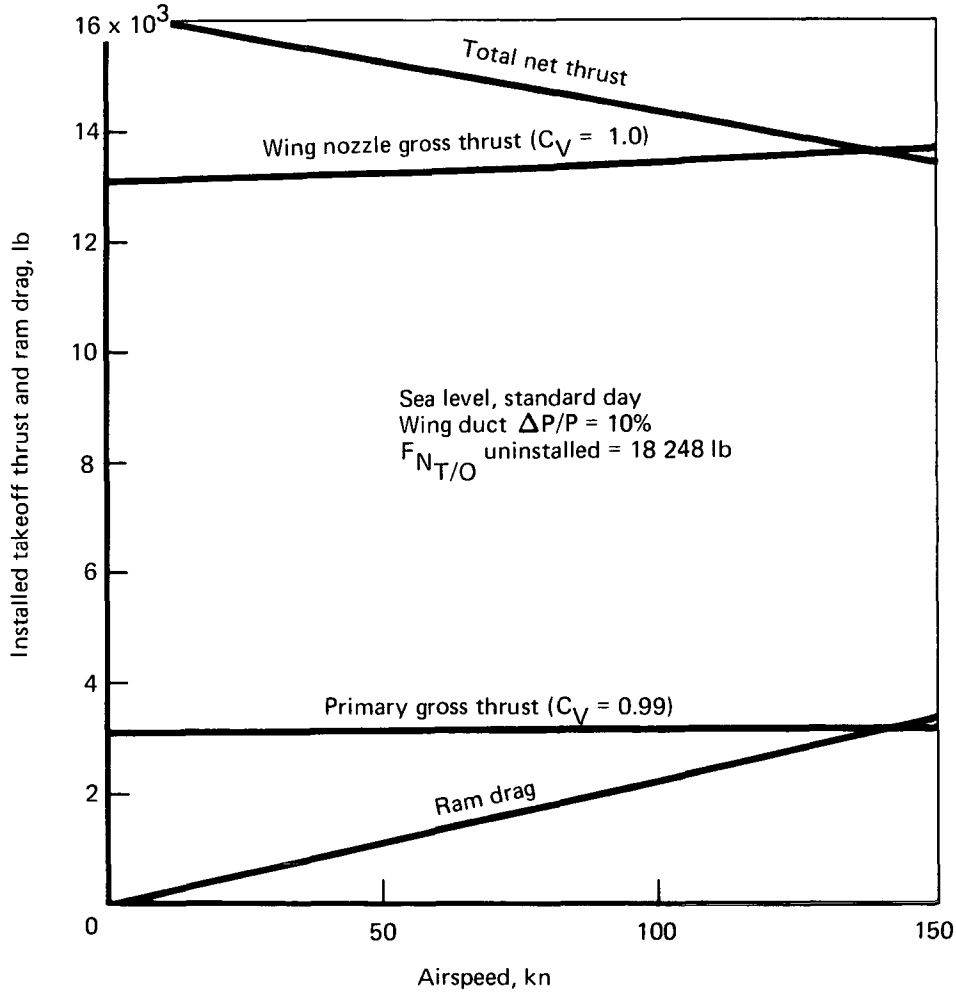

FIGURE 21.–TAKEOFF PERFORMANCE, INSTALLED–STF-395D (BM-2), FPR = 3.2

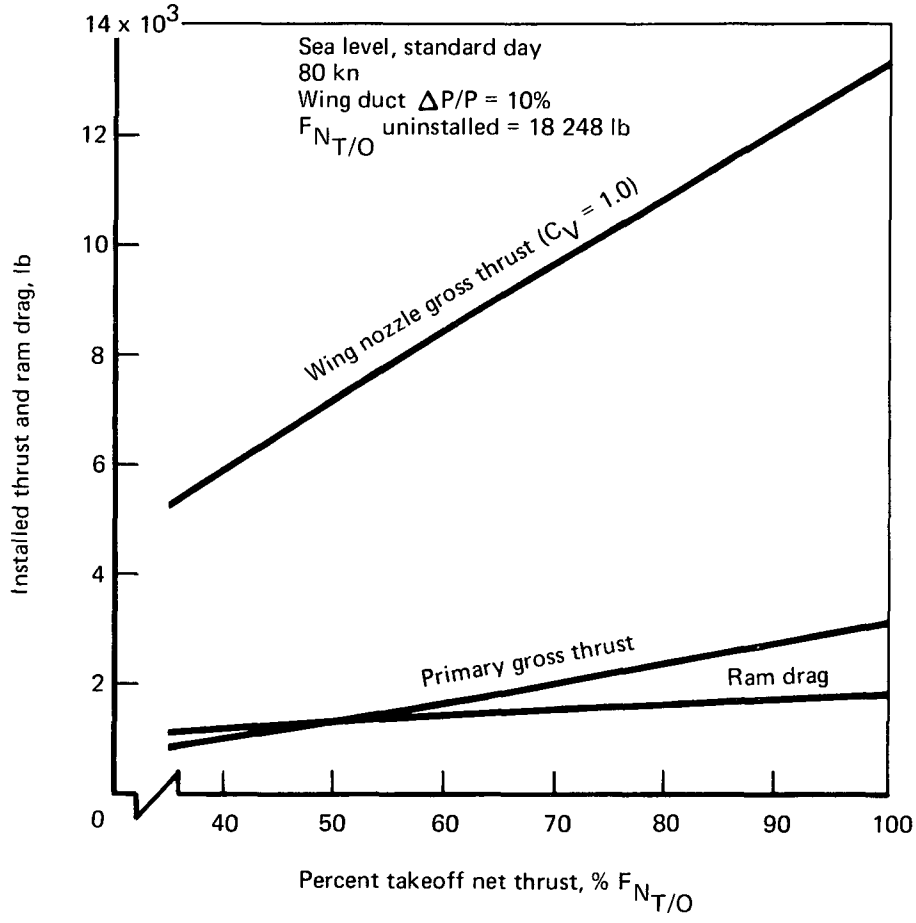

FIGURE 22.–APPROACH PERFORMANCE, INSTALLED–STF-395D (BM-2), FPR = 3.2

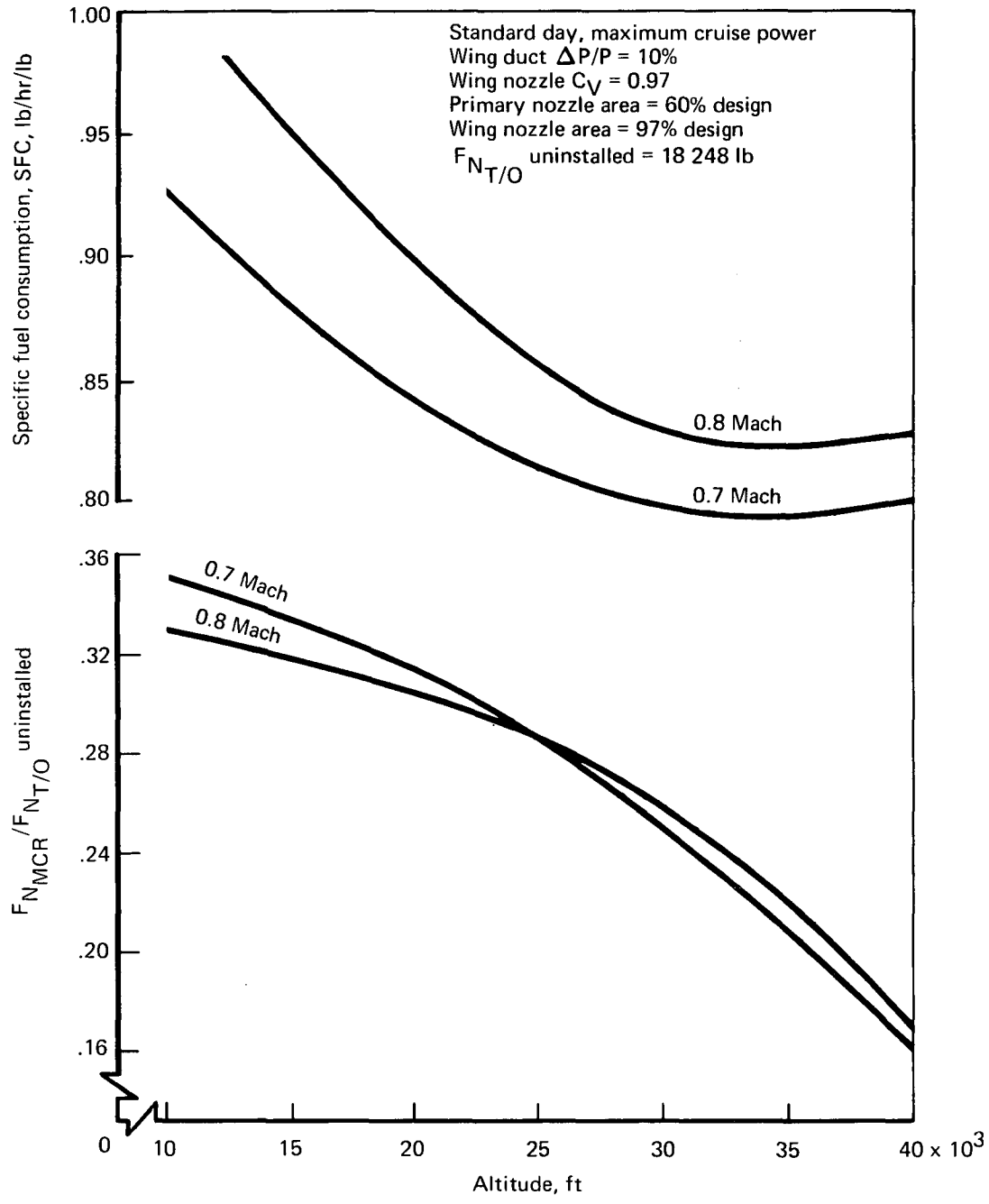

FIGURE 23.—CRUISE PERFORMANCE, INSTALLED—STF-395D (BM-2), FPR = 3.2

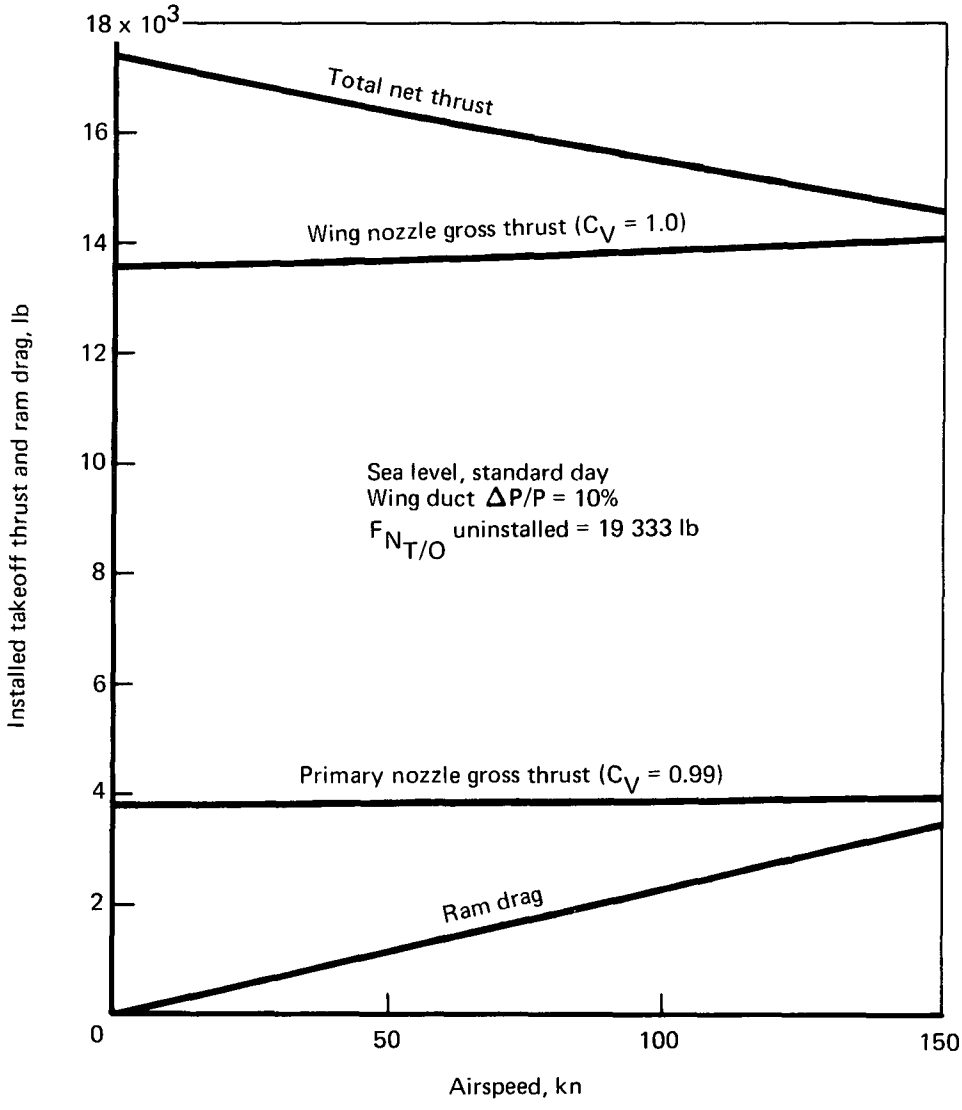

FIGURE 24.–TAKEOFF PERFORMANCE, INSTALLED–HP-1 CYCLE, FPR = 3.75

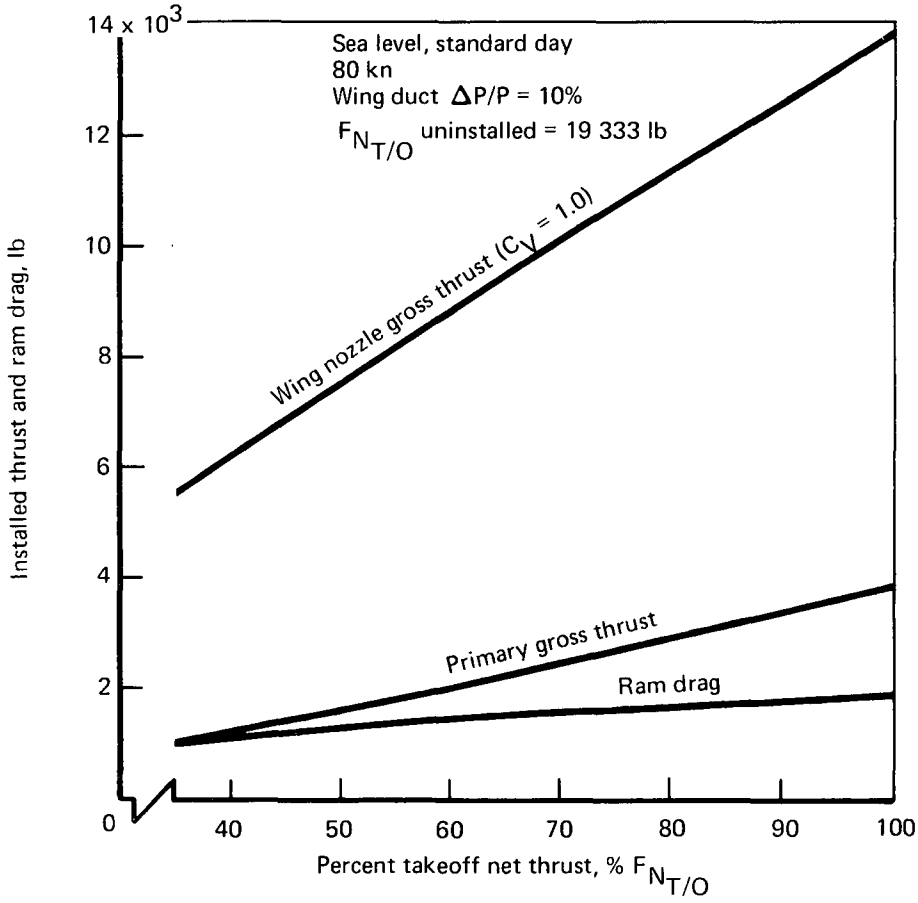

FIGURE 25.–APPROACH PERFORMANCE, INSTALLED–HP-1 CYCLE, FPR = 3.75

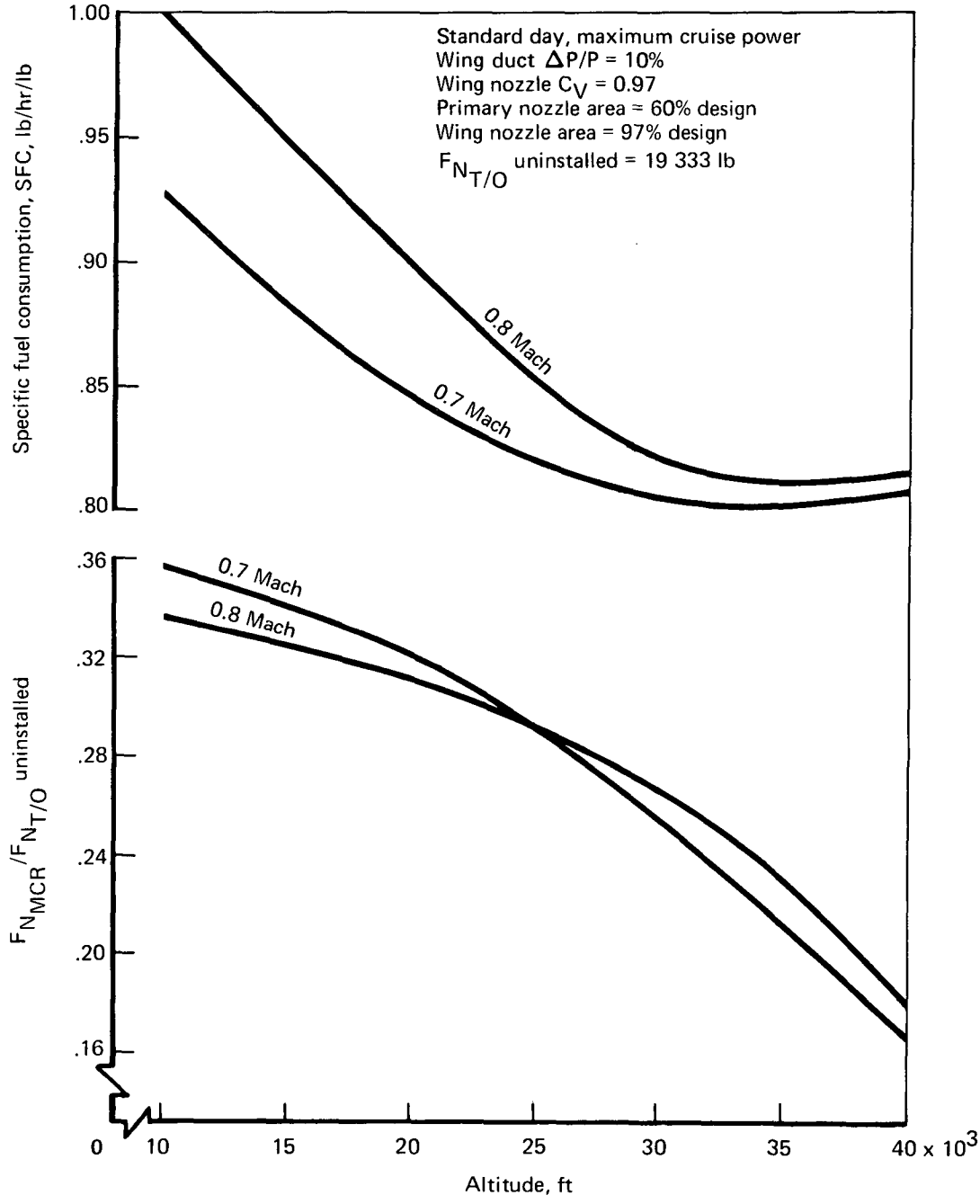

FIGURE 26.–CRUISE PERFORMANCE, INSTALLED–HP-1 CYCLE, FPR = 3.75

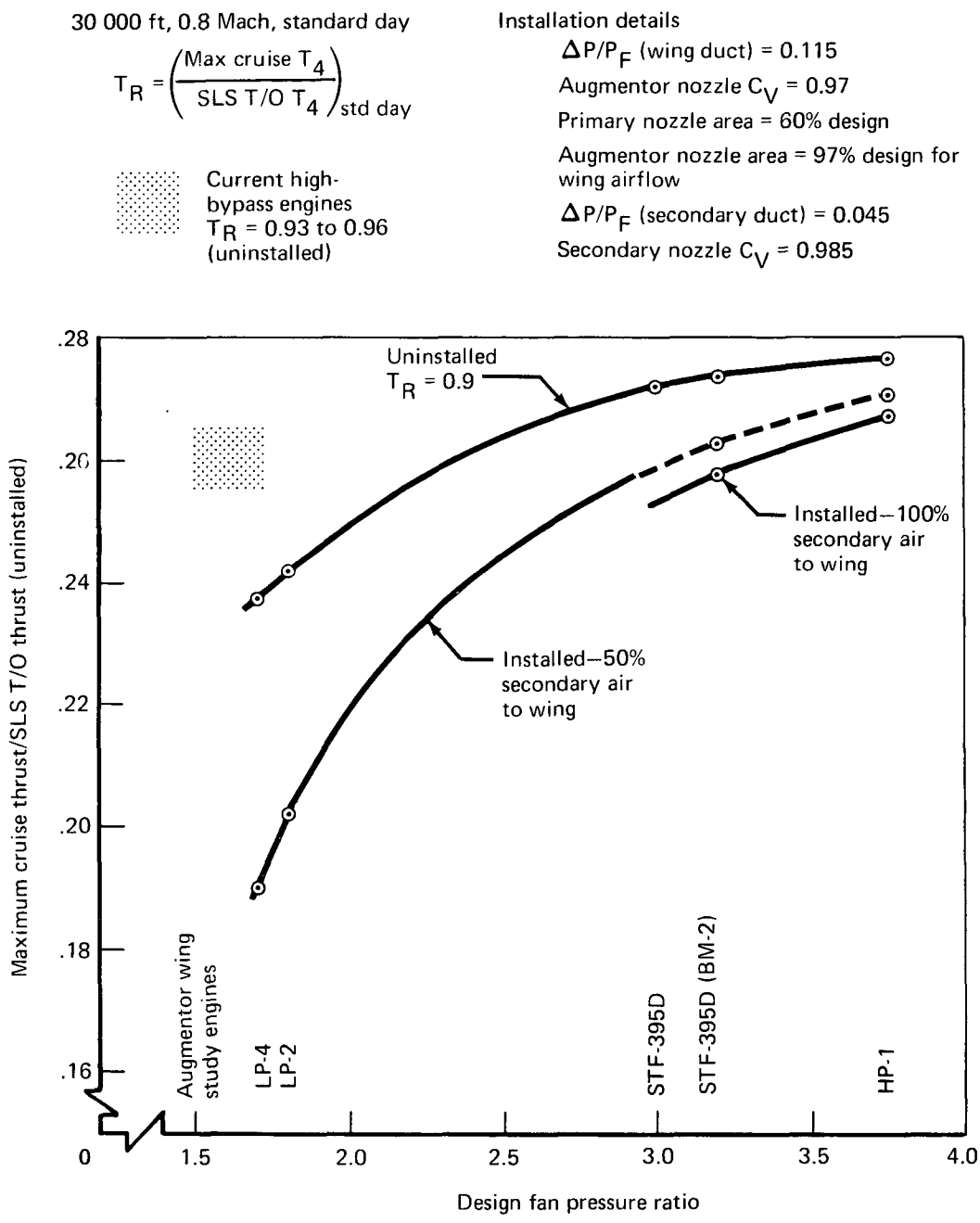

FIGURE 27.—CRUISE THRUST LAPSE VS DESIGN FAN PRESSURE RATIO

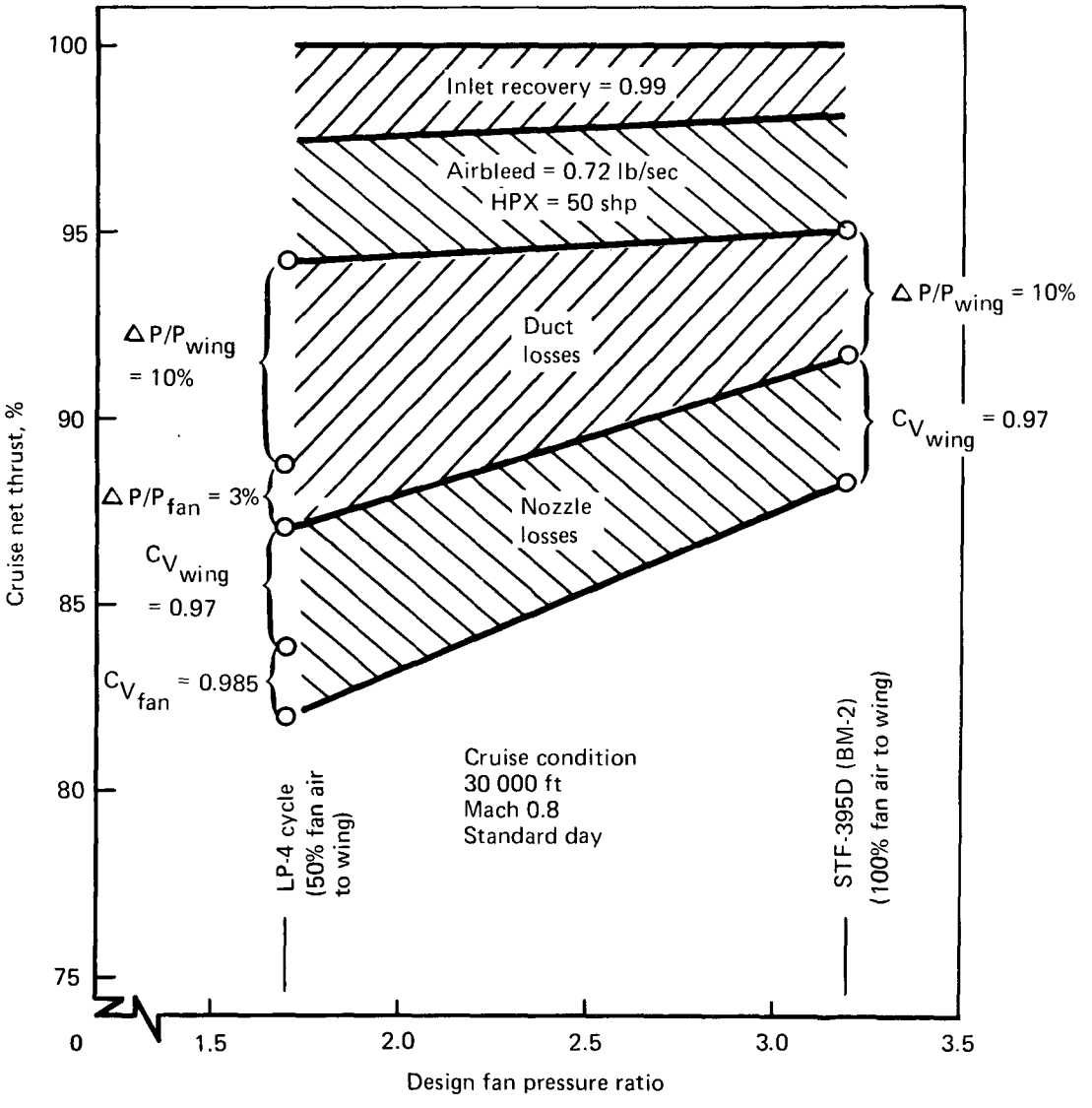

FIGURE 28.–EFFECT OF INSTALLATION LOSSES ON CRUISE NET THRUST

thrust loss differences can readily be seen to be caused primarily by duct pressure and nozzle losses. As shown in figure 28, the total net thrust loss due to all installation losses is approximately 12% for the high-pressure STF-395D (BM-2) cycle and 18% for the low-pressure LP-4 cycle.

The temperature ratio for the augmentor study engines was held the same (T_R = 0.9) as that of the basic engine, STF-395D, and was selected as appropriate for the STOL duty cycle. With low fan pressure ratio cycles the airplane tends to become cruise thrust limited, and a higher cruise-to-takeoff thrust ratio might be considered. The turbine temperature was held constant, however, because the complexity of takeoff/cruise temperature trades is beyond the scope of the present study.

By suitable turbine temperature trades a cruise thrust increase of 5% to 6% might be realized, but at the expense of takeoff thrust, which will also affect the engine thrust-to-weight ratio. It should be noted that the high performance losses due to the installation would still be evident. Referring to section 4.6, the gross weight of the airplane with the low-pressure system (LP-4) is approximately 40 000 lb higher than that of the airplane with high pressure. An increase in cruise thrust could reduce this only 3000 to 6000 lb.

All engine cycles were developed on the basis of the same high-pressure core. The LP compression ratio was held constant at 3.0 for the low-pressure cycles. For cycles with a fan pressure ratio greater than 3.0, the LP compressor pressure ratio was made equal to the fan pressure ratio. This changed the overall pressure ratio from 24 for the low-pressure cycles to 30 for the HP-1 cycle, as shown in figure 29a.

The bare engine weights for the cycles in table 2 may not be directly compared since the engine takeoff thrust size is also changing. The thrust-to-weight ratios are consistent, however, as shown by the curve on figure 29b. The weight of the HP-1 cycle is significantly higher due to the four-stage fan and increase in overall pressure ratio. Also, the STF-395D (BM-2) cycle requires one less LP turbine stage than the other cycles.

Installed cruise SFC is tabulated in table 2, and figure 29c presents curves of installed and uninstalled cruise SFC. From figure 29c the uninstalled SFC increases as the fan pressure ratio increases. The curve flattens out at the high fan pressure ratios because the increase in overall pressure ratio results in a more optimum match for these cycles.

As figure 29c shows, the installed curve crosses the uninstalled curve. The crossing occurs because closing the primary nozzle at cruise causes a proportionately larger decrease in SFC for the high fan pressure ratio cycles. The installed SFC curve also tends to flatten out because the low-pressure systems are more sensitive to a given amount of duct pressure loss.

4.3 ENGINE INSTALLATIONS

4.3.1 High-Pressure Installations

The high-pressure cruise blowing two-stream engine installation is similar to the two-stream installation shown in figure 4 of NASA CR-114284. Both use the modified STF-395D

(a) Overall pressure ratio

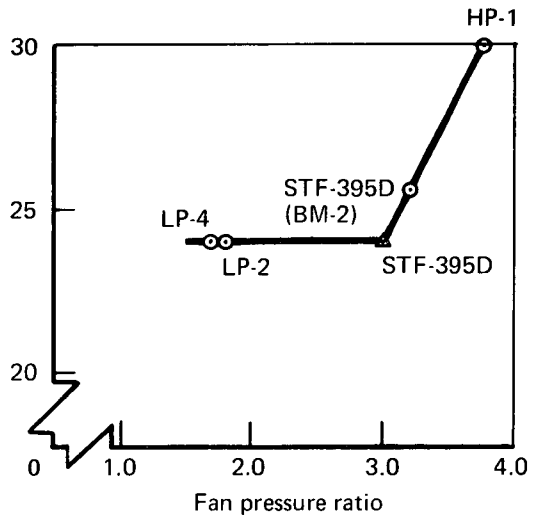

(b) Thrust/bare engine weight, T/W

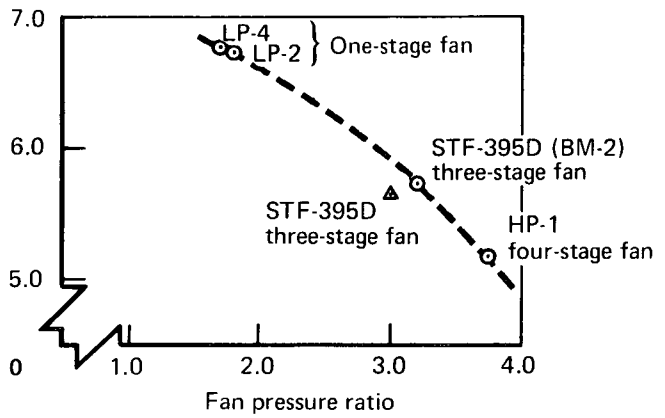

(c) Cruise SFC, lb/hr/lb

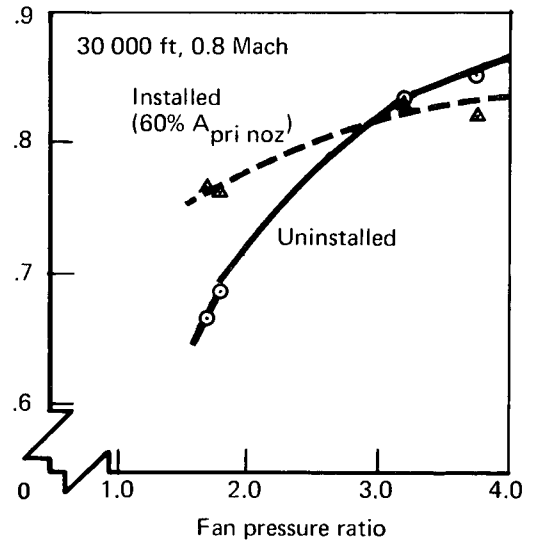

FIGURE 29.—CHARACTERISTICS OF AUGMENTOR WING STUDY ENGINES

engine cycle. The major difference is the elimination of diverter valves and separate cruise nozzles on the high-pressure cruise blowing system. The deletion of the diverter valve allows the engine-collector to wing-duct "wye" to be contoured for minimum pressure losses.

4.3.2 Low Pressure

The low-pressure cruise blowing system requires a separate fan nozzle because all of the fan air cannot be ducted into the wing while maintaining a reasonable wing loading. An overwing engine installation (fig. 30) was chosen for the low-pressure systems to make use of wing shielding to alleviate the aft fan noise associated with the separate fan nozzle. Fifty percent of the fan airflow is ducted to the wing, and the remaining fan air and primary exhaust exits through the overwing nacelle nozzle. The overwing installation also improves the engine and fuselage interference drag. The outboard engine is shifted outboard relative to the wing duct feeder spanwise location to further improve engine spacing. The overwing nacelle and strut for the LP-2 engine is approximately 33% heavier than the underwing installation for the high-pressure STF-395D (BM-2) engine at the same engine thrust. This is about 3000 lb OWE per airplane for the same thrust.

4.3.3 Thrust Vectored Nacelle

Vectoring of the thrust not ducted to the wing was briefly investigated to determine the effect on airplane performance. A hooded or clamshell combination vectoring thrust reverser as shown on figure 31 was chosen as a representative concept. Figure 32 shows the effect of vector angle on takeoff field length with a 50% fan air to wing split and a 5.5 aspect ratio. The optimum vector angle is about 15°, and vectoring reduces the T/W requirement for a 2000-ft field length by 0.02 (3.5%) at a wing loading of 100 lb/sq ft and by 0.007 at a wing loading of 70 lb/sq ft. Similar results are obtained at a 7.5 aspect ratio (fig. 33). Since the cruise thrust requirement, shown on figures 32 and 33, establishes the engine size for wing loadings less than 100 lb/sq ft, the reduction in takeoff thrust with vectoring is not useful. Any thrust losses caused by the vectoring mechanism would increase the cruise thrust requirement still further. The thrust vectoring would, however, measurably improve landing performance and glide slope control by allowing high engine thrust and high C_J in the augmentor flap. The thrust vectoring would increase the engine jet noise by about 3 PNdB, and increases in landing power would add to the approach noise. The weight of the concept shown in figure 31 is estimated to be about the same as that of the overwing nacelle (fig. 30), but it is not likely that the wing strength and flutter requirements for the vectored thrust nacelle can be achieved within a practical weight penalty on the 20%-50% chord wing box.

4.4 DUCT PERFORMANCE EVALUATION

4.4.1 Duct Performance Comparisons

Augmentor wing installed thrust depends primarily on available wing duct volume, engine cycle fan pressure ratio, and wing duct flow velocity (Mach) at critical wing duct stations. Available duct volume in terms of the resultant blowing nozzle area per square foot of wing

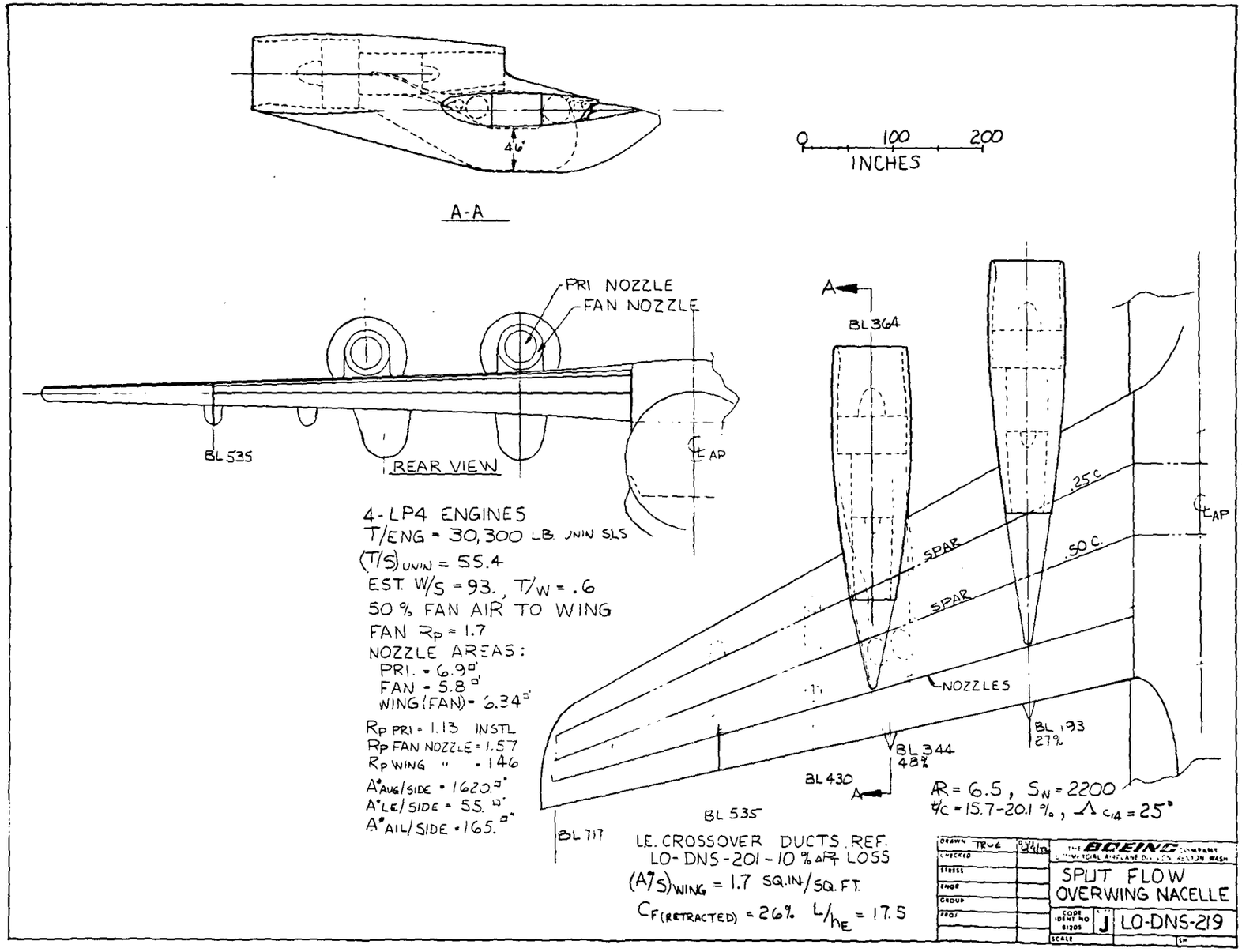

FIGURE 30.—LO-DNS-219—SPLIT FLOW, OVERWING NACELLE

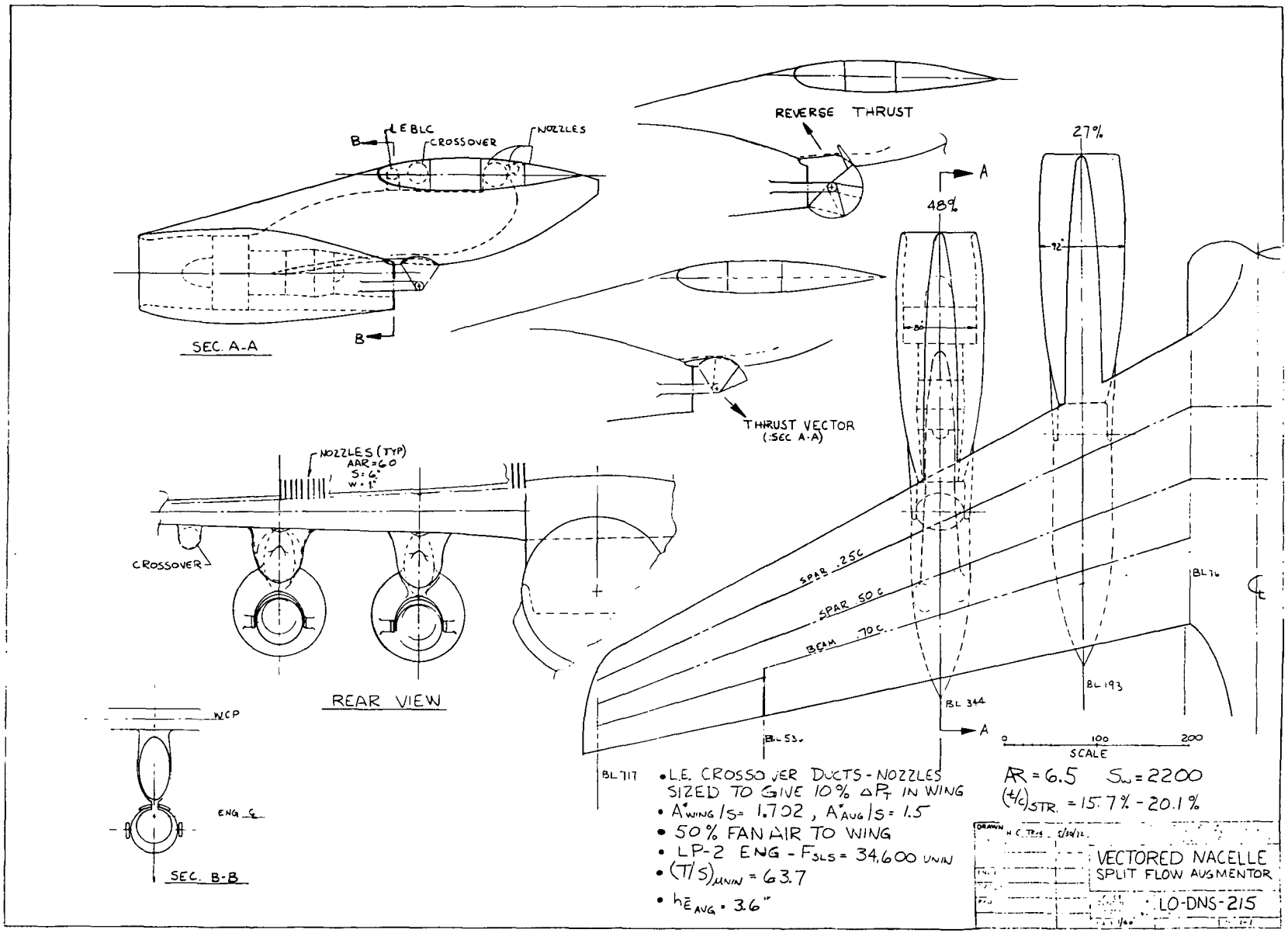

FIGURE 31.—LO-DNS-215, THRUST-VECTORING NACELLE INSTALLATION

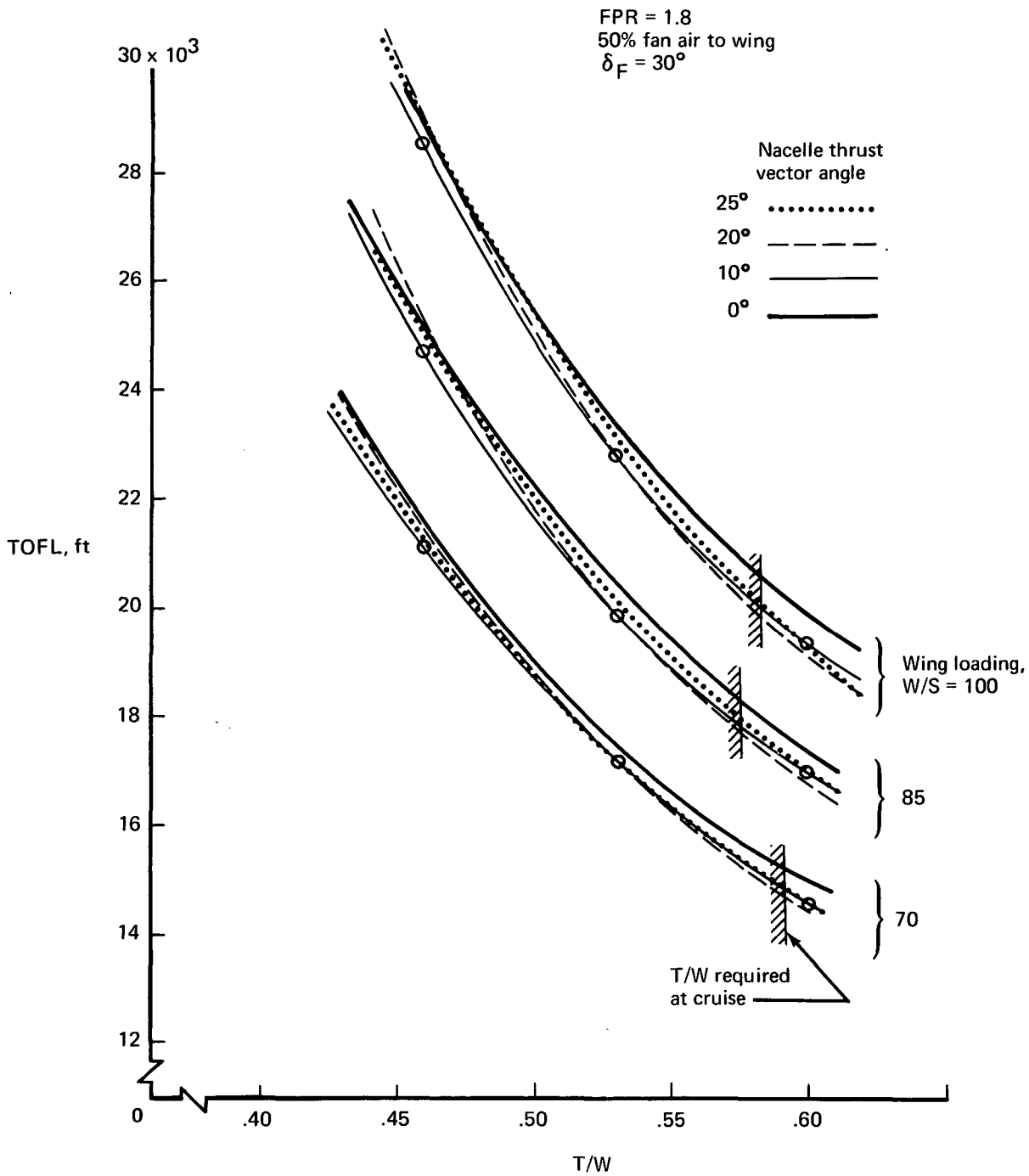

FIGURE 32.–EFFECT OF VECTORED NACELLE THRUST ON TAKEOFF PERFORMANCE, AR = 5.5

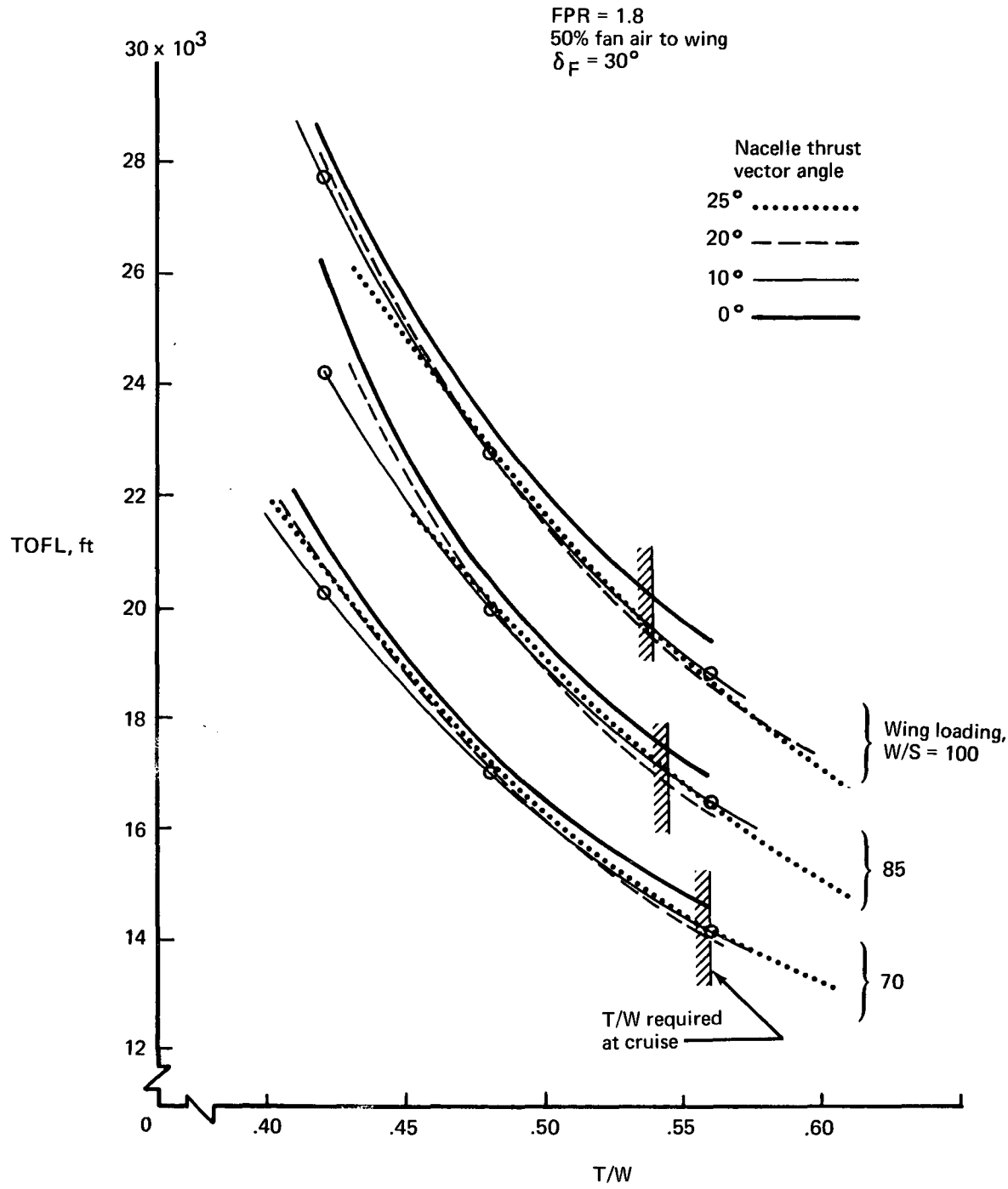

FIGURE 33.—EFFECT OF VECTORED NACELLE THRUST ON TAKEOFF PERFORMANCE, AR = 7.5

area (A_N/S) plotted against wing aspect ratio for wing thicknesses of 0.157_{outbd}; 0.201_{SOB} and 0.132;0.176 is shown in figure 34. Available duct volume was determined by the design layouts described in section 4.1.2 for the duct system configurations.

The effect of augmentor duct pressure loss on fan flow thrust loss relative to fan pressure ratio is shown in figure 35. This study shows that ducting thrust loss relative to the engine FPR is considerably more sensitive to duct $\Delta P/P_F$ at low than at high FPR. This characteristic indicates that high-pressure air can be transported much more efficiently than low-pressure air with a fixed duct configuration.

The effect of engine cycle fan pressure ratio on installed thrust per square inch of wing nozzle area (T/A_N) is shown in figure 36 for a duct pressure loss $\Delta P/P_F$ = 10%. Combining these data with those of figure 34 results in wing thrust loading capability $(T/S)_{in}$ as shown in figure 37. Using a wing loading requirement of W/S = 80 lb/sq ft as a criterion for possible airplane design point studies, the data shown in figure 37 indicate engine cycles which could provide acceptable airplane designs.

The LP-2 and LP-4 engine cycles (FPR = 1.8 and 1.7, respectively) cannot meet 80 lb/sq ft wing loading with these ducting configurations with 100% fan flow ducted to the wing.

Thrust loading $(T/S)_{in}$ can be increased considerably by ducting only 50% fan air to the wing. The other 50% would exhaust through a nacelle nozzle either below or above the wing using this concept. Thrust loading $(T/S)_{in}$ for the LP-2 and LP-4 engine cycles with leading edge cross ducts is shown in figure 38. These data indicate that 80 lb/sq ft wing loading capability is attainable, although because of the fan nozzle noise the split flow design would result in higher airplane noise levels than a 100% ducted configuration at the same fan pressure ratio.

4.4.2 Computerized Performance Analysis

Pressure loss analysis to evaluate wing thrust distribution as a function of wing nozzle area can best be accomplished on a digital computer, since an iterative analysis involving several variables is required.

A duct system performance analysis was computed for the LP-2 engine cycle (FPR = 1.8) using the independent duct system with leading edge cross ducts (fig. 11). The analysis assumed a scaleable engine size for a fixed cycle. The augmentor nozzle area $(A_N/S)_{aug}$ was varied as the independent variable, with fan flow pressure distribution and thrust distribution as dependent variables. The duct system pressure loss coefficients used in the analysis are shown in figure 39. The analysis further assumes a wing blowing distribution based on 88% augmentor flow, 9% aileron flow, and 3% leading edge flow.

Augmentor duct system pressure loss relative to wing nozzle area is shown in figure 40. The LP-2 total engine installed thrust (T/A_N) and installed wing thrust (F_W/A_N) are shown in figure 41 relative to wing nozzle area (A_N/S). Combining the data of figures 40 and 41 results in the thrust loading $(T/S)_{in}$ capability of the LP-2 engine cycle with 50% fan air ducted to the wing (fig. 42).

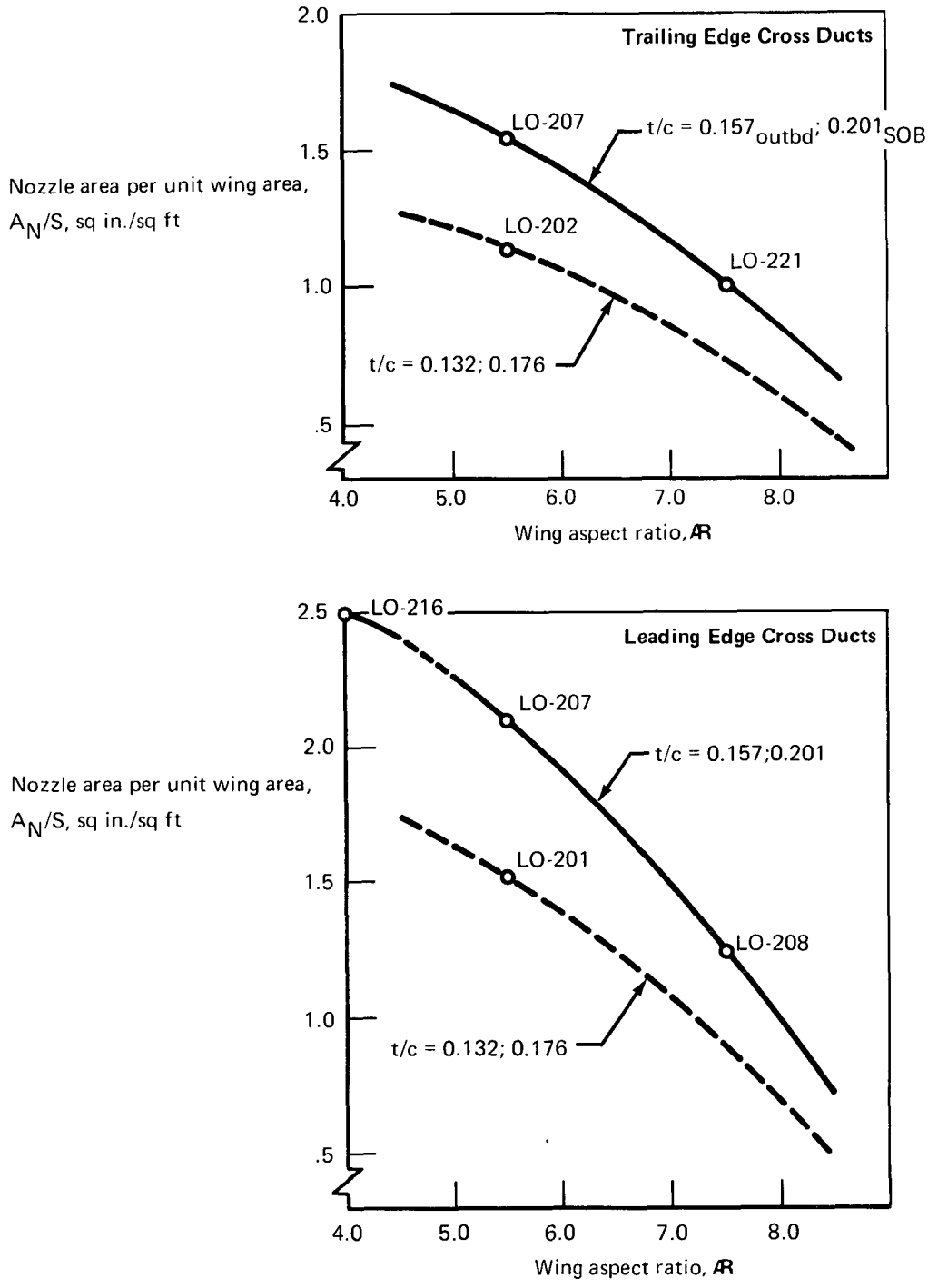

FIGURE 34.—AVAILABLE NOZZLE AREA CRUISE BLOWING SYSTEMS, DUCT FLOW LOSS, $\Delta P/P_F$ = 10%

E

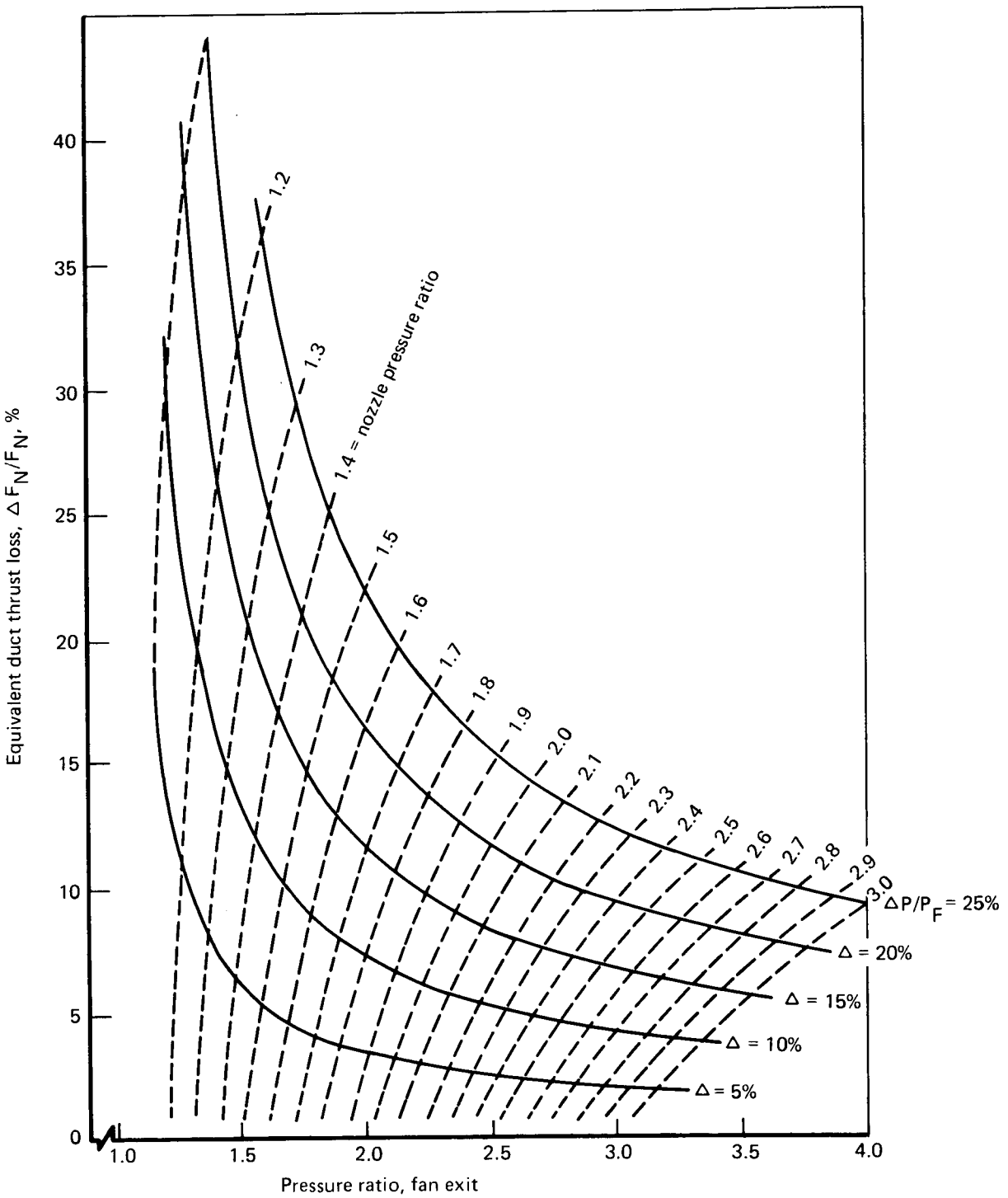

FIGURE 35.—PRESSURE LOSS—THRUST LOSS CORRELATION

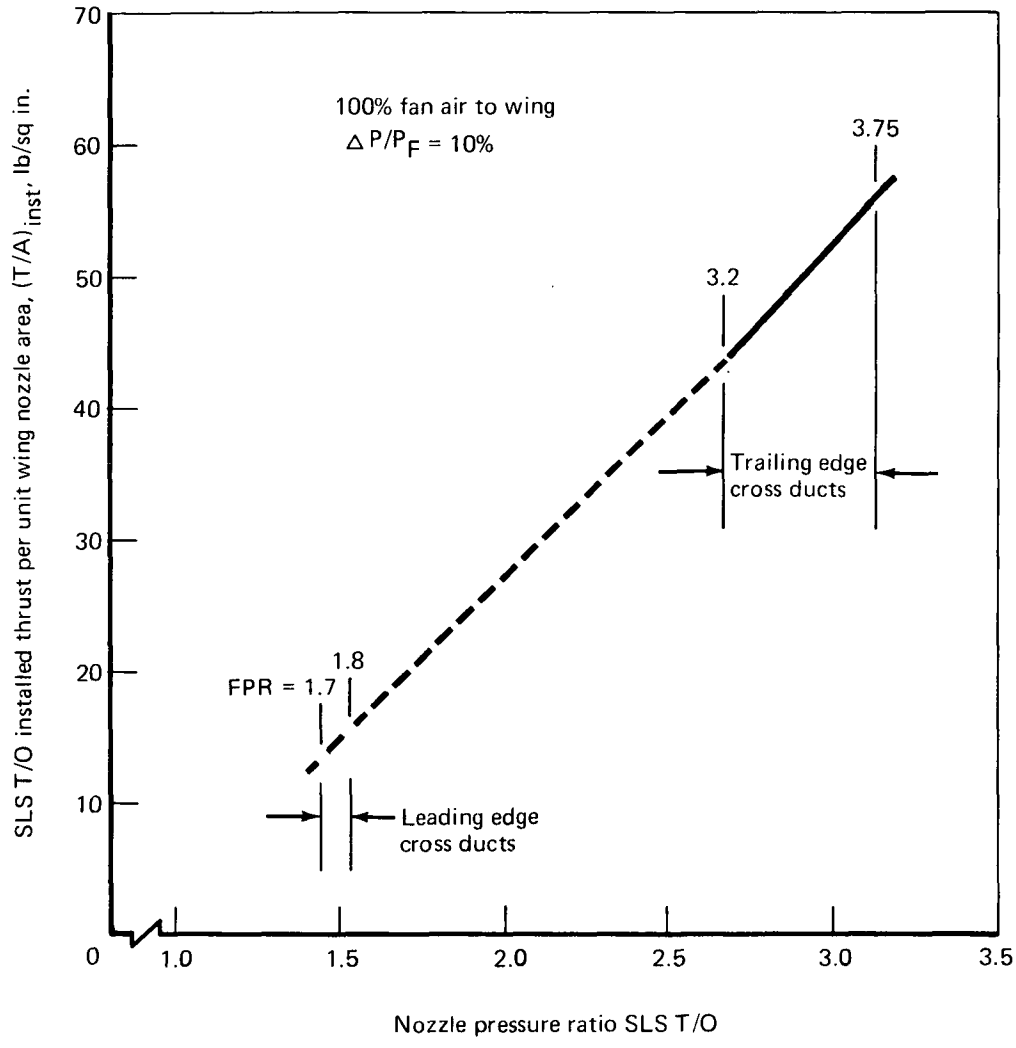

FIGURE 36.—INSTALLED THRUST PER UNIT WING NOZZLE AREA AS FUNCTION OF PRESSURE RATIO

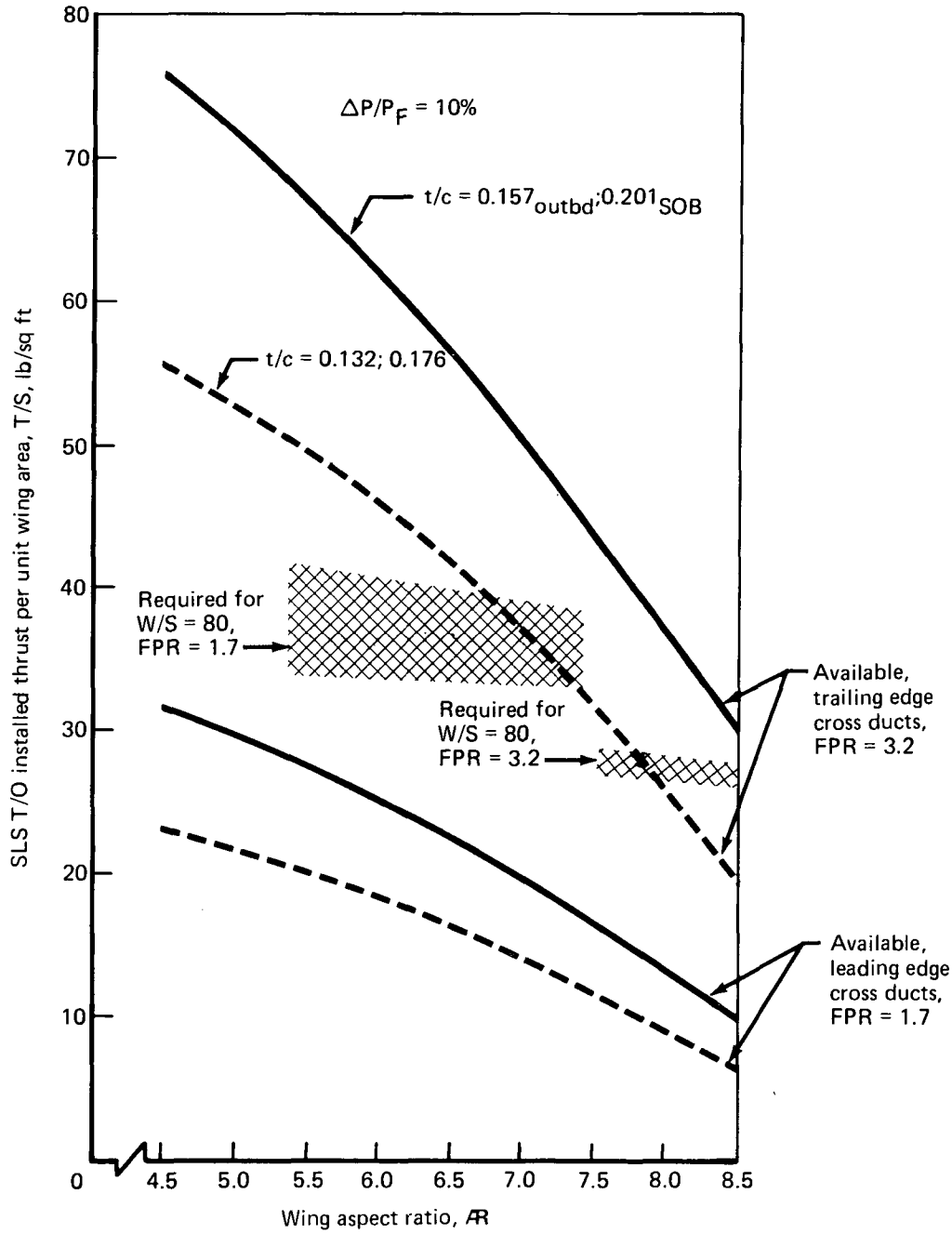

FIGURE 37.–INSTALLED THRUST PER UNIT WING AREA AS FUNCTION OF WING ASPECT RATIO, t/c, AND CROSS DUCT CONFIGURATION, 100% FAN AIR TO WING

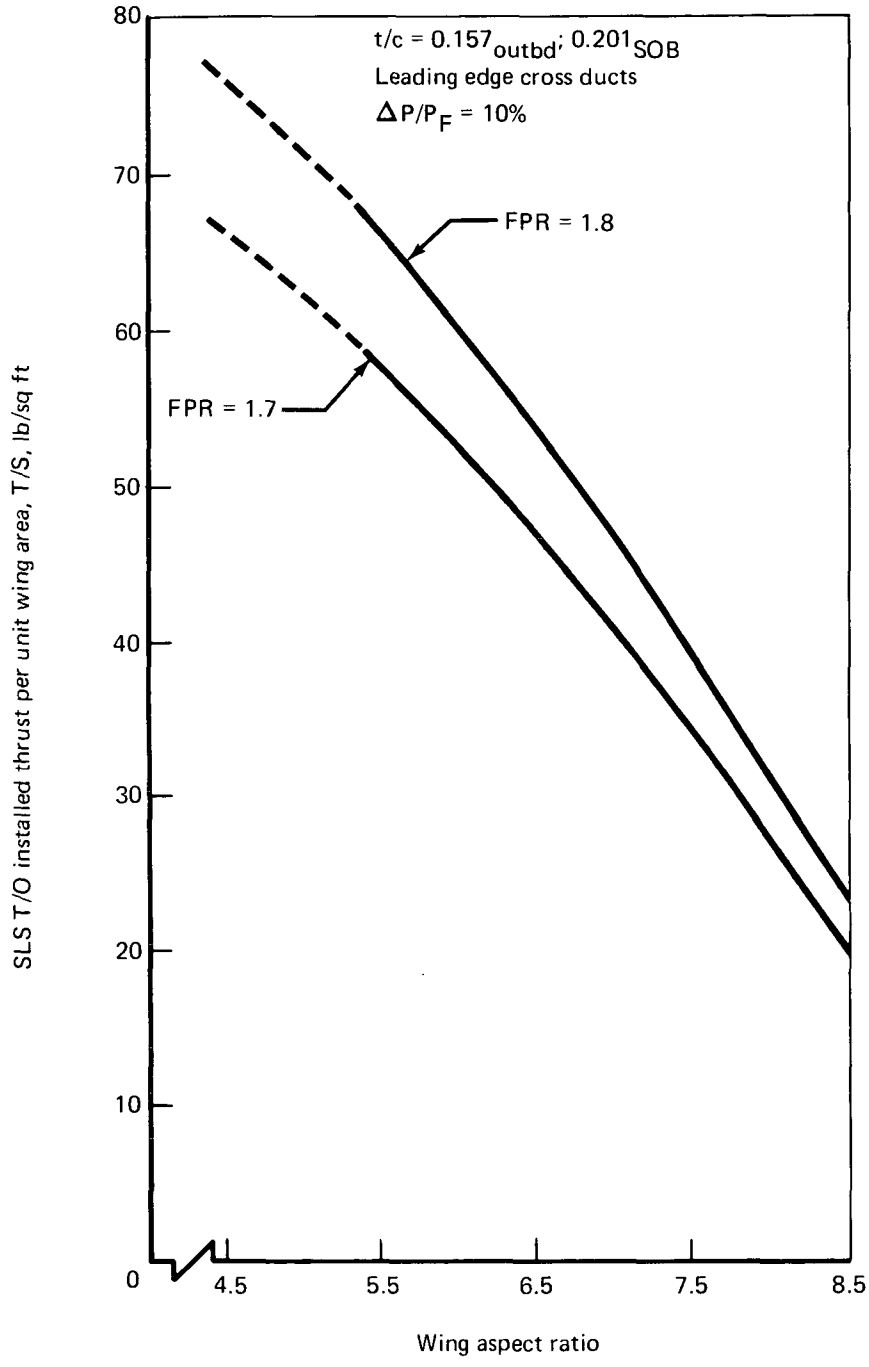

FIGURE 38.–INSTALLED THRUST PER UNIT WING AREA AS FUNCTION OF WING ASPECT RATIO, 50% FAN AIR TO WING

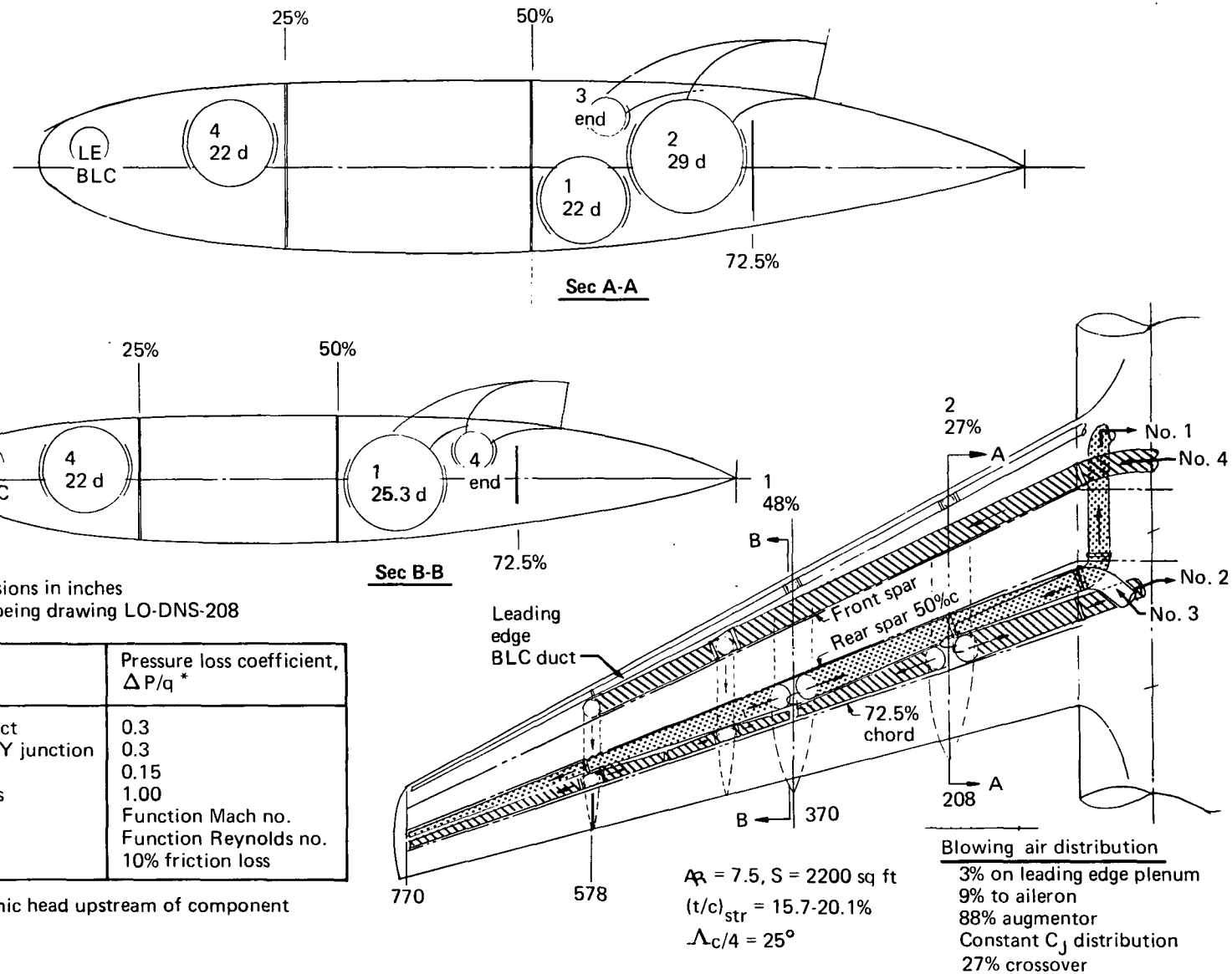

Dimensions in inches
Ref. Boeing drawing LO-DNS-208

Component	Pressure loss coefficient, $\Delta P/q$ *
Fan collector duct	0.3
Strut-wing duct Y junction	0.3
Flex joints	0.15
Body cross ducts	1.00
Nozzle off-takes	Function Mach no.
Friction	Function Reynolds no.
Roughness	10% friction loss

*q = flow dynamic head upstream of component

FIGURE 39.—AUGMENTOR DUCTING SYSTEM—LEADING EDGE CROSS DUCTS

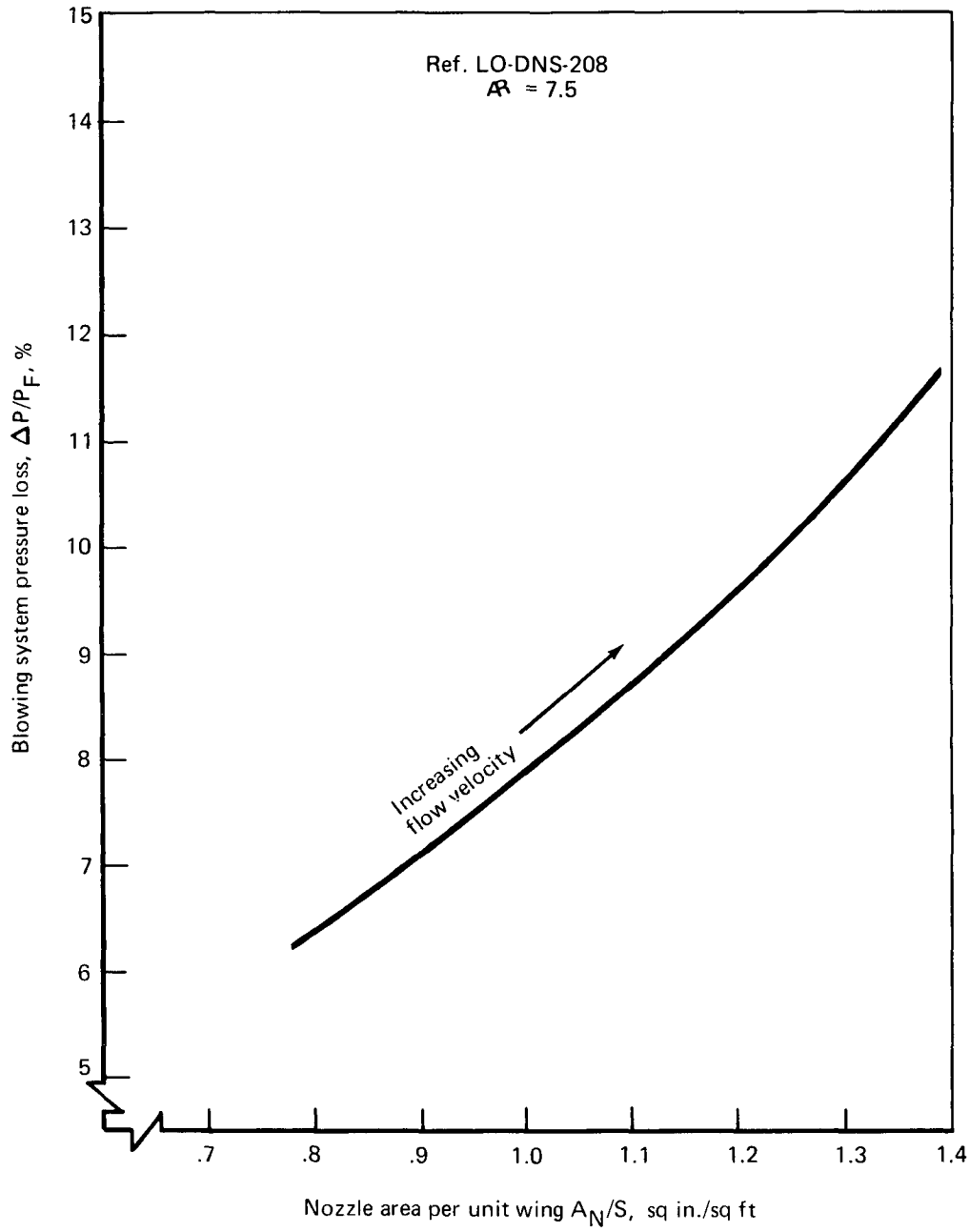

FIGURE 40.–PRESSURE LOSS CHARACTERISTICS, LEADING EDGE CROSS DUCT SYSTEM

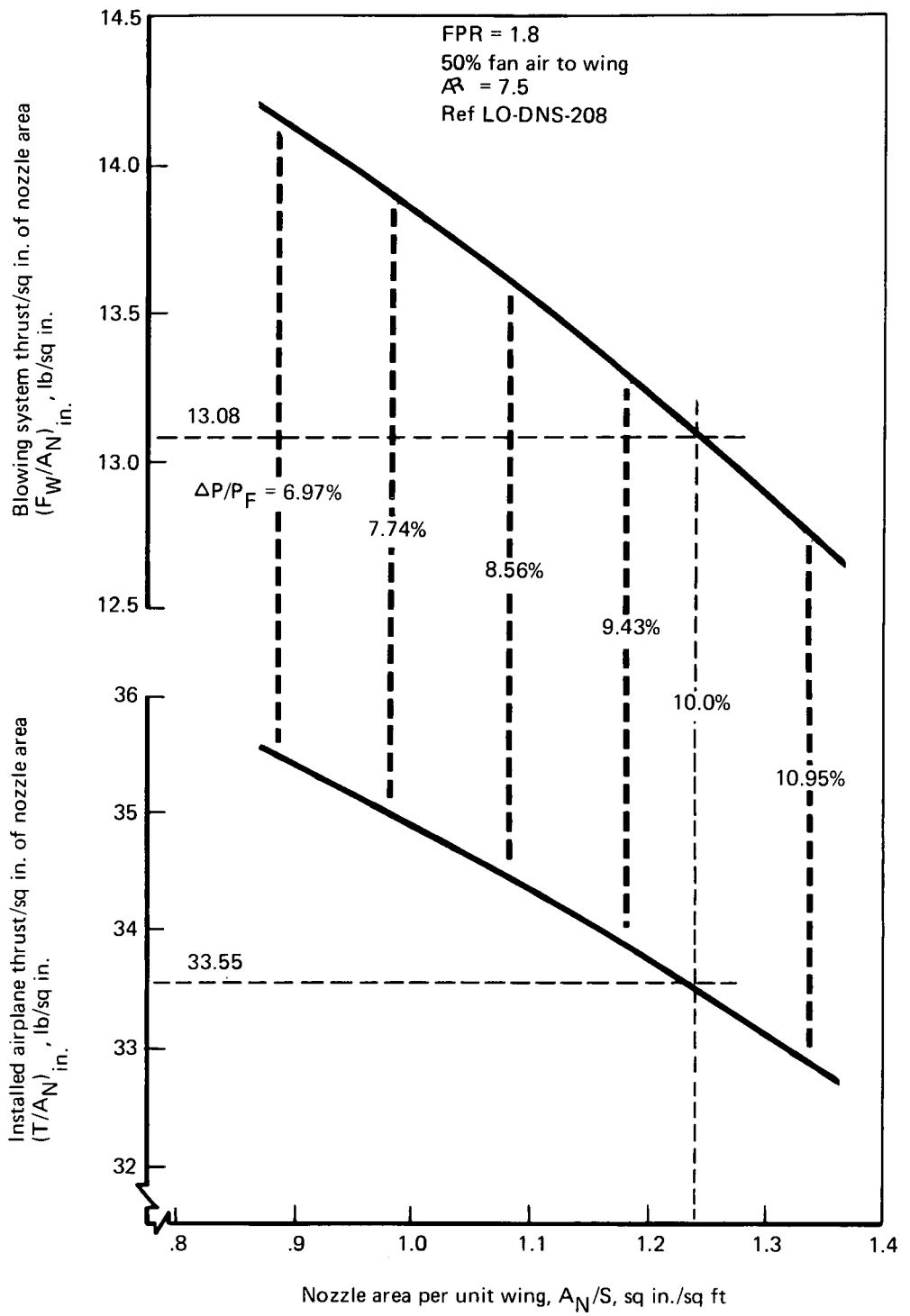

FIGURE 41.—BLOWING THRUST AND AIRPLANE INSTALLED THRUST CHARACTERISTICS, LEADING EDGE CROSS DUCT SYSTEM

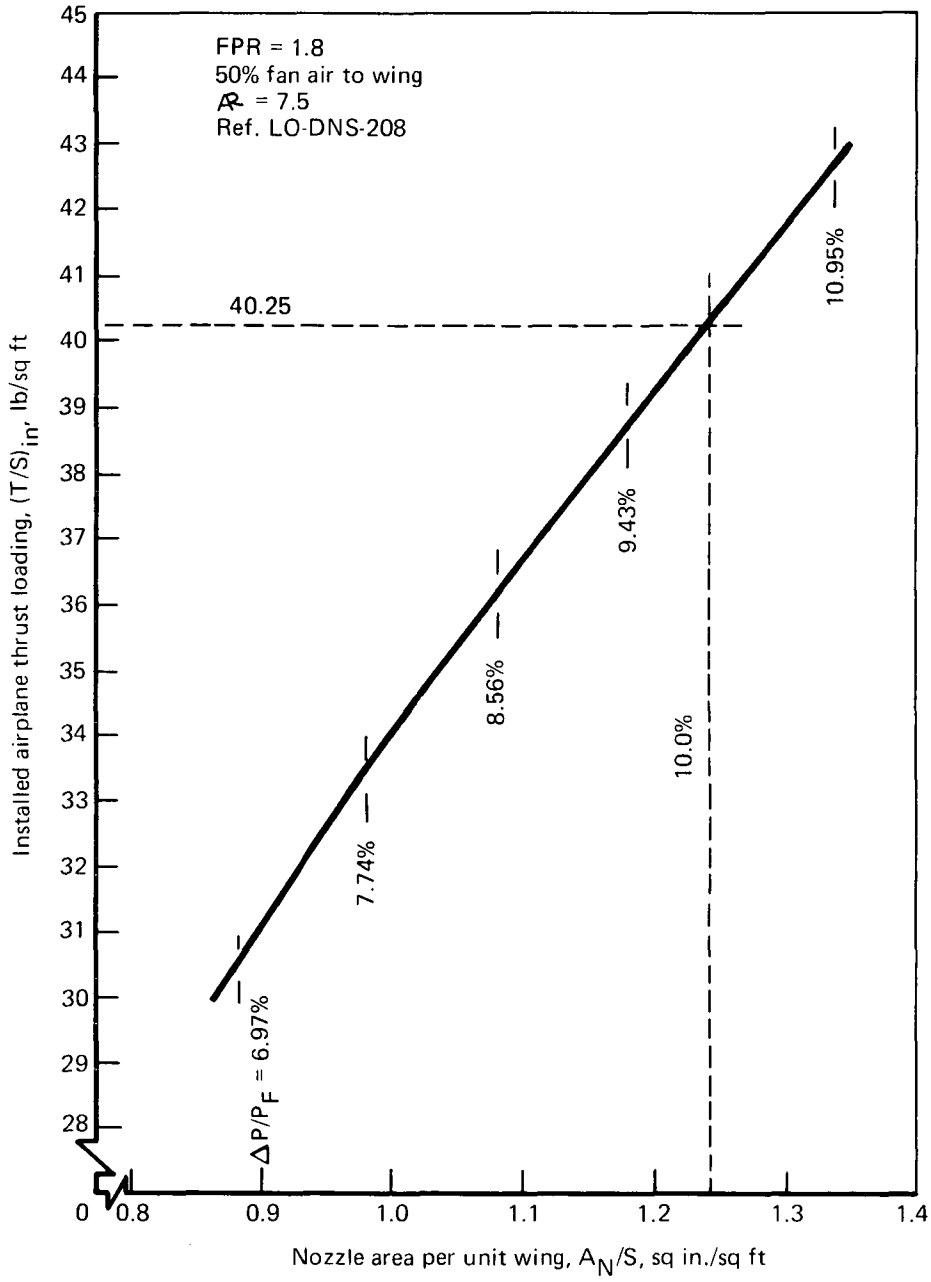

FIGURE 42.–INSTALLED AIRPLANE THRUST LOADING, LEADING EDGE CROSS DUCT SYSTEM

The same analysis was conducted on a trailing edge cross duct configuration (fig. 43), using the STF-395D (BM-1) engine cycle (FPR = 3.2) based on ducting 100% fan air to the wing. This analysis was based on the same assumptions used for the leading edge cross duct system analysis. The pressure loss characteristic for this duct system is shown in figure 44. Total installed thrust (T/A_N) and installed wing thrust (F_W/A_N) relative to wing nozzle area (A_N/S) and $\Delta P/P_F$ is shown in figure 45. Thrust loading $(T/S)_{in}$ relative to A_N/S and $\Delta P/P_F$ is shown in figure 46.

The duct volume capacities (A_N/S) shown in figure 34 can be applied to the computer results for $\Delta P/P_F = 10\%$ to determine uninstalled airplane thrust $(T/S)_{un}$ relative to aspect ratio and wing thickness for the LP-2 and STF-395D (BM-1) engine cycles. The results, shown in figures 47 and 48, were used in the airplane sizing analyses discussed in section 4.6.2.

4.5 AUGMENTOR SYSTEM DESIGN INTEGRATION

4.5.1 Augmentor Performance

The thrust augmentation capability of an augmentor is mainly a function of the ratio of the flap length to equivalent slot nozzle height or nozzle area ($L/h_{\overline{E}}$), and the nozzle array area ratio (AAR). Figure 49 shows the basic relationship of static augmentation (ϕ_S) with $L/h_{\overline{E}}$ and AAR. This figure is based on the reference (CR-114284) data and was adjusted for the estimated effects of cruise blowing. The nozzles on top of the wing are not volume critical and give good augmentor nozzle ventilation, so the nozzle ventilation correction (L_N/H_A) described in NASA CR-114284, section 4.2.2, would not be applicable. Figure 49 was derived from the 172-lobe nozzle test of the reference study ($L/h_{\overline{E}} = 55$) as follows:

CR-114284 data	ϕ_S =	1.48	172-lobe, long extended nozzle
		-0.03	Lower cruise blowing fairing
		-0.03	Screech shields
		-0.02	Reduced breakup of tall lobes compared with 172 lobe
		1.40	
1978 improvement		+0.05	
	ϕ_S =	1.45	($L/h_{\overline{E}} = 55$, AAR = 8)

The augmentor mixing length ($L/h_{\overline{E}}$) is a function of the augmentor extended flap chord and the nozzle area in the augmentor per unit wing area, A_A/S (see fig. 50). For the cruise blowing rigid duct systems, $A_A/S = 0.88\ A_N/S$ since 12% of the airflow goes to the leading edge and ailerons.

Figure 50 can be cross plotted with figure 49 to yield ϕ_S as a function of A_N/S, as shown in figure 51. Low-pressure augmentors tend to have high A_N/S values, since a large-capacity duct system is required to obtain enough thrust in the wing for reasonable C_J and wing loadings. Low-pressure augmentors have typical A_N/S values of about 1.5 to 2.0 for a 50% fan air

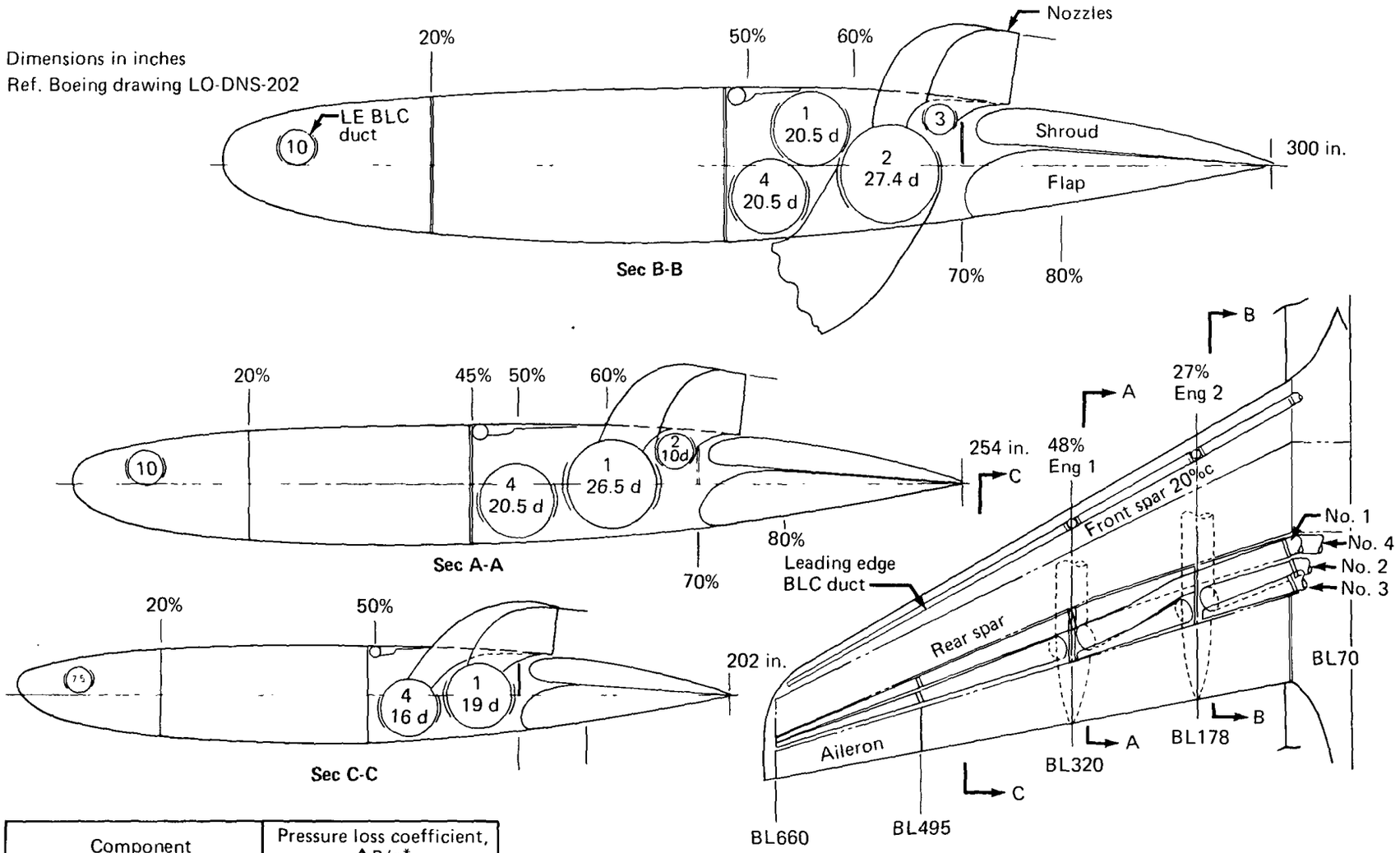

Component	Pressure loss coefficient, $\Delta P/q^*$
Fan collector duct	0.3
Strut-wing duct Y junction	0.3
Flex joint	0.15
Body cross ducts	1.00
Nozzle off-take	Function Mach no.
Friction	Function Reynolds no.
Roughness	10% friction loss

$\mathcal{A}$ = 5.5
S = 2200 sq ft
t/c_{str} = 13.2–17.6%
$\Lambda_{c/4}$ = 25°

Blowing air distribution

3% on leading edge plenum
9% to aileron
88% augmentor
Constant C_J distribution
27% crossover

*q = flow dynamic head upstream of component.

FIGURE 43.–AUGMENTOR DUCTING SYSTEM–TRAILING EDGE CROSS DUCTS

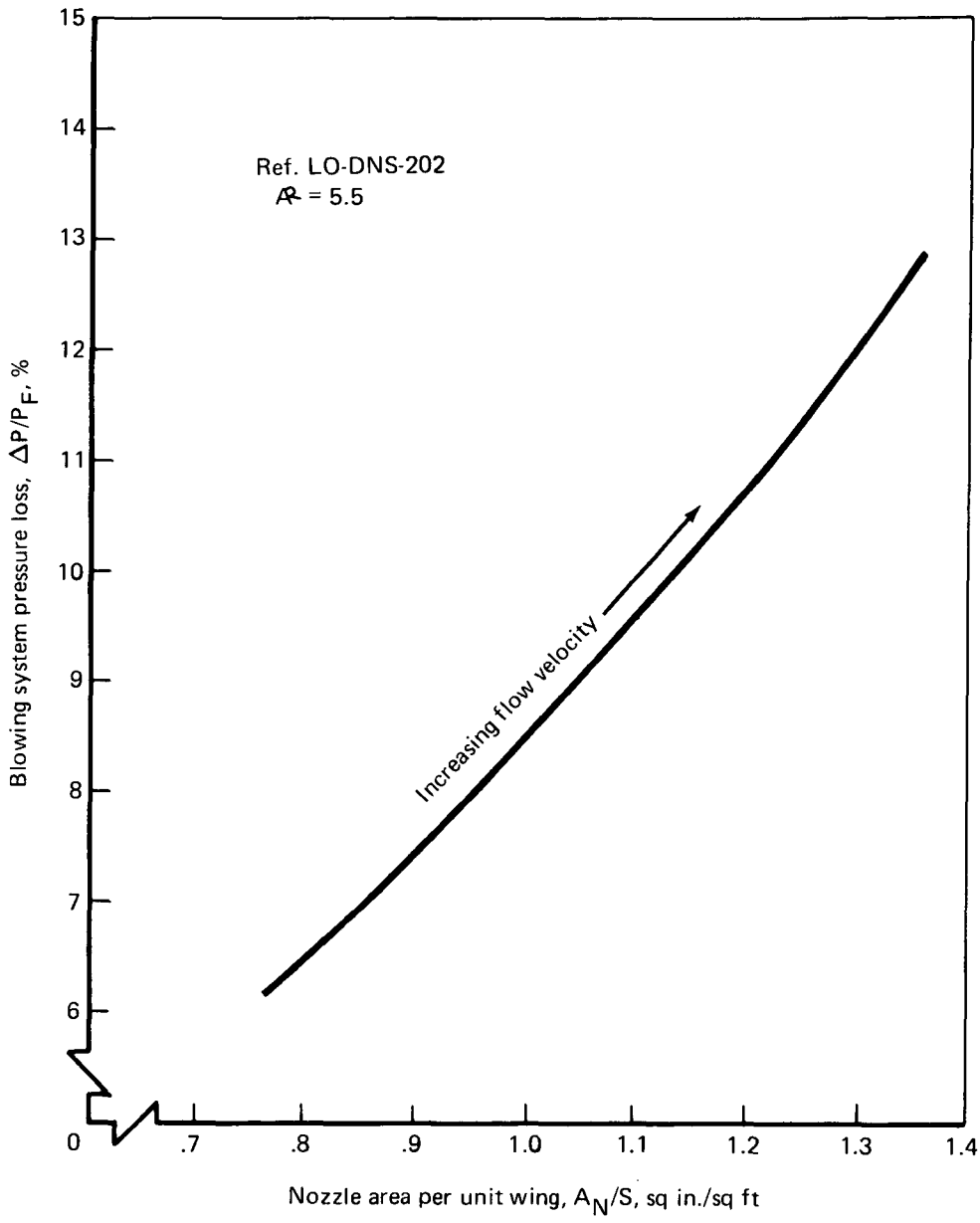

FIGURE 44.–PRESSURE LOSS CHARACTERISTIC, TRAILING EDGE CROSS DUCT SYSTEM

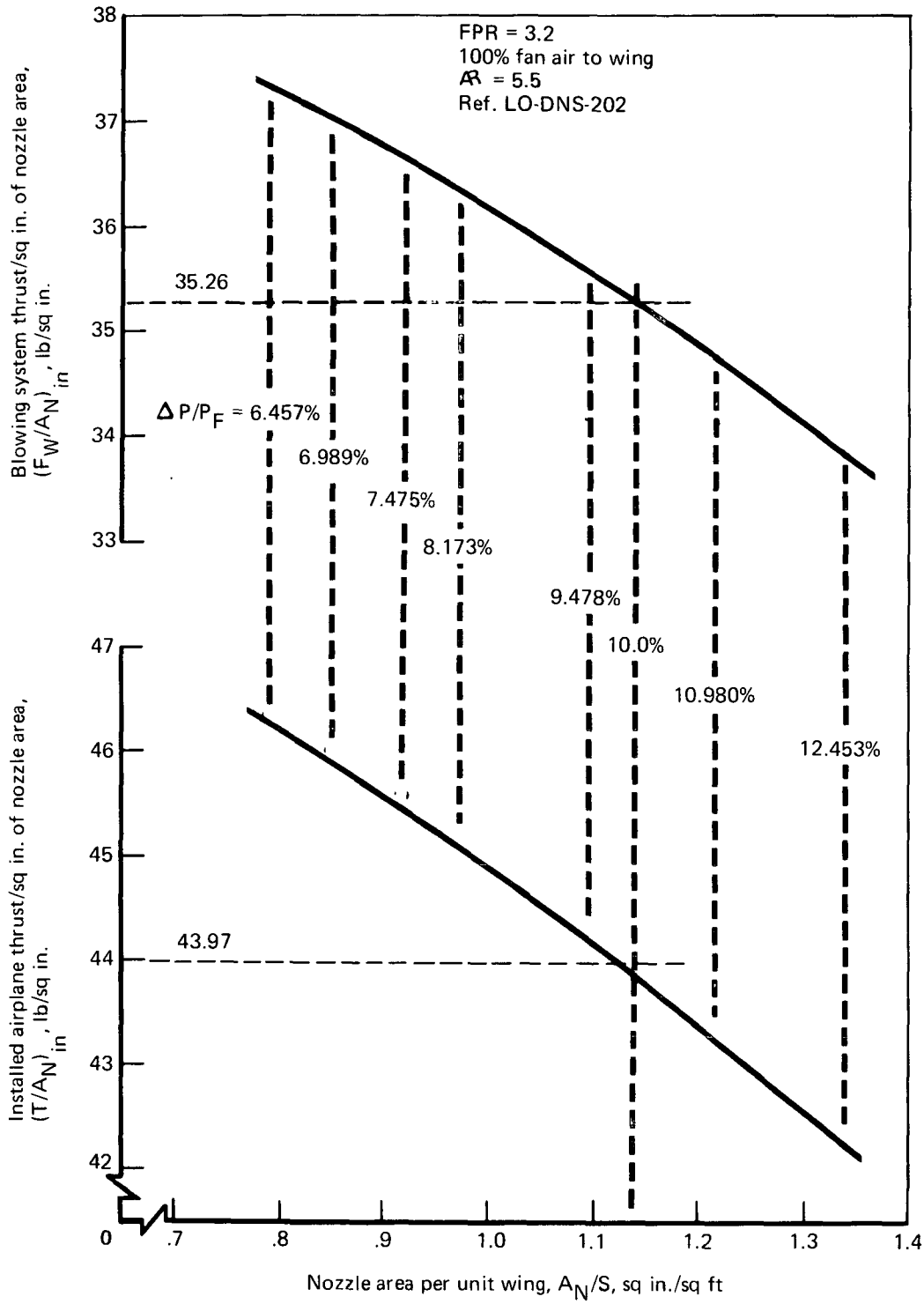

FIGURE 45.—BLOWING THRUST AND AIRPLANE INSTALLED THRUST, CHARACTERISTICS, TRAILING EDGE CROSS DUCT SYSTEM

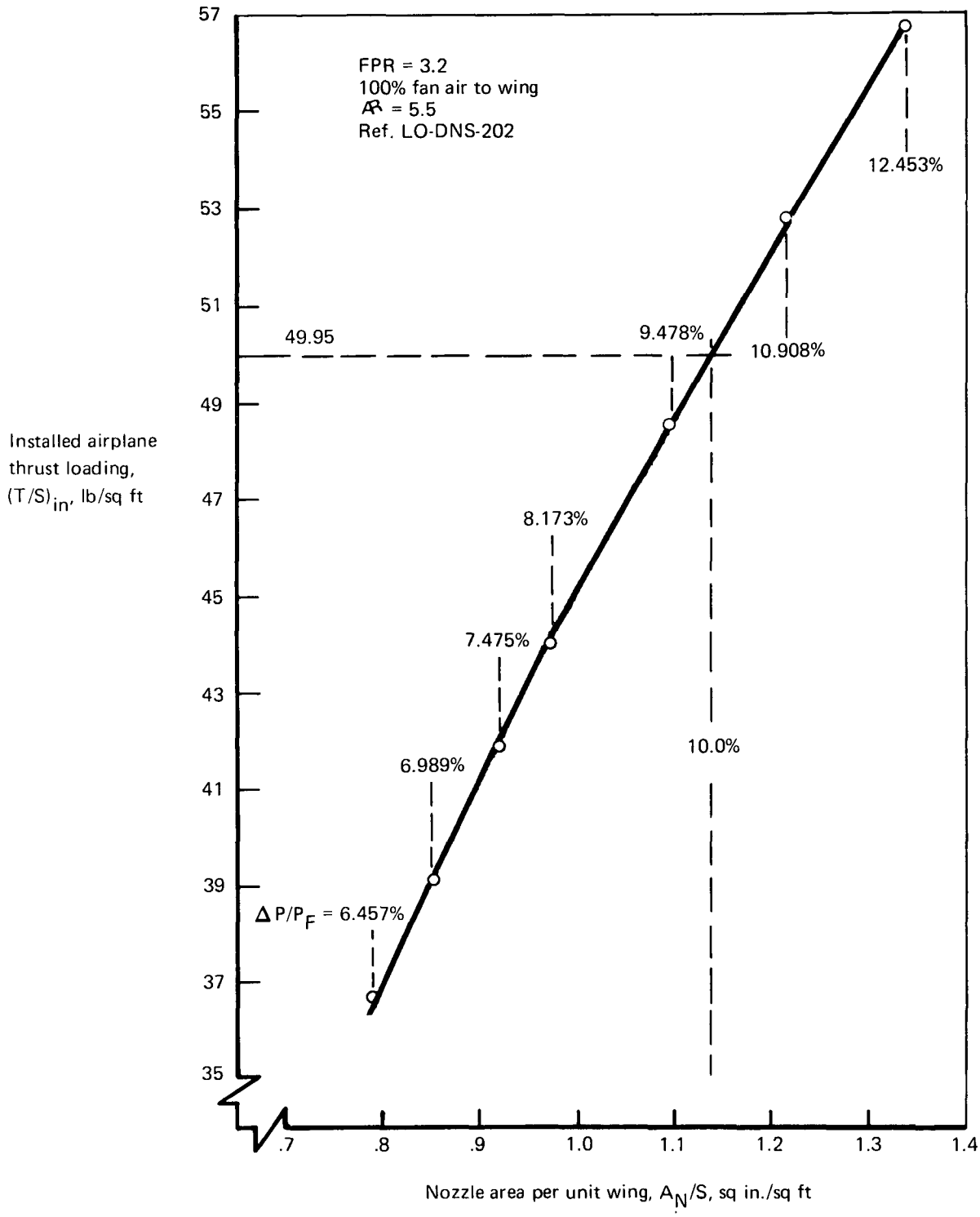

FIGURE 46.—INSTALLED AIRPLANE THRUST LOADING, TRAILING EDGE CROSS DUCT SYSTEM, FPR = 3.2

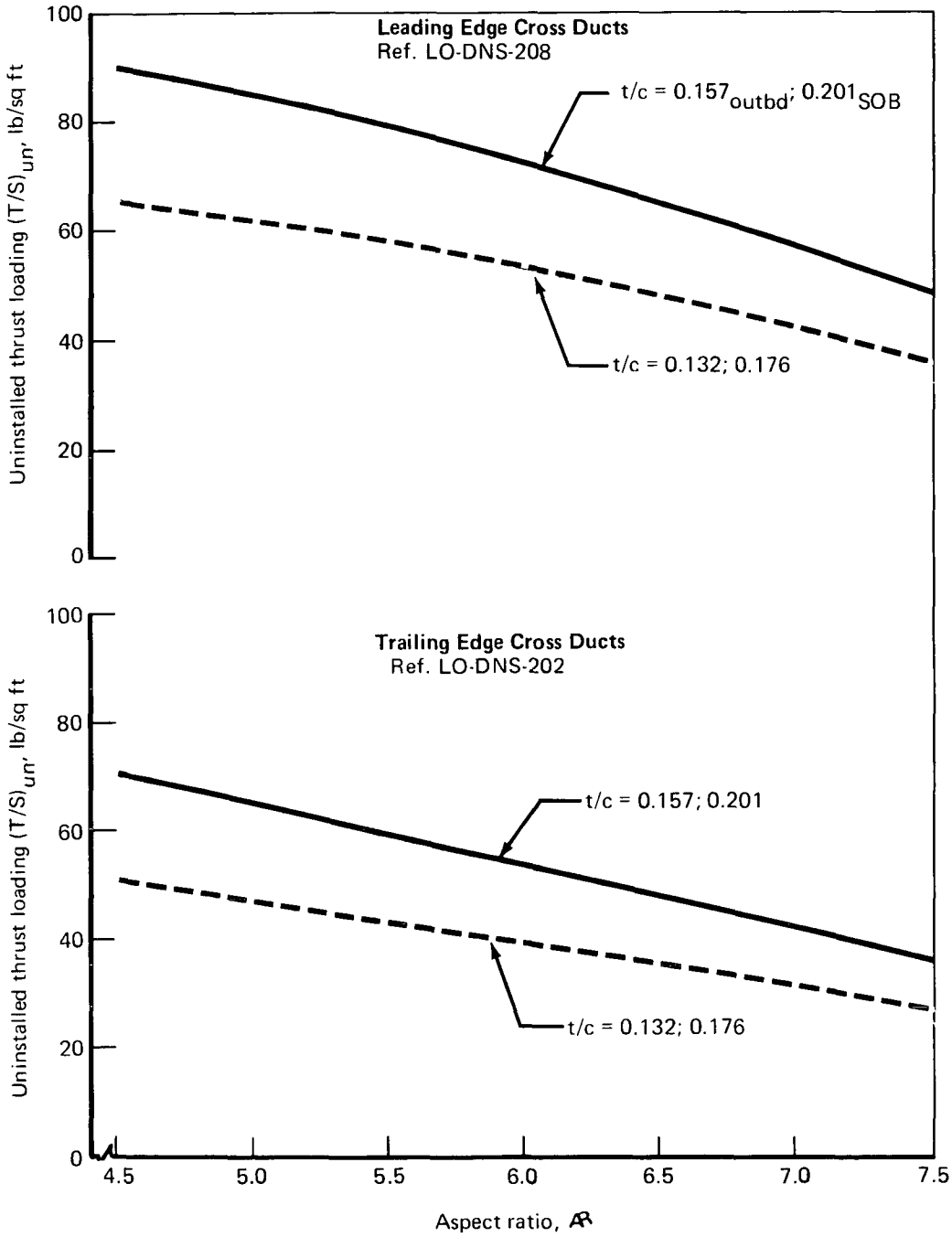

FIGURE 47--WING PLANFORM AND THICKNESS EFFECT ON UNINSTALLED THRUST LOADING, FPR = 1.8, $\Delta P/P_F$ = 10%, 50% FAN AIR TO WING

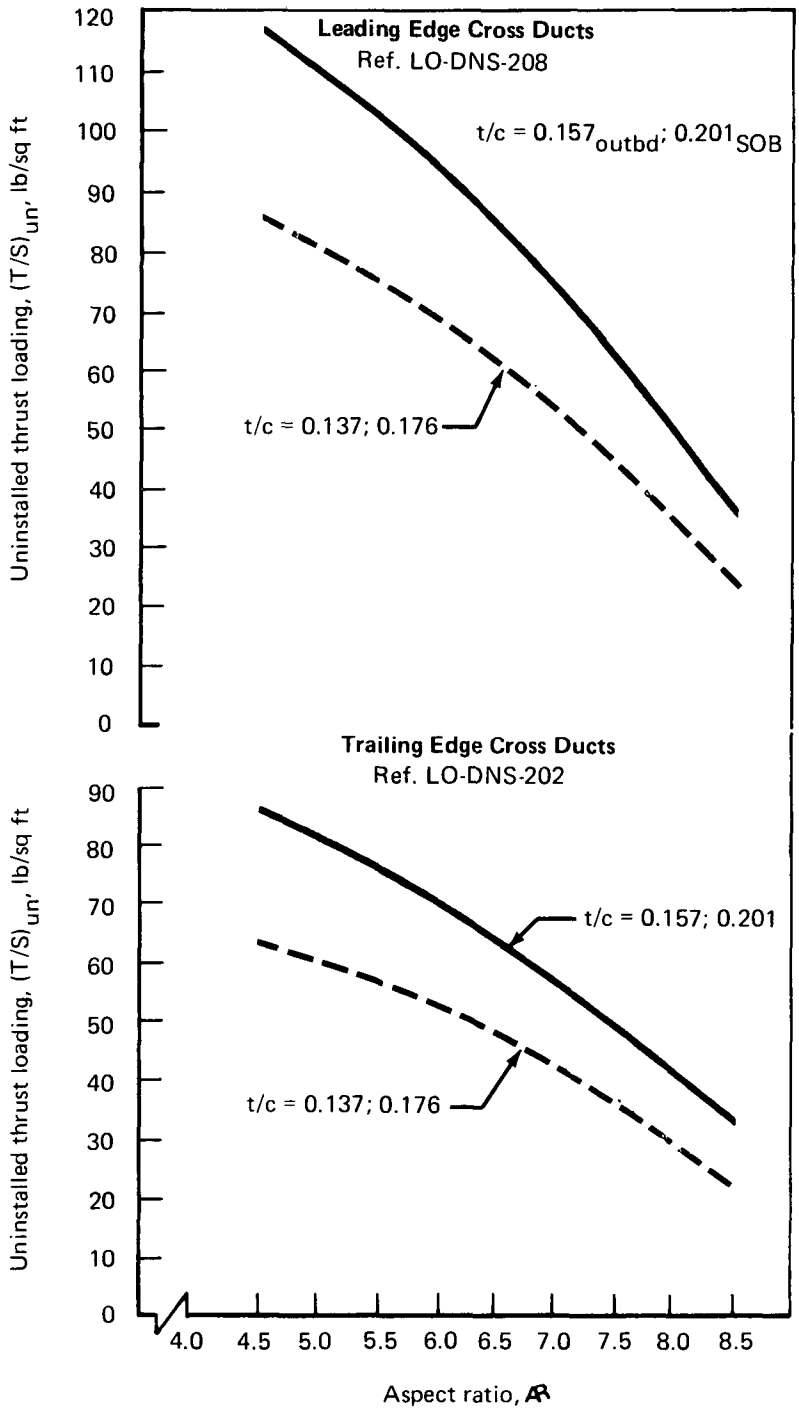

FIGURE 48-- WING PLANFORM AND THICKNESS EFFECT ON UNINSTALLED THRUST LOADING, FPR = 3.2, $\Delta P/P_F$ = 10%, 100% FAN AIR TO WING

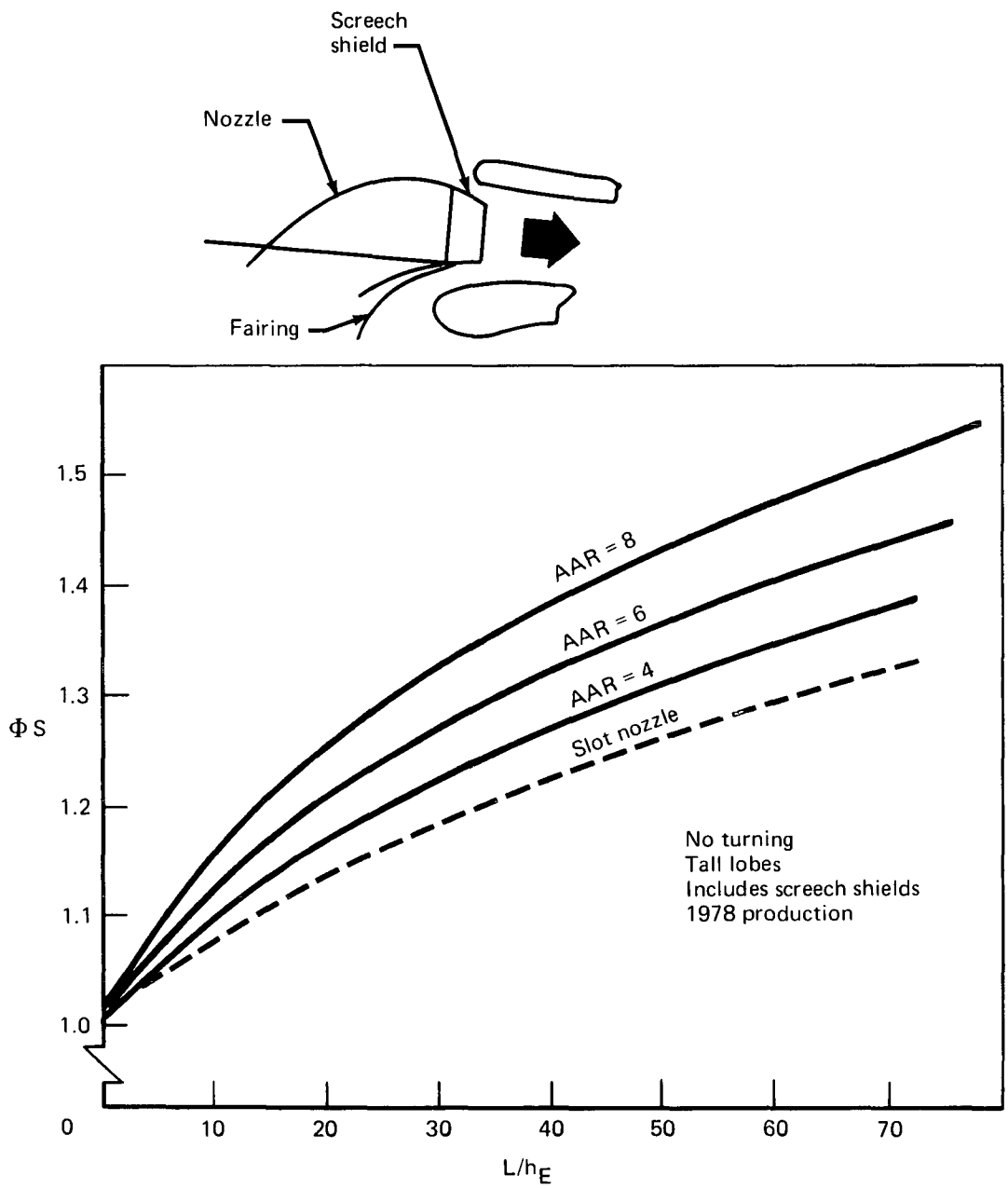

FIGURE 49.–STATIC AUGMENTATION AS FUNCTION OF NOZZLE ARRAY AREA AND FLAP LENGTH, CRUISE BLOWING SYSTEM

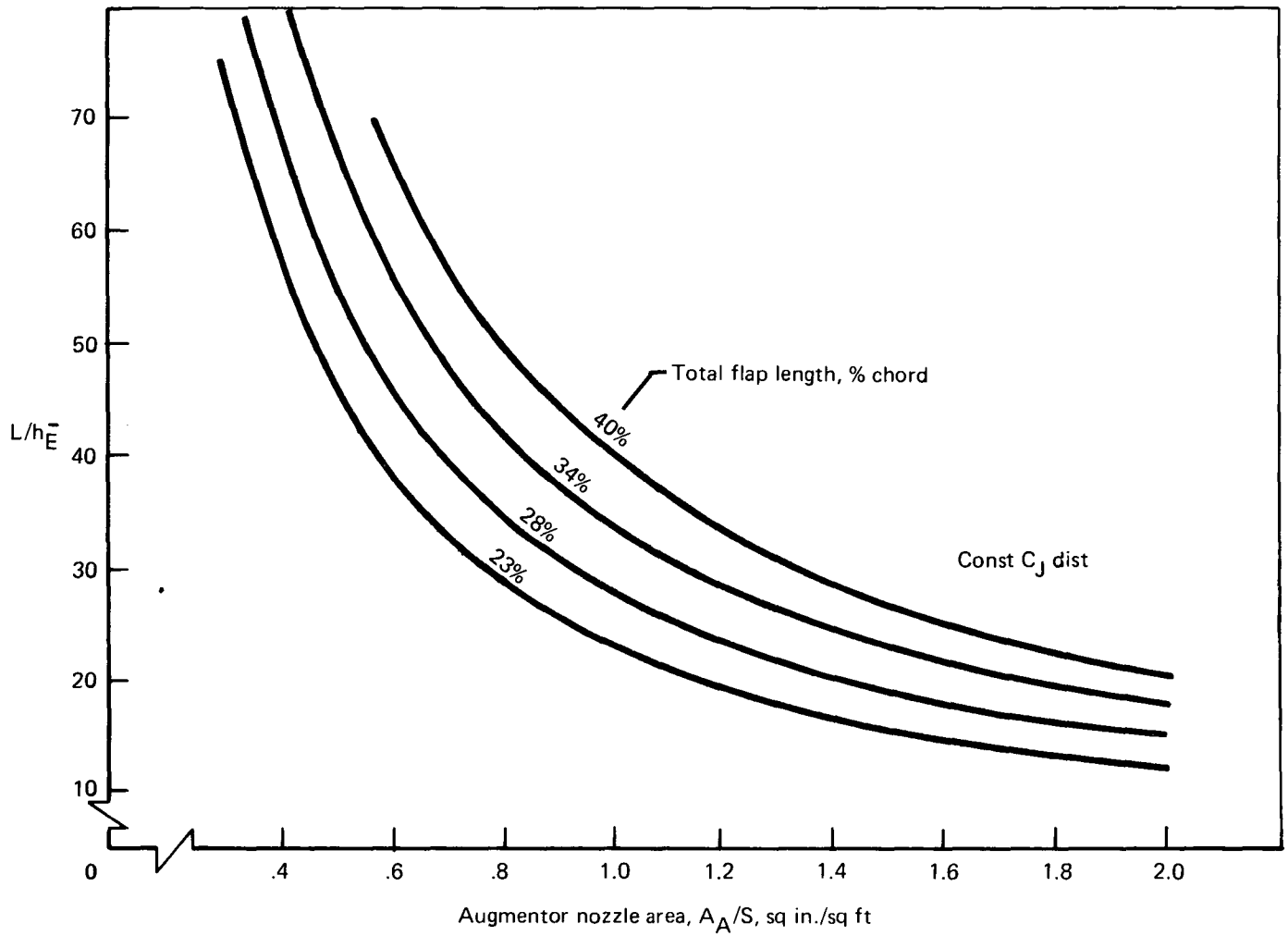

FIGURE 50.–RATIO OF FLAP LENGTH TO EQUIVALENT NOZZLE HEIGHT AS FUNCTION OF NOZZLE AREA AND FLAP CHORD

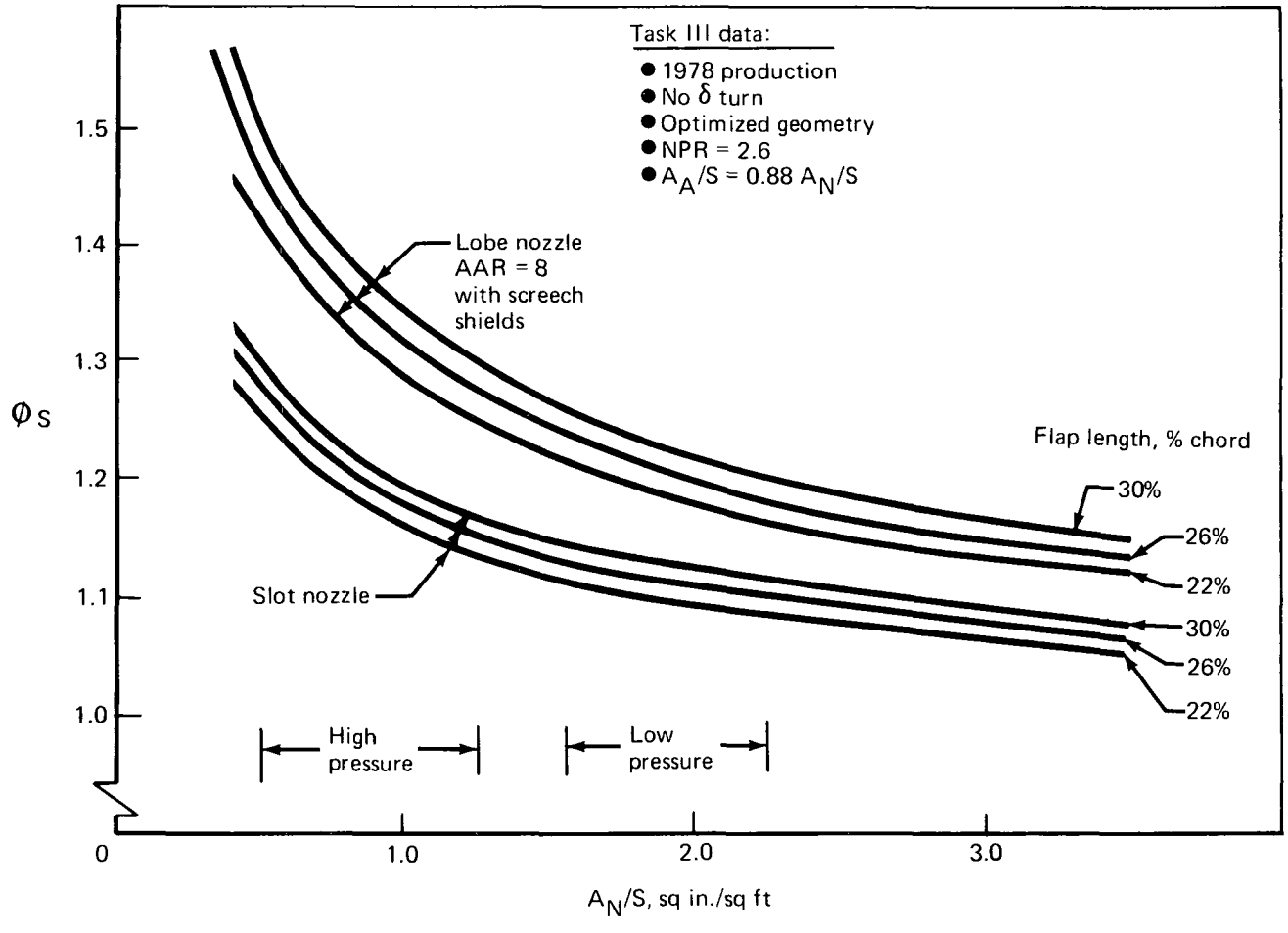

FIGURE 51.—STATIC THRUST AUGMENTATION AS FUNCTION OF WING NOZZLE AREA AND FLAP CHORD

to wing flow split, and the high-pressure augmentor has an A_N/S value of 0.5 to 1.0 for systems with all the air to the wing. This gives $L/h_{\overline{E}}$ values of 12 to 20 for the low-pressure system and 30 to 60 for the high-pressure system.

As the A_N/S increases, the nozzle height becomes a sizeable percentage of the wing chord. Figure 52 gives nozzle array height in percent of chord (H_A/C) as a function of A_N/S and nozzle array area ratio (AAR). For reasonable values of H_A/C (for example, less than 6% chord) it can be seen that a nozzle with AAR = 8 is limited to A_N/S less than 0.9, which implies nozzle pressure ratios above 2.5. If a limit is placed on nozzle array height, the lower pressures tend toward lower array area ratios, but lower array area ratios have increased blockage of the air over the wing because the ratio of nozzle spacing to nozzle width is a function of the array area ratio.

Figure 53 shows a cruise blowing flap system. This figure uses the ducts and wing planform of figure 14. The t/c values are 0.132 and 0.176, and the aspect ratio is 7.5. The airfoil was recontoured to match the airfoil to be used in the exploratory two-dimensional high-speed wind tunnel test (NASA CR-114560). The trailing edge lower cusp causes the airfoil trailing edge to be thin, and this reduces the lower flap chord by about 2%. The nozzles are directed 8° downward from the wing chord plane to be aligned with the wing upper surface. Assuming a takeoff flap angle of 35°, a flow turning angle of 35° - 8° = 27° is required, and reference data indicate a reduction in augmentation associated with flow turning. The effects of flow turning on augmentation together with those of acoustic linings and nozzle pressure are estimated in figure 54. The reduction in augmentation for 27° of flow turning is estimated to be 0.08 in static augmentation ratio for an AAR = 8 nozzle. Utilizing the nozzle areas established in section 4.6.2, revised augmentation estimates for the design point high- and low-pressure system are shown below. The low-pressure system is evaluated with both an AAR = 8 lobe nozzle and a slot nozzle. The flap chord for the high-pressure system is from figure 53, and the flap chord for the low-pressure system with the thicker wing is estimated from figure 10, which shows that the ducts extend about 4% chord further aft than on the thinner wing. This shortens the flap chord by a similar amount.

	High Pressure	Low Pressure	
	AAR = 8	AAR = 8	AAR = 1 (slot)
FPR	3.2	1.7	1.7
% fan air to wing	100%	50%	50%
Wing aspect ratio	7.5	6.5	6.5
t/c	0.132-0.176	0.157-0.201	0.157-0.201
Cross-duct configuration	TE	LE	LE
A_N/S (sq in./sq ft)	0.64	1.7	1.7
A_A/S	0.56	1.5	1.5
C_F, % c	26%	22%	22%
$L/h_{\overline{E}}$	46.0	14.0	14.0
ϕ (fig. 49)	1.42	1.21	1.11
$\Delta\phi_{Turning}$	-0.08	-0.08	0
$\Delta\phi_{Lining}$	-0.04	-0.02	-0.02
$\Delta\phi_{NPR}$	0	+0.03	+0.03
ϕ_{Static}	1.30	1.14	1.12

Additional airplane sizing iterations would be required to completely reconcile these values of static augmentation with those of the selected design point configurations, but it was not deemed warranted at this preliminary stage as it could not substantially affect the recommendation.

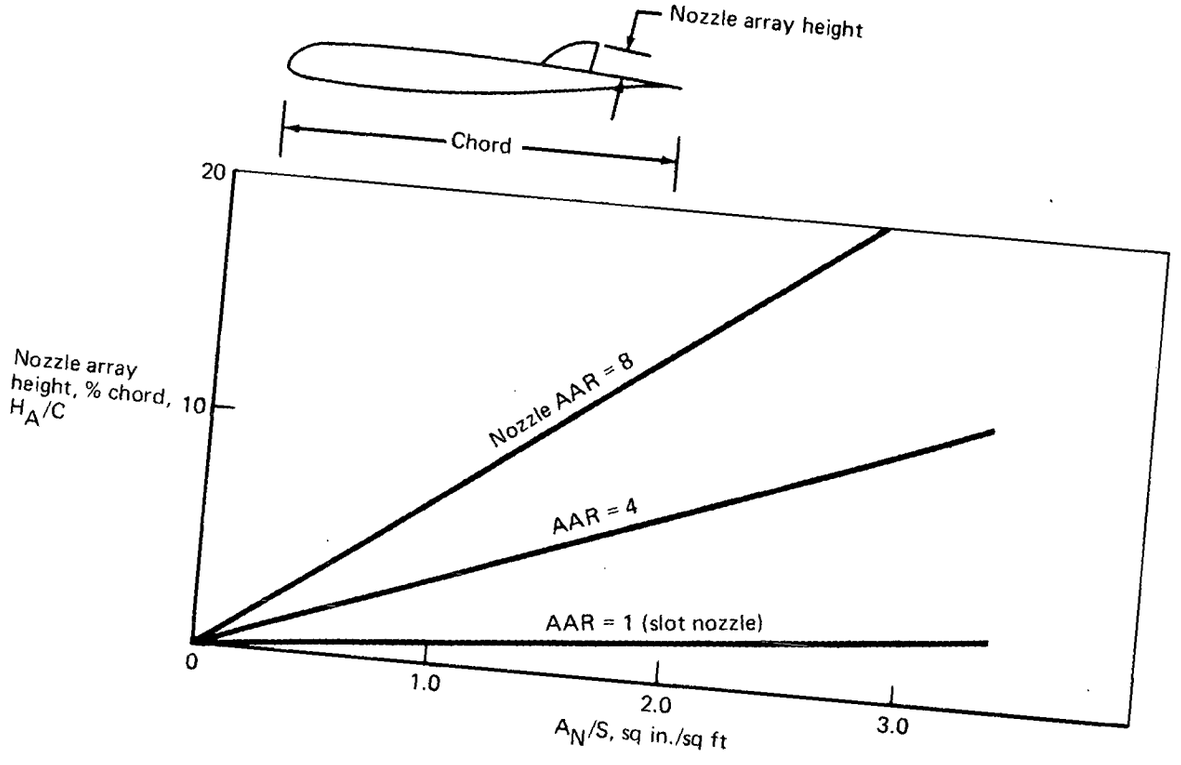

FIGURE 52.—NOZZLE ARRAY HEIGHT AS FUNCTION OF NOZZLE AREA AND ARRAY AREA RATIO

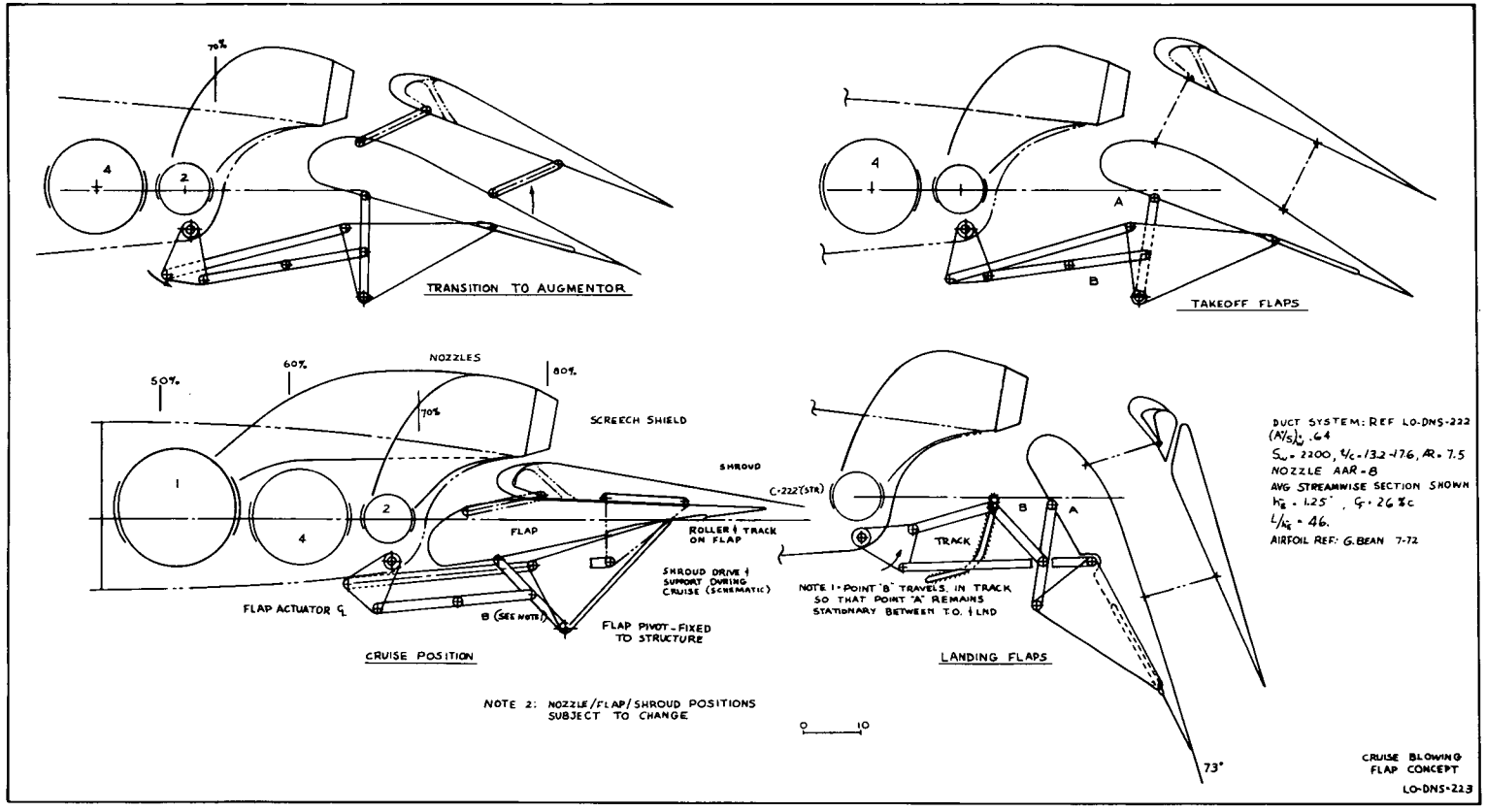

FIGURE 53.—LO-DNS-223—CRUISE BLOWING FLAP CONCEPT

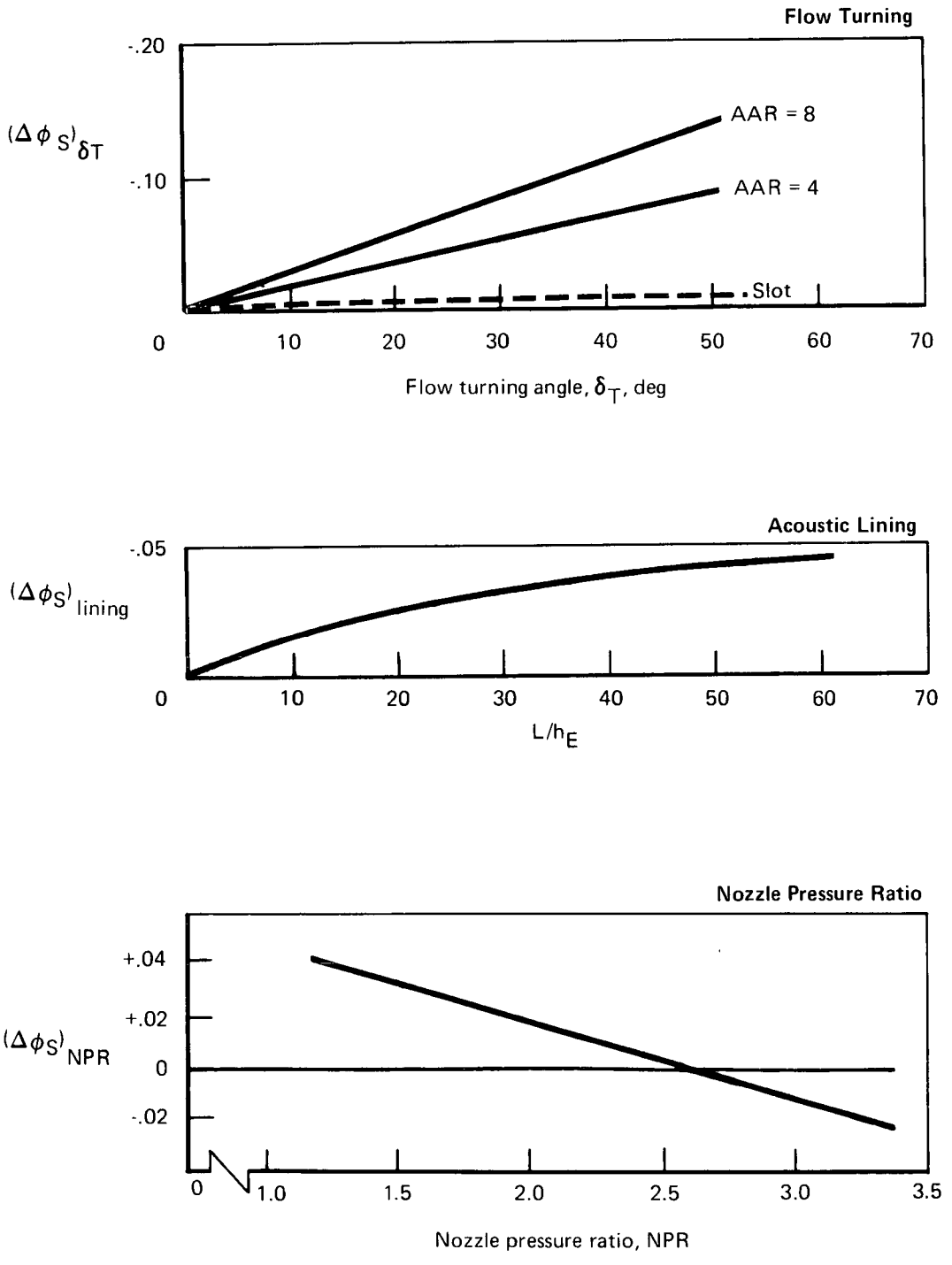

FIGURE 54.—ESTIMATED CORRECTIONS TO STATIC AUGMENTATION

This shows that the estimated turning loss almost eliminates the benefit of the large AAR nozzle on the low-pressure system. The AAR = 8 nozzle on the low-pressure system would give a nozzle height equal to 12% chord compared to 4.5% chord on the high-pressure system.

The short flap chord associated with a single-piece lower flap on the thick, low-pressure wing limits $L/h_{\overline{E}}$ and augmentation ratio. One way to enlarge the flap chord is with a separate vane, as shown in figure 55. This vane extends the lower flap by about 10% chord and may either be fixed as shown in figure 55 or rotated with the flap. The jet flap configuration approximately doubles the $L/h_{\overline{E}}$, and would improve landing performance and acoustic shielding. The loss in augmentation on the low-pressure designs may not be a significant handicap in itself, because the low-pressure system tends to be cruise thrust limited rather than takeoff thrust limited.

As indicated above, the nozzle secondary air ventilation parameter used in NASA CR-114284 is not considered applicable to the cruise blowing configurations discussed. The effect of nozzle spacing parameters is the subject of static tests in DNS task V. It will be necessary to evaluate the results of those tests as applicable to the cruise blowing system and to test the cruise blowing configuration to confirm both ventilation and flow turning assumptions.

4.5.2 Noise

Airplane and augmentor flap noise at the 500-ft sideline is summarized in figures 56 and 57 for the high- and low-pressure split-flow systems. The high-pressure, two-stream system is similar to the reference system, and uses a choked inlet. The aft fan noise is contained and suppressed within the ducting and is not considered a noise source. The low-pressure split-flow system has the fan jet and aft fan as additional noise sources, and these sources control the airplane noise. The low-pressure jet exhaust noise is rather high, but since this noise is related to the fan pressure ratio, it is constrained by duct volume and airplane gross weight. If the fan pressure ratio is reduced, the airplane gross weight increases for a given mission because the wing planform must be unduly compromised to contain the required wing blowing airflow at a 50% split. It may be possible to reduce the split slightly while maintaining adequate values of flap thrust coefficient during landing.

The augmentor flap noise does not respond readily to decreases in NPR because the suppression capability of a multielement nozzle decreases with decreasing NPR, and also because the $L/h_{\overline{E}}$ of the flap becomes shorter as A_N/S increases. In order to maintain reasonable amounts of thrust in the wing, the A_N/S tends to increase as NPR decreases. This is summarized in the table below.

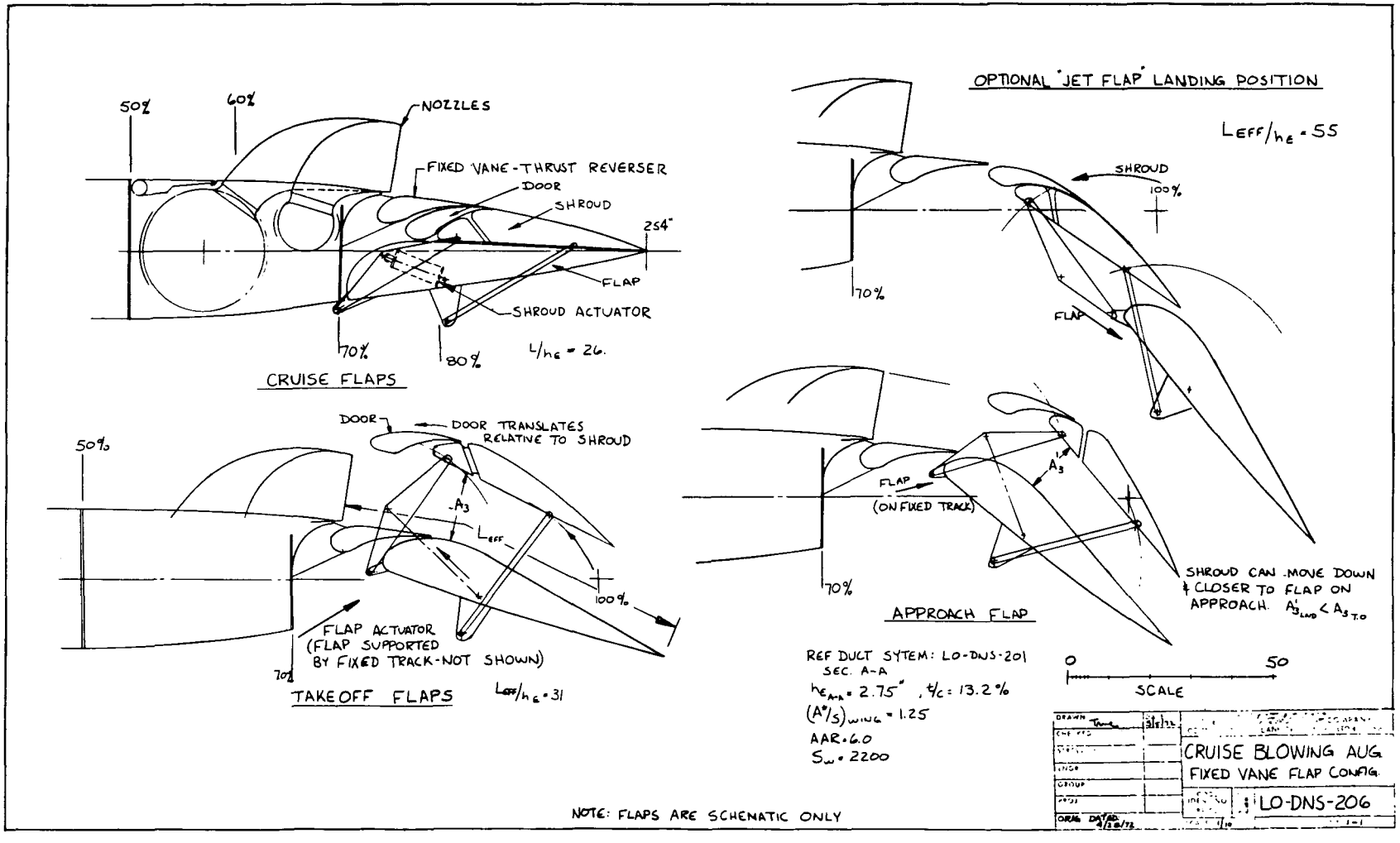

FIGURE 55.—AUGMENTOR WING CRUISE BLOWING SYSTEM FIXED VANE FLAP CONFIGURATION

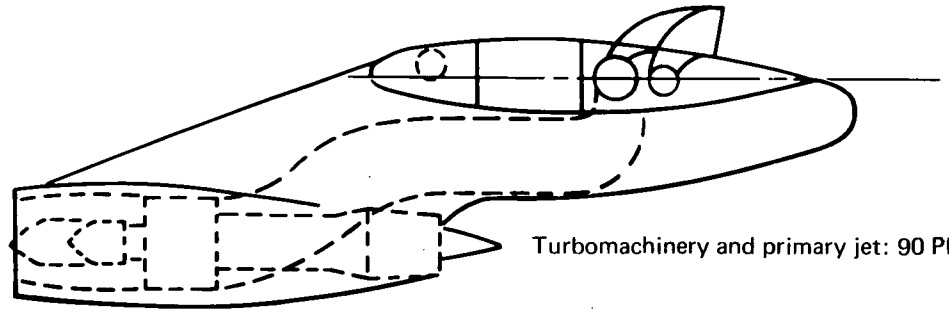

Turbomachinery and primary jet: 90 PNdB

Ref. NASA CR-114472*, fig. 4

Inlet:	115 PNdB
Choked:	-25
Net	90 PNdB

Augmentor flap	
Bare lobe nozzle:	106 PNdB
Screech shields	-4
Lined flaps	-12
Net: (1978 tech)	90 PNdB

FPR = 3.2
NPR = 2.7
Four engines at 18 300 lb SLST
Thrust split: primary jet 20%
augmentor 80%
Overall peak noise = 90 PNdB

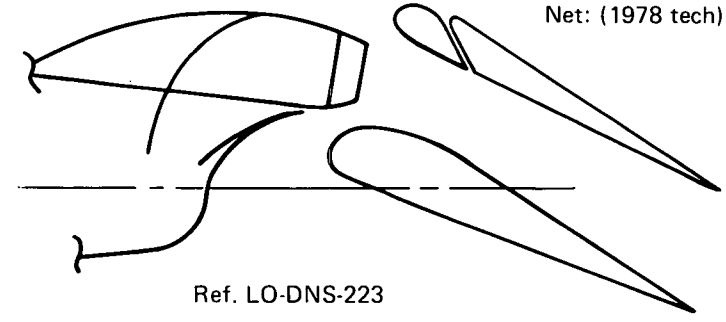

Ref. LO-DNS-223

FIGURE 56.—ESTIMATED AIRPLANE TAKEOFF NOISE—500-FT SIDELINE, FPR = 3.2, 100% FAN AIR TO WING

*Originally issued as CR-114284.

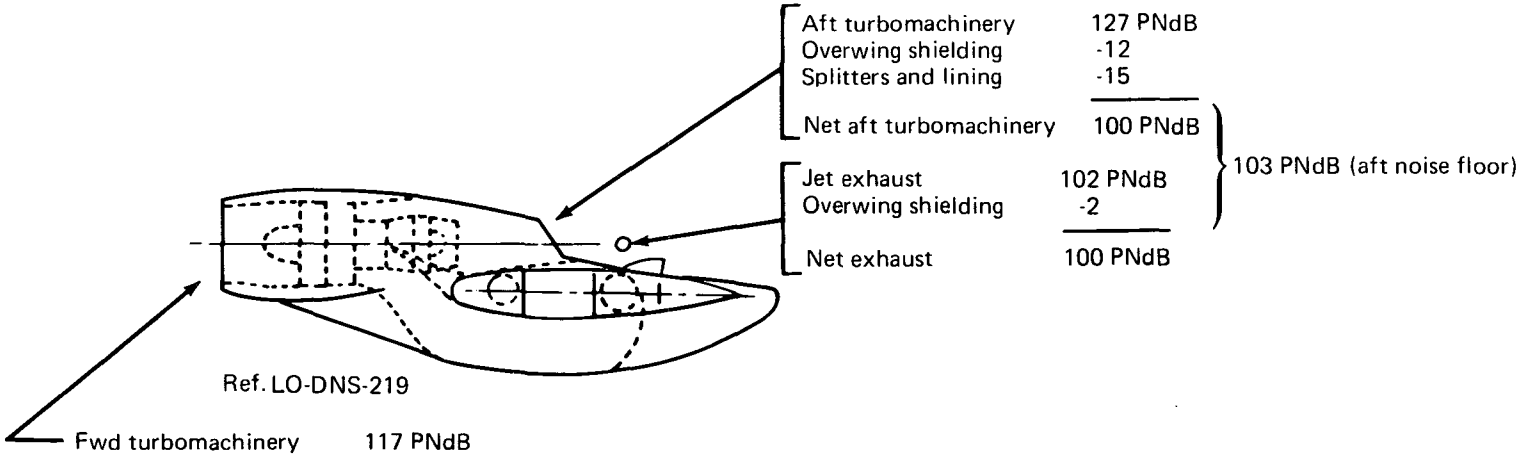

FPR = 1.7
NPR = 1.52
Four engines at 34 700 lb SLST
Thrust split: Primary jet 20%
Secondary jet 40%
Augmentor 40%
Overall peak noise = 103 PNdB

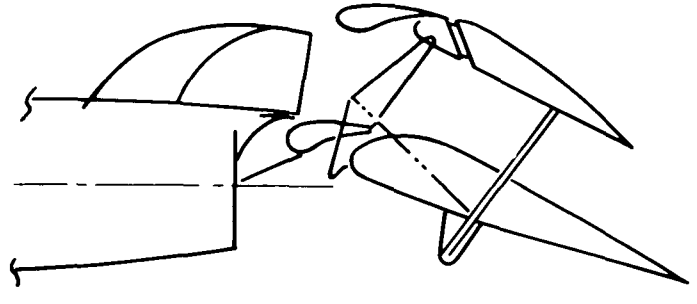

Ref. LO-DNS-206

Bare nozzle 102 PNdB
Flaps -3
Lining -3
Net augmentor noise 96 PNdB

FIGURE 57.–ESTIMATED AIRPLANE TAKEOFF NOISE–500-FT SIDELINE, FPR = 1.7, 50% FAN AIR TO WING

	Augmentor Noise Characteristics	
	High Pressure	Low Pressure
FPR	3.2	1.7
NPR	2.7	1.52
A_N/S	0.64	1.7
$L/h_{\overline{E}}$	46.0	14.0
Nozzle area	1280 sq in.	3750 sq in.
500-ft sideline peak noise		
Slot nozzle noise (ref.)	116 PNdB	102 PNdB
ΔPNdB screech	-4	0
ΔPNdB multielement nozzle	-10	0
ΔPNdB flaps with lining	-12	-6
Net PNL (1978)	90 PNdB	96 PNdB

4.6 AIRPLANE INTEGRATION

4.6.1 Airplane/System Parameters

The airplane ground rules for the study (similar to those of NASA CR-114472*) are:

150-passenger capacity
2000-ft TOFL
Four engines
Mach 0.8 at 30 000-ft cruise altitude
500-nmi STOL range
1500-nmi CTOL range
90-PNdB maximum noise objective at 500-ft sideline

The airplanes were sized by means of the "thumbprint", figure 58. Here the TOGW is determined parametrically for a matrix of thrust loadings (T/W) and wing loading (W/S). The airplane design point is determined by the critical combination of the takeoff line, duct volume, fuel volume, and cruise thrust constraints. The general determinants of these constraints are listed below.

Constraint	is a function of
Takeoff line	T/W, W/S, augmentation ratio, wing aspect ratio
Duct volume	Wing t/c and aspect ratio, NPR, duct routing, rear spar location, and flap chord
Fuel volume	W/S, t/c, rear spar location
Cruise thrust	Cruise drag, thrust lapse rate

*Originally issued as CR-114284

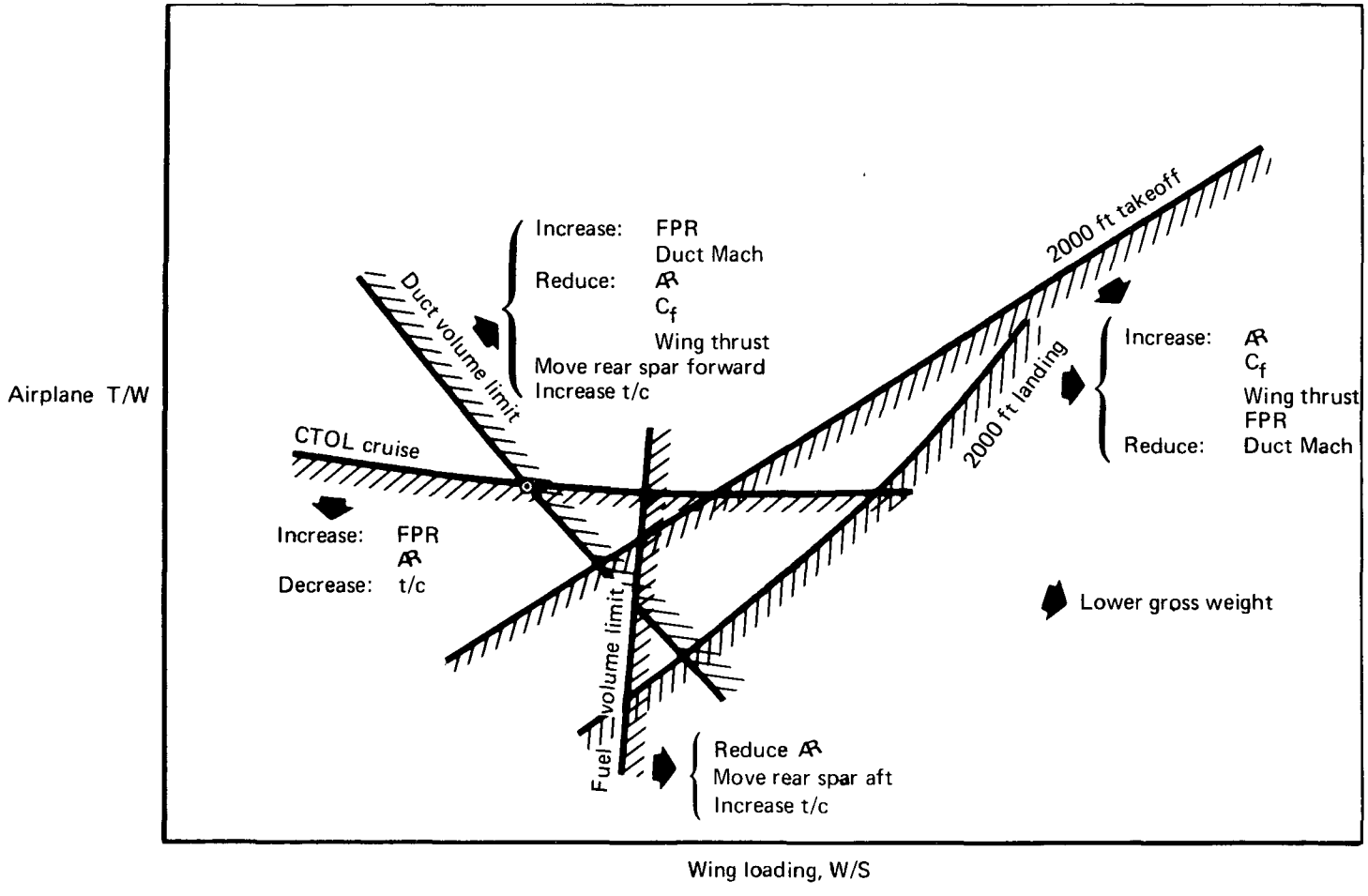

FIGURE 58.–AUGMENTOR WING AIRPLANE DESIGN PARAMETERS

These constraints are basically sensitive to wing planform and fan pressure ratio. The following sections describe an overview of some engine and augmentor characteristics which influence the airplane weight and constraints.

4.6.1.1 Engine Characteristics—The two low-pressure and two high-pressure engines used in the study were parametrically based on a common core engine, with bypass ratios adjusted to balance primary jet noise with other system component noise. The upper line in figure 59 describes the thrust/weight ratio of the uninstalled engines varying typically with fan pressure ratio. The other lines on figure 59 show successively the effect of installation thrust loss (including duct losses), the effect of engine pod installation weight and, finally, the overall installed thrust/weight including the weight of the augmentor blowing duct and nozzle system. It is significant that the 25% advantage of the low-pressure bare engine is given up in installation thrust loss and pod weight.

Another important parameter affecting relative airplane/engine matching characteristics is the thrust lapse at the cruise condition. This parameter is given in figure 60 for the uninstalled and installed low- and high-pressure engines in the study. Although the performance curve for the low-pressure, installed engine cycles includes the advantage of 50% fan air discharged from a nozzle in the nacelle without incurring duct losses, the cruise/SLS takeoff installed thrust fraction is 0.19 or about 73% of the high-pressure cycle, which has all the fan air directed through the wing blowing system. Because of this, the low-pressure engines tend to be sized by the cruise thrust requirement.

4.6.1.2 Augmentor System Characteristics—The thrust losses associated with distribution duct flow losses are shown in figure 61 for the range of pressure ratios and duct pressure losses studied. Except for assessment of duct velocity effects and the iteration to the selected airplane match point, the studies assumed a duct flow loss ($\Delta P/P_F$) = 10%. The increasing thrust loss as supply pressure ratio is reduced below 3.0 is a basic influence favoring the high-pressure system. Considering a typical distribution system with given duct geometry, the installed thrust capacity may be adjusted as a function of duct flow Mach number by varying the blowing nozzle area. This effect is illustrated in figure 62, in which changes in blowing nozzle area, thrust per unit nozzle area, and resultant airplane thrust per unit wing area are plotted against $\Delta P/P_F$ as an index of velocity. The Mach number at the critical duct section is 0.4 for the 10% overall duct loss reference point.

This installed thrust characteristic provides latitude for iteration to the final airplane sizing match point. The resulting variation in A_N/S does affect the augmentor geometry parameter ($L/h_{\bar{E}}$) and in turn requires appropriate adjustment of the augmentation ratio.

Figure 63 is typical of the variation in propulsion system thrust capacity of the airplane for two wing thicknesses over a ringe of wing aspect ratios. While the higher aspect ratio is desirable for aerodynamic efficiency, the duct installation space constrains thrust loading $(T/S)_{un}$, leading to larger wing area or greater thickness. The lower fan pressures (FPR = 1.7 and 1.8) demand larger duct flow capacity than is available with the trailing edge cross-duct system of figure 63. For these pressures, leading edge cross ducts described in section 4.1 with half the fan air discharged through a nozzle in the nacelle were used to achieve a match with airplane requirements at acceptable wing loadings. The trailing edge cross ducts

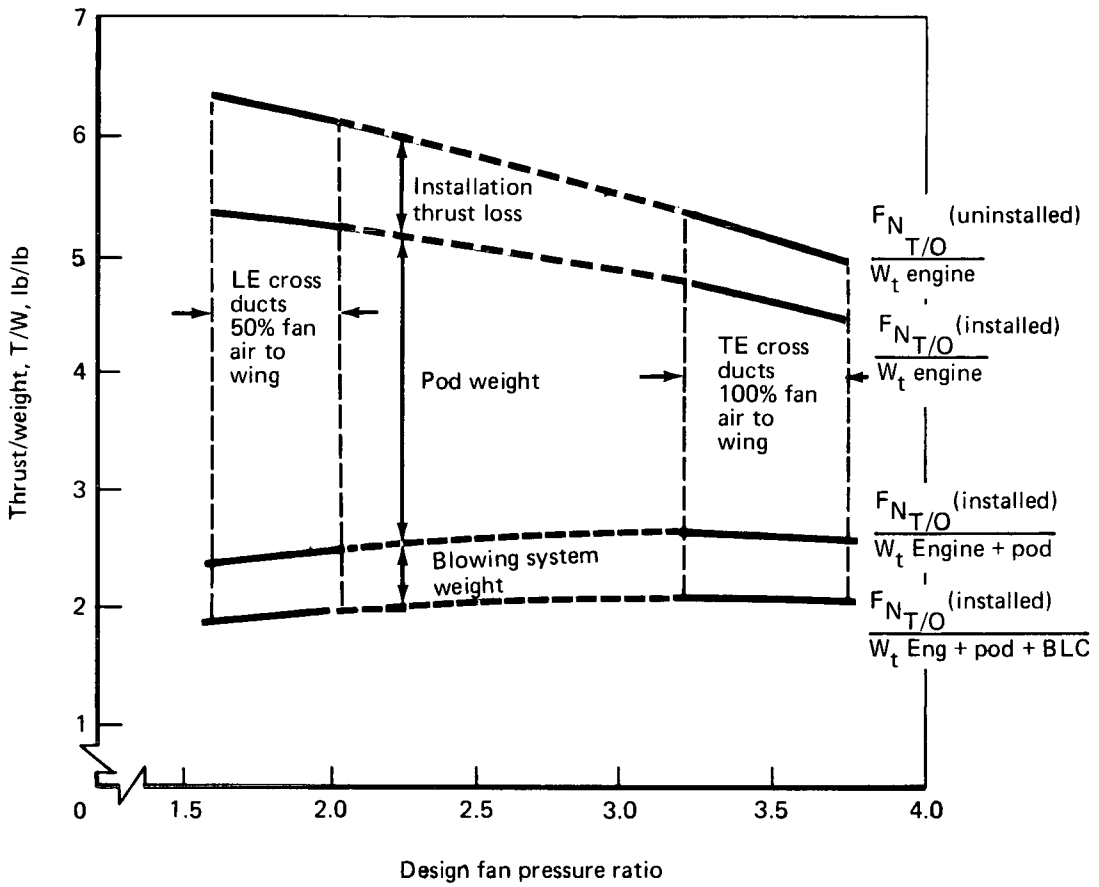

FIGURE 59.–EFFECTS OF INSTALLATION ON PROPULSION THRUST/WEIGHT

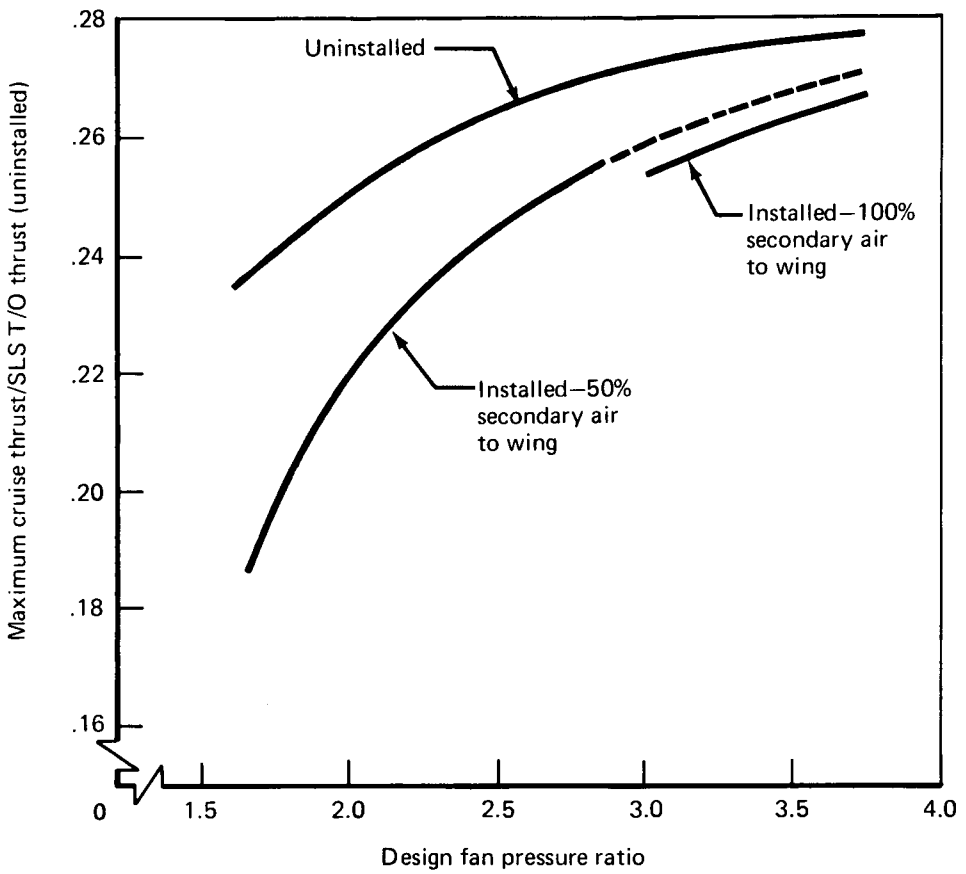

FIGURE 60.–CRUISE THRUST FRACTION AS FUNCTION OF DESIGN FAN PRESSURE RATIO

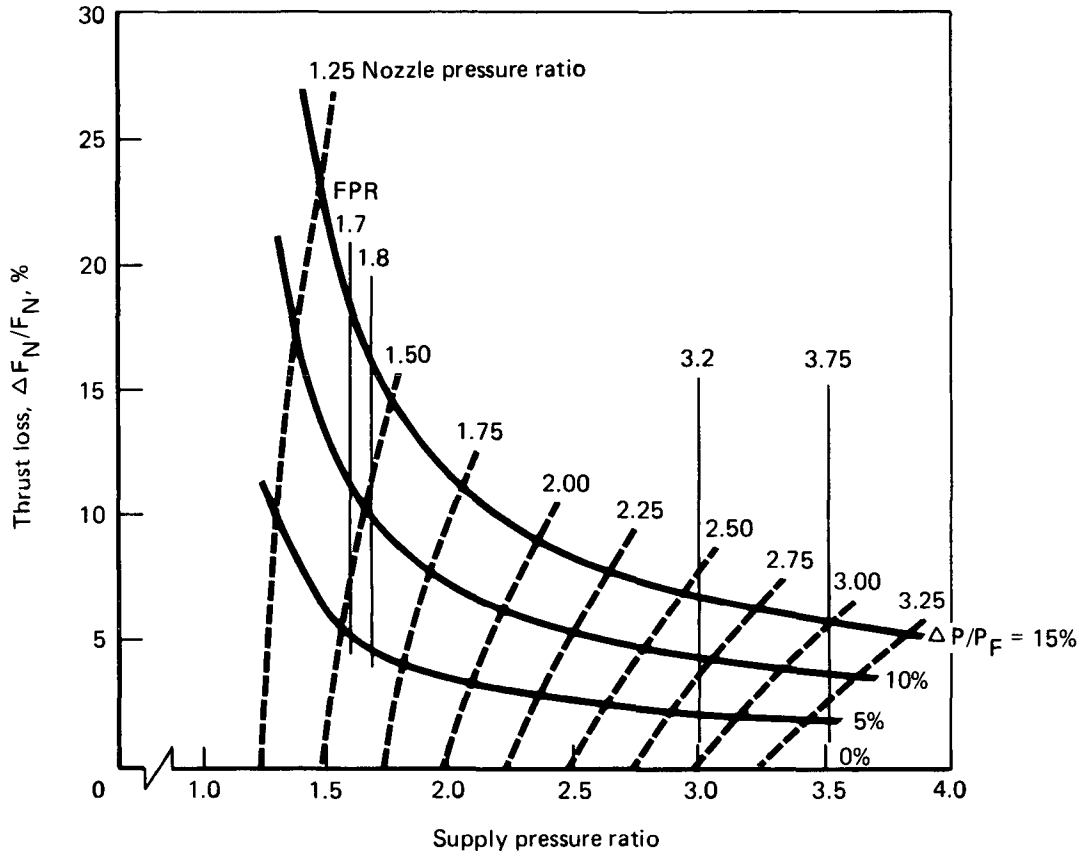

FIGURE 61.—DUCT PRESSURE LOSS-THRUST LOSS CORRELATION

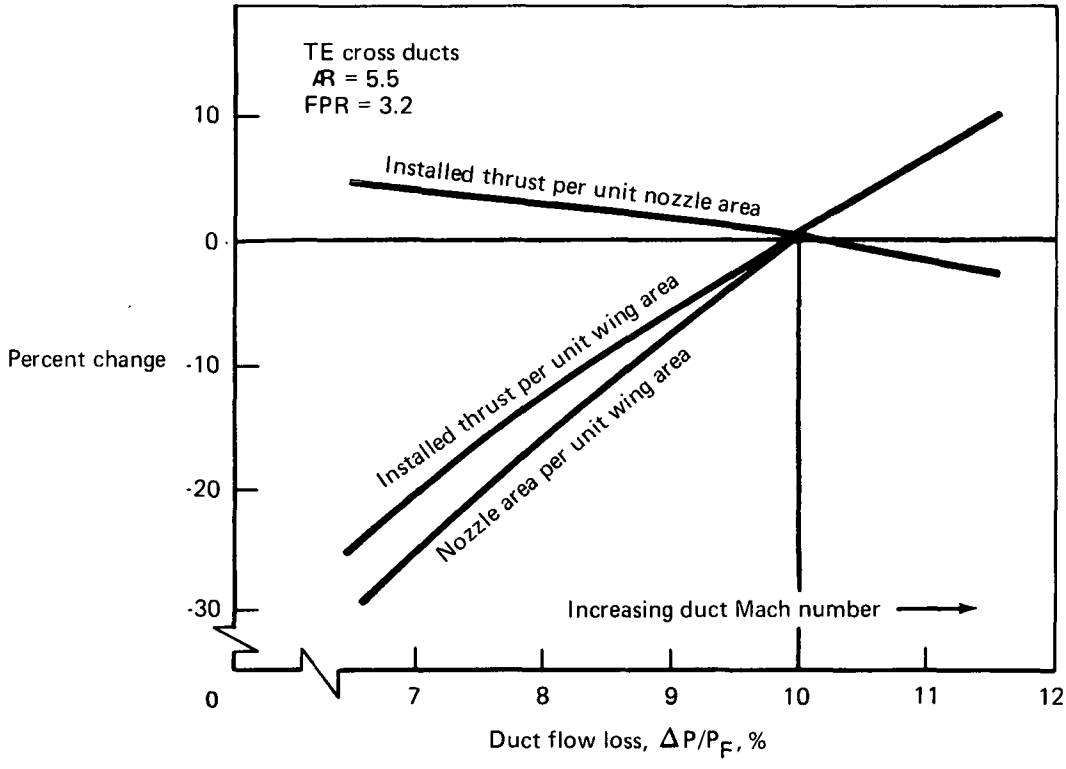

FIGURE 62.—BLOWING NOZZLE SIZE AND THRUST AS FUNCTION OF DUCT VELOCITY

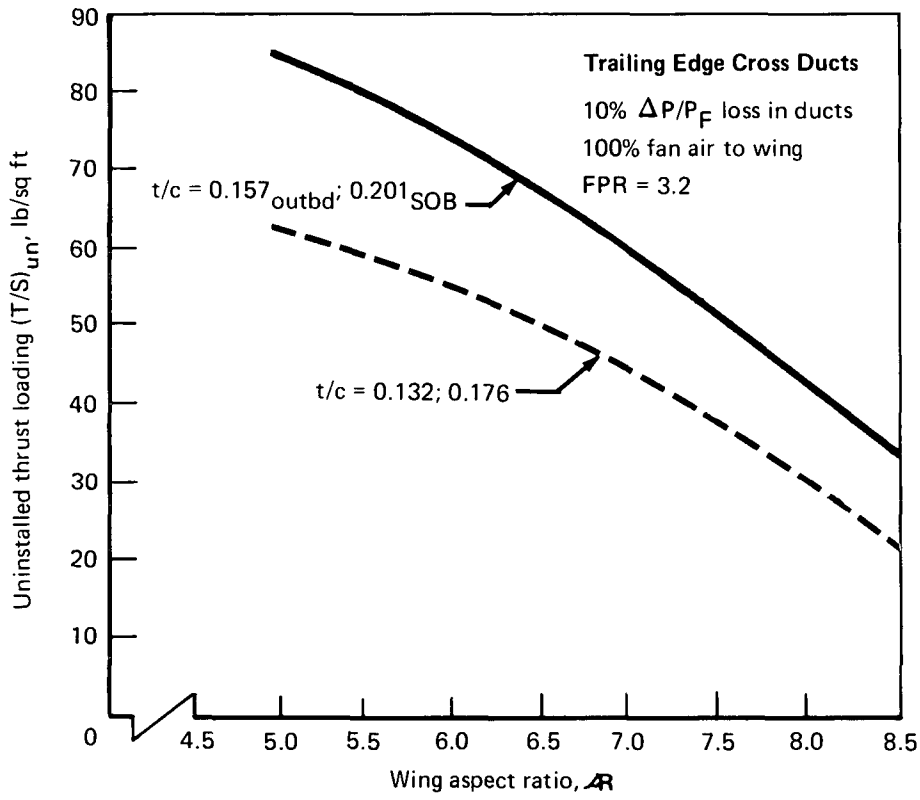

FIGURE 63.—UNINSTALLED ENGINE THRUST AS FUNCTION OF WING ASPECT RATIO AND THICKNESS

with 100% fan air to the wing were used with the high-pressure systems (FPR = 3.2 and 3.75). The two approaches are compared in figure 64 as a function of fan pressure ratio.

The size (H_A) of the wing nozzles, an important factor in the performance of the augmentor (see section 4.5), is a function of the wing duct capacity and favors the high-pressure systems. Figure 65 displays the range of thrust augmentation ratio (ϕ) as adjusted for nozzle size and other related effects in the low- and high-pressure systems. The advantage of high system pressure is clearly evident in this parameter.

4.6.2 Airplane Sizing

Design trades for the valveless augmentor system were determined within the payload, field length, range, speed, and altitude requirements listed in section 4.6.1. Low-speed performance is based on the 40- by 80-ft wind tunnel test of a swept wing augmentor (Working Paper 271, NASA-Ames, April 1971; TM X 62, 029). These data were modified to account for differences in airplane wing planform, flap chord, wing leading edge blowing, and nozzle C_V. The augmentation levels used were developed from the static tests of task III. Augmentor thrust lapse with velocity was accounted for by assuming that gross thrust was reduced by the effects of 10% total pressure losses at the augmentor inlet and diffuser and using a theoretical momentum drag term based on augmentor secondary mass flow.

The assumed cruise drag values due to the upper-wing-mounted nozzles needed for these valveless designs were:

Scrubbing	C_D =	.00090 for 100% fan air to wing
	=	.00045 for 50% fan air to wing
Nozzle Drag	C_D =	.00030 for 100% fan air to wing
	=	.00040 for 50% fan air to wing

When leading edge ducts were used, an additional C_D = .0003 accounted for the drag of the external ducts.

The studies encompassed low-pressure systems (FPR = 1.7 and 1.8) and high-pressure systems (FPR = 3.2 and 3.75) utilizing duct configurations, engine data, and augmentor system performance characteristics described in sections 4.1, 4.2, 4.4, and 4.5. Airplanes were sized for the wing fan pressures and cross-duct configurations indicated in table 3.

4.6.2.1 Low-Pressure Systems—Two wing thickness ($t/c = 0.157_{outbd}; 0.201_{SOB}$ and $0.132_{outbd}; 0.176_{SOB}$) were investigated to examine the potential advantage of this avenue in providing thrust capacity. However, the large wing volumes necessary to house ducts for the low-pressure systems cause low wing loadings, resulting in poor passenger ride quality, and heavy airplanes. Accordingly, only 50% of the fan air was ducted through the wing for the low-pressure systems. The remaining 50% exits through a conventional nozzle in the nacelle. Splitting the fan air in this manner has the following effects:

- Increased takeoff thrust requirements because of reduction in powered lift and augmented thrust
- Higher cruise thrust because of lower installation loss of the fan air discharged through the tailpipe
- Increased noise from fan air discharged through the tailpipe
- Increased angle of attack and body attitude during landing approach
- Required thrust reversal during landing approach to reduce the fan air tailpipe thrust

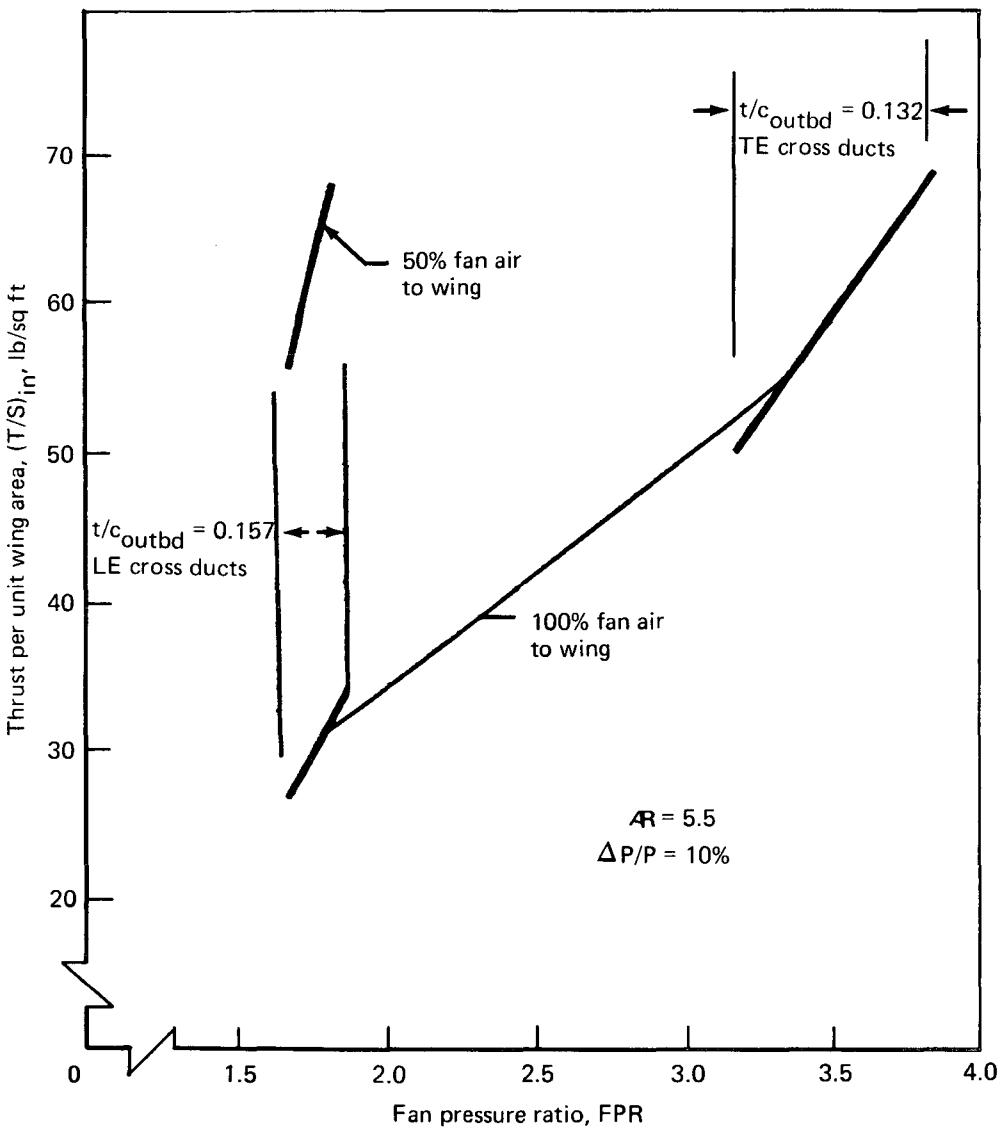

FIGURE 64.—INSTALLED THRUST CAPACITY AS FUNCTION OF DUCT SYSTEM AND PRESSURE RATIO

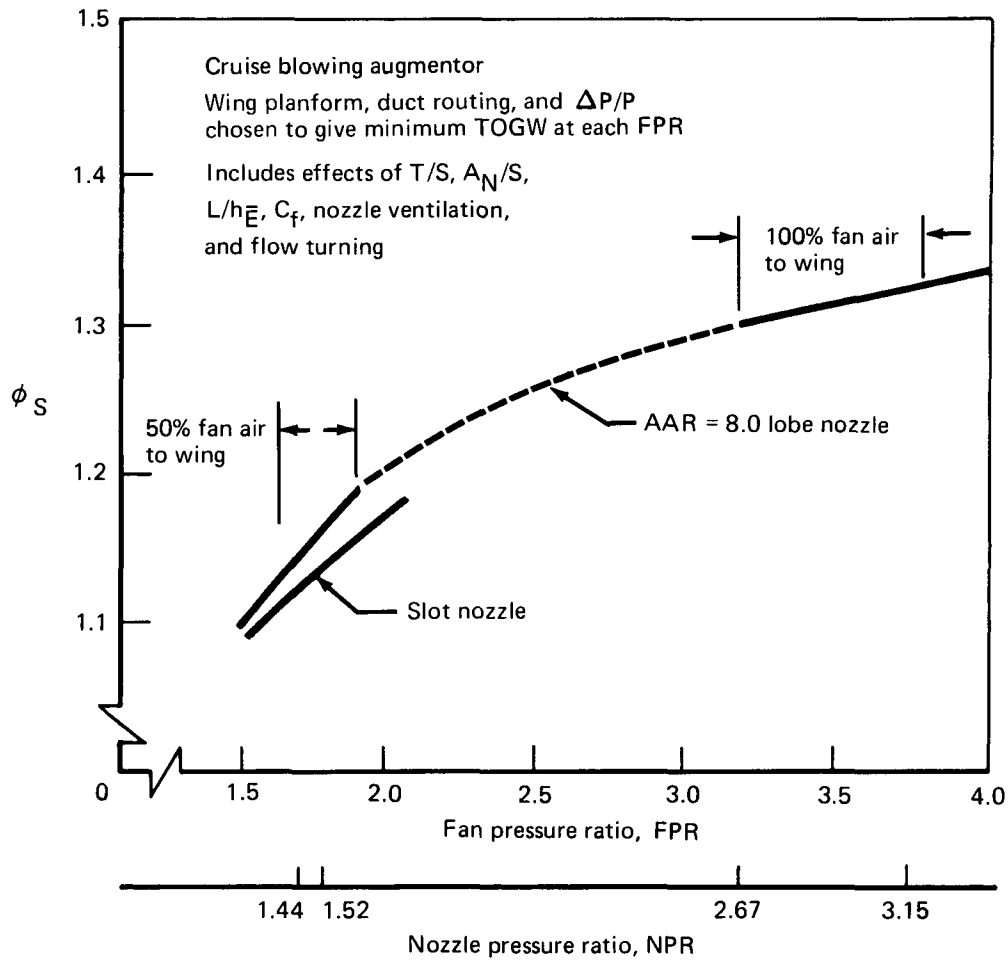

FIGURE 65.– THRUST AUGMENTATION TRENDS AS FUNCTION OF FAN PRESSURE RATIO

TABLE 3.–MATRIX OF AIRPLANE SIZING STUDIES

Wing aspect ratio		5.5		6.5		7.5		8.5	
Wing t/c (outboard)		0.132	0.157	0.132	0.157	0.132	0.157	0.132	0.157
FPR and. cross-duct configuration	1.7		LE		LE				
	1.8		TE		TE		LE		
	3.2					TE	TE		
	3.75					TE	TE		TE

To reduce the adverse noise effects of a 50-50 fan air split, the engines were mounted over the wing as shown in figure 30 (without exhaust flow attachment) to utilize the wing as a noise shield. However, this installation caused an OWE penalty of about 3000 lb compared with an underwing installation for the high-pressure STF-395D (BM-2) engine at the same thrust.

4.6.2.1.1 Fan Pressure Ratio = 1.7: The lowest pressure system studied used the duct configuration of figure 8 adjusted to the thick wing ($t/c_{outbd} = 0.174$) as in figure 10, and the LP-4 engine cycle with FPR = 1.7 (section 4.2.2). Accounting for the various losses resulted in an NPR = 1.46. Figure 66 shows the engine/airplane design relationships for 5.5 aspect ratio. The design point is determined by the intersection of the STOL takeoff thrust requirement, with the duct volume limit at W/S = 104.7 and T/W = 0.656, giving a TOGW of 236 800 lb.

The relatively high T/W required for STOL operation is caused by:

- Reduction in powered lift and total thrust resulting from using only 50% of the fan air in the wing
- Reduction in augmentation ratio due to the large nozzle area required for low-pressure air

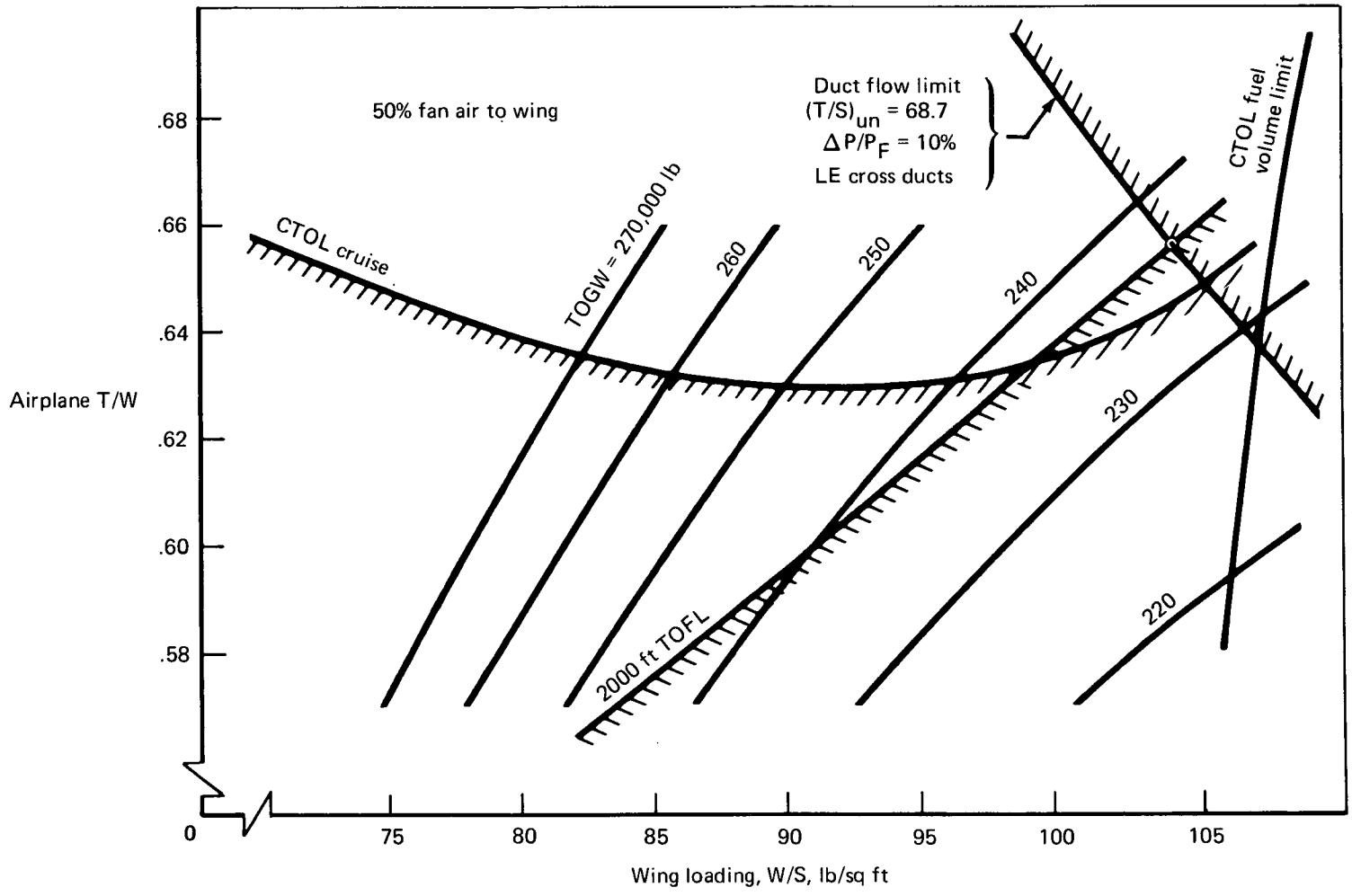

FIGURE 66.–AUGMENTOR WING CRUISE BLOWING SYSTEM AIRPLANE SIZING PARAMETERS, AR = 5.5, t/c = 0.157$_{outbd}$-0.201$_{SOB}$, FPR = 1.7

- Low wing aspect ratio
- Relatively high losses in fan jet thrust associated with ducting low-pressure air
- Ram drag associated with high-BPR engine cycle

The very high T/W needed for CTOL cruise is caused by:

- High thrust lapse with high-BPR engine cycle
- Thrust losses due to duct pressure drops and nozzle C_V that affect 50% of fan thrust
- Drag of relatively large nacelles
- Engine cruise/takeoff temperature ratio selected to account for the STOL duty cycle

At the chosen design point, the T/W requirements for CTOL cruise and STOL takeoff are quite close, indicating that the choice of 50% split of fan air to the wing gives near minimum TOGW for this engine/airplane/mission combination. However, a small reduction in TOGW would result from increasing slightly the percentage of fan air fed to the wing to reduce the takeoff thrust requirements. Concurrently, the CTOL cruise thrust requirements would slightly increase because the wing duct losses would affect a greater portion of the total cruise thrust. The greater duct volume requirements of the higher split would also reduce W/S. The maximum available reduction in TOGW from increasing the fan air split would be about 2000 lb.

The FPR = 1.7,LP-4 cycle was also examined with a 6.5 aspect ratio wing. The parametric relationships are shown in figure 67. The duct volume limit intersects the CTOL cruise requirement at T/W = 0.597 and a wing loading of W/S = 93.0. At the design point, TOGW = 232 100 lb and all mission requirements are met. This is approximately 5000 lb lighter in TOGW than the 5.5 aspect ratio wing because the higher aspect ratio requires less T/W for STOL takeoff and CTOL cruise.

If the CTOL cruise requirements were ignored, the design point would be the intersection of the duct volume limit with the STOL takeoff thrust requirement at W/S = 95 and T/W = 0.585, and the airplane TOGW would be 225 100 lb.

Since the CTOL cruise and STOL takeoff thrust requirements are somewhat mismatched along the duct volume limit line, TOGW could be slightly reduced by decreasing the fan air split, i.e., reducing the amount of fan air used in the wing. This would decrease the CTOL cruise thrust requirement and increase the duct-volume-limited W/S. However, takeoff thrust requirements would increase because of the reduction in thrust used for powered lift and augmentation. The maximum reduction in TOGW due to changing the fan air split would be about 2000 to 3000 lb, thus yielding TOGW = 229 000 lb for an airplane meeting the mission requirements.

Although increasing aspect ratio from 5.5 to 6.5 with the LP-4 cycle saved 5000 lb in TOGW, further increases would not yield substantial reduction in TOGW because the duct

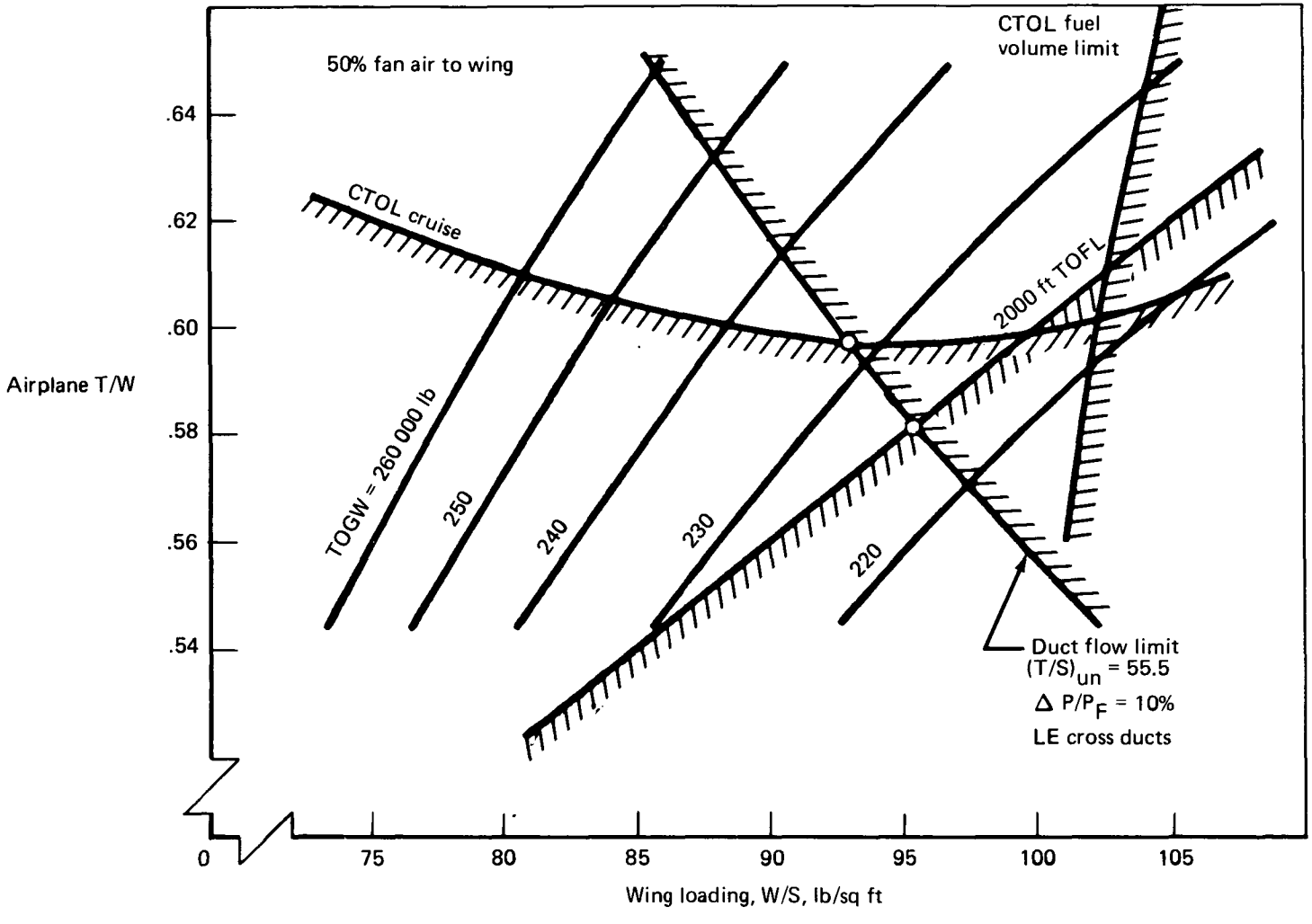

FIGURE 67.—AUGMENTOR WING CRUISE BLOWING SYSTEM AIRPLANE SIZING PARAMETERS, AR = 6.5, t/c = 0.157$_{outbd}$, 0.201$_{SOB}$, FPR = 1.7

volume limit rapidly reduces the maximum W/S, causing relatively heavy wings. Increased aspect ratio would significantly reduce the takeoff thrust requirement and slightly reduce the CTOL cruise thrust requirement, thus increasing the mismatch between cruise and takeoff requirements. The higher aspect ratio design could be rematched by decreasing the fan split, which would also increase the allowable W/S. However, since the changes in CTOL thrust requirements due to increasing aspect ratio beyond 6.5 and decreasing fan split would be small, the increased weight of higher aspect ratio and lower W/S would offset most of the potential weight reduction. Thus the 229 000-lb TOGW of the rematched 6.5 aspect ratio airplane is near the minimum possible for an LP-4 powered (FPR = 1.7) airplane which will meet the CTOL and STOL mission requirements.

4.6.2.1.2 Fan Pressure Ratio = 1.8: The LP-2 engine cycle has an FPR of 1.8, which gives an NPR of 1.52 after accounting for installation losses. The increase of FPR from 1.7 gives the following advantages:

- Increased cruise thrust at M = 0.8 and 30 000 ft– $F_{N_{MCR}}/SLST$ = 0.204 for LP-2 vs 0.190 for LP-4 or 7% more installed cruise thrust
- Reduced duct volume requirements–15% more thrust can be installed with the same installation losses.
- Improved augmentation due to smaller nozzles, thus giving more favorable augmentor flap/nozzle geometry.

At 5.5 and 6.5 aspect ratios, the reduction in duct volume requirements of the FPR = 1.8 cycle eliminates the need for the relatively heavy leading edge cross ducts that were necessary with FPR = 1.7.

Figure 68 shows the characteristics of a 5.5 aspect ratio airplane powered with the LP-2 engine cycle. The airplane is defined by the intersection of the duct volume limit with the takeoff thrust requirement at W/S = 99.6, T/W = 0.598, and TOGW = 227 000 lb.

Increasing aspect ratio to 6.5 reduces the duct volume limit, and the airplane becomes cruise thrust limited as shown in figure 69. The reduction in thrust requirement (T/W = 0.543 vs 0.598) due to increased aspect ratio more than offsets the heavier weight of the duct-volume-limited lighter wing loading (W/S = 88 vs 99.6) and results in a TOGW of 224 700 lb or 2300 lb less than that of the 5.5 aspect ratio airplane.

Figure 70 shows the engine/airplane matching characteristics of a 7.5 aspect ratio airplane with the LP-2 cycle. This aspect ratio requires use of the leading edge cross-duct distribution system to keep W/S in the desired region. The airplane is CTOL cruise thrust limited, with T/W = 0.532 at W/S = 87.2, giving a TOGW of 224 500 lb, only 200 lb lighter than for 6.5 aspect ratio.

The improved aerodynamic efficiency of 7.5 vs 6.5 aspect ratio does not translate into substantial TOGW reduction because at the relatively low wing loading (forced by duct volume limits) the airplane is cruise thrust limited, although induced drag is not large during

C2

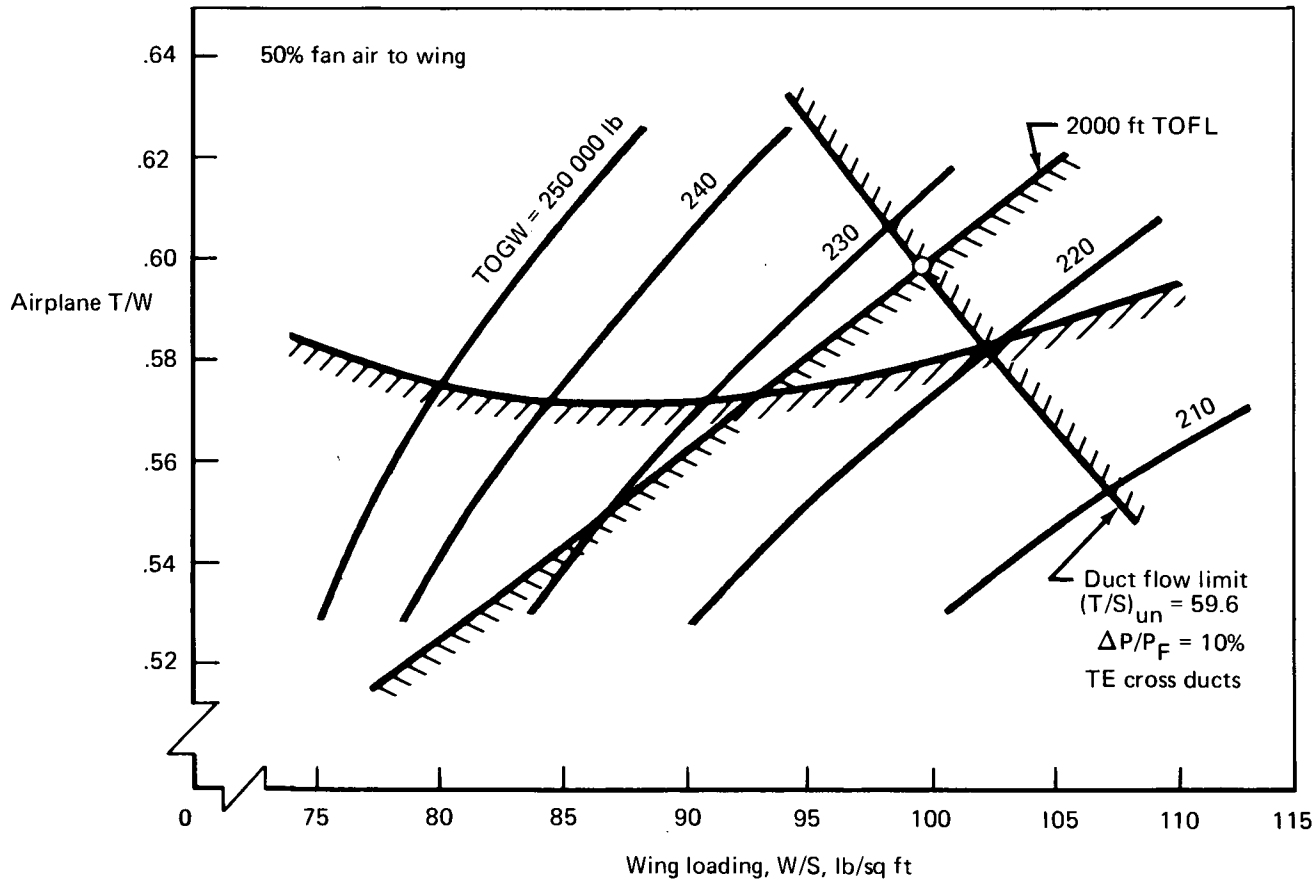

FIGURE 68.—AUGMENTOR WING CRUISE BLOWING SYSTEM AIRPLANE SIZING PARAMETERS, AR = 5.5, t/c = 0.157$_{outbd}$, 0.201$_{SOB}$, FPR = 1.8

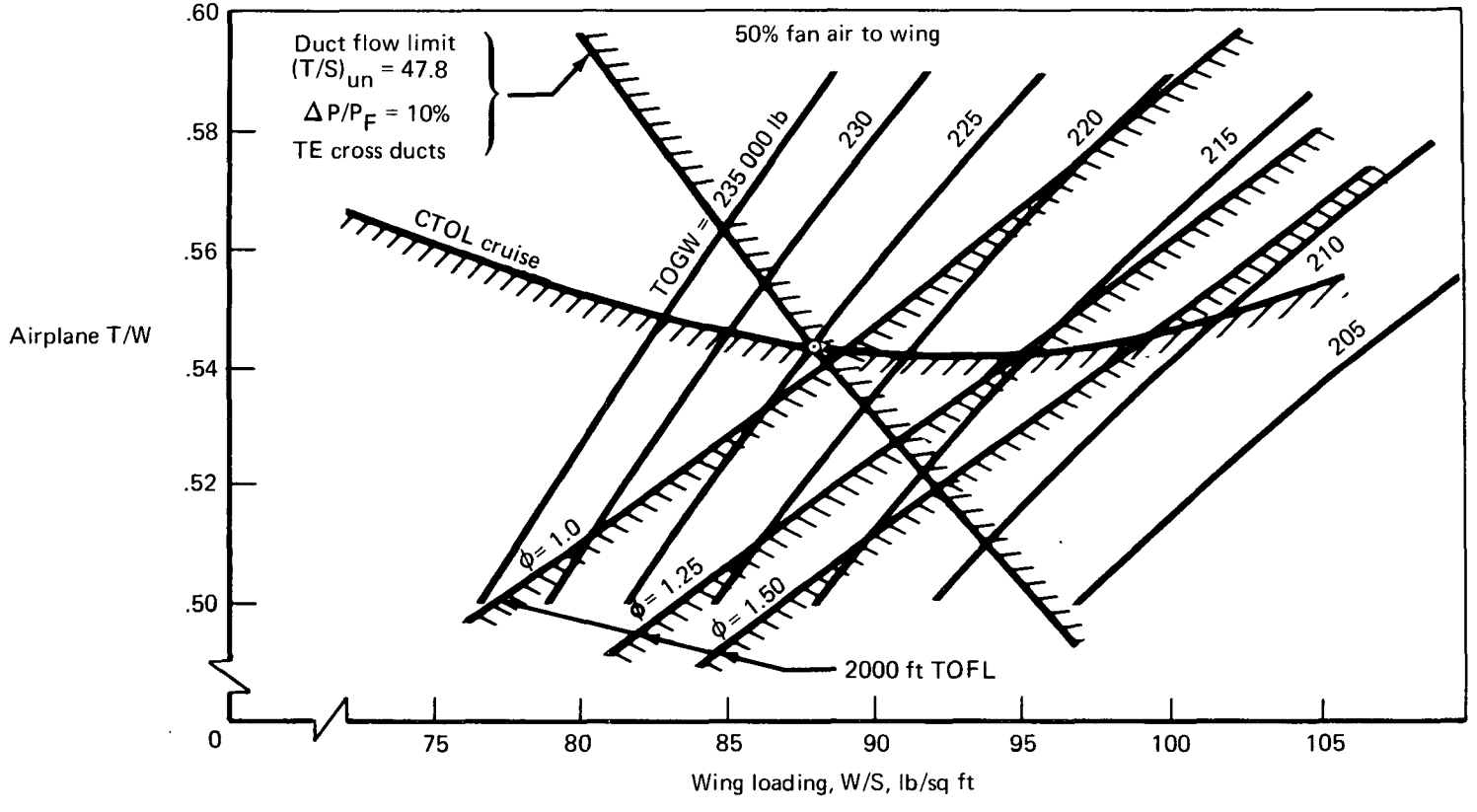

FIGURE 69.—AUGMENTOR WING CRUISE BLOWING SYSTEM AIRPLANE SIZING PARAMETERS, AR = 6.5, t/c = 0.157$_{outbd}$, 0.201$_{SOB}$, FPR = 1.8

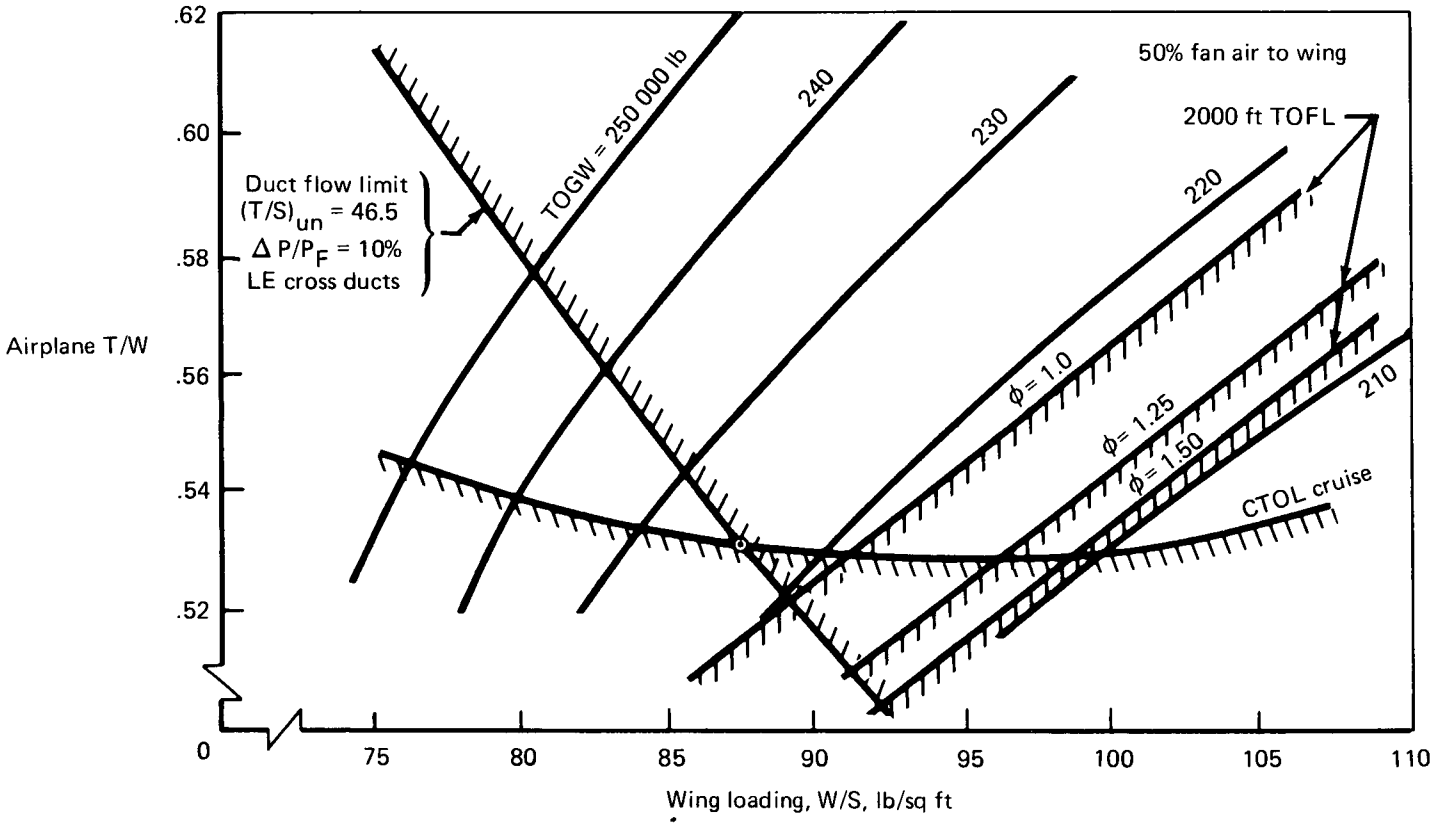

FIGURE 70.—AUGMENTOR WING CRUISE BLOWING SYSTEM AIRPLANE SIZING PARAMETERS, AR = 7.5, t/c = 0.157$_{outbd}$, 0.201$_{SOB}$, FPR = 1.8

cruise at these wing loadings. The slight reduction in T/W has been offset by the heavier cross-duct system and the increase in wing weight due to higher aspect ratio.

4.6.2.2 High-Pressure Systems–The high-pressure ratio systems studies used underwing mounting of the engines to save weight because overwing mounting was not needed for fan noise suppression. All of the fan air was used for augmentor, aileron, and leading edge blowing to increase powered lift and to reduce fan air noise. Wing thicknesses of 0.157_{outbd}; 0.201_{SOB} and 0.132_{outbd}; 0.176_{SOB} were investigated to determine effects on TOGW.

Two high-pressure engine cycles were studied:

- STF-395D (BM-2) with FPR = 3.2, giving an NPR = 2.7 with 10% $\Delta P/P_F$ duct pressure losses
- HP-1 with FPR = 3.75 resulting in NPR = 3.17 after installation losses are accounted for

4.6.2.2.1 Fan Pressure Ratio = 3.2: Figure 71 shows the characteristics of an airplane with the STF-395D (BM-2) engine cycle and with a wing aspect ratio of 7.5 and t/c = 0.157_{outbd}; 0.201_{SOB}. The design point is defined by the intersection of the fuel volume limit and the takeoff thrust requirement at W/S - 95.6 lb/sq ft, T/W = 0.43, and TOGW = 189 490 lb, or about 34 000 lb lighter than the best FPR = 1.8 design.

The relatively lower takeoff and cruise T/W limits are inherent characteristics of the higher pressure system. The engine size needed to satisfy the takeoff thrust requirement of the FPR = 3.2 system is reduced more than 20% from that of the FPR = 1.7 system primarily because of the increase in powered lift and augmented thrust due to using 100% of the fan air in the wing rather than 50%. The higher pressure system also results in reduced installation losses and improved augmentation ratio. In terms of installed cruise performance, the FPR = 3.2 thrust is 26% greater than that of the FPR = 1.8 cycle, i.e., $(F_{N_{MCR}}/F_{SLS})_{un} = 0.258$ vs 0.204.

Since the airplane design point is defined by the CTOL fuel volume limit at a wing loading well below the duct volume limit, the excess duct capacity would permit further optimization by:

- Increasing aspect ratio to improve aerodynamic efficiency
- Reducing duct Mach number to reduce installation thrust losses
- Decreasing wing thickness to reduce basic cruise drag and minimize technical risk of lower than predicted Mach critical.

Figure 72 shows the characteristics of the above airplane adjusted to a thinner (t/c = 0.132_{outbd}; 0.176_{SOB}) wing. The fuel volume limit has moved close to a match with the duct volume, the cruise thrust, and the takeoff requirements. The new design point is T/W = 0.404, W/S = 88.2 lb/sq ft, and TOGW = 190 000 lb, or a penalty of 1400 lb while reducing the engine thrust size by 6% and providing the reduced technical risk of a substantially thinner wing.

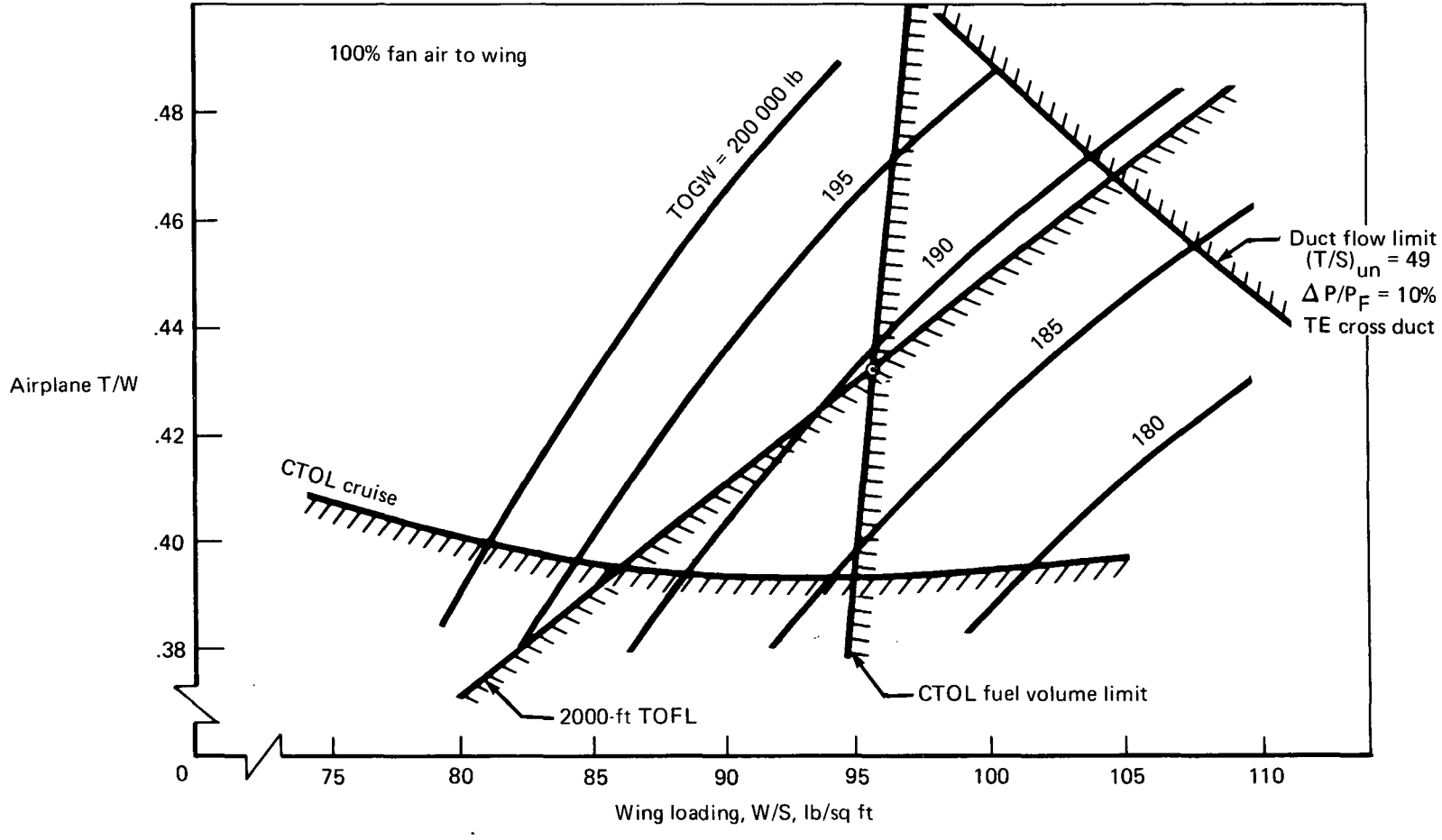

FIGURE 71.—AUGMENTOR WING CRUISE BLOWING SYSTEM AIRPLANE SIZING PARAMETERS, AR = 7.5, t/c = 0.157$_{outbd}$, 0.201$_{SOB}$, FPR = 3.2

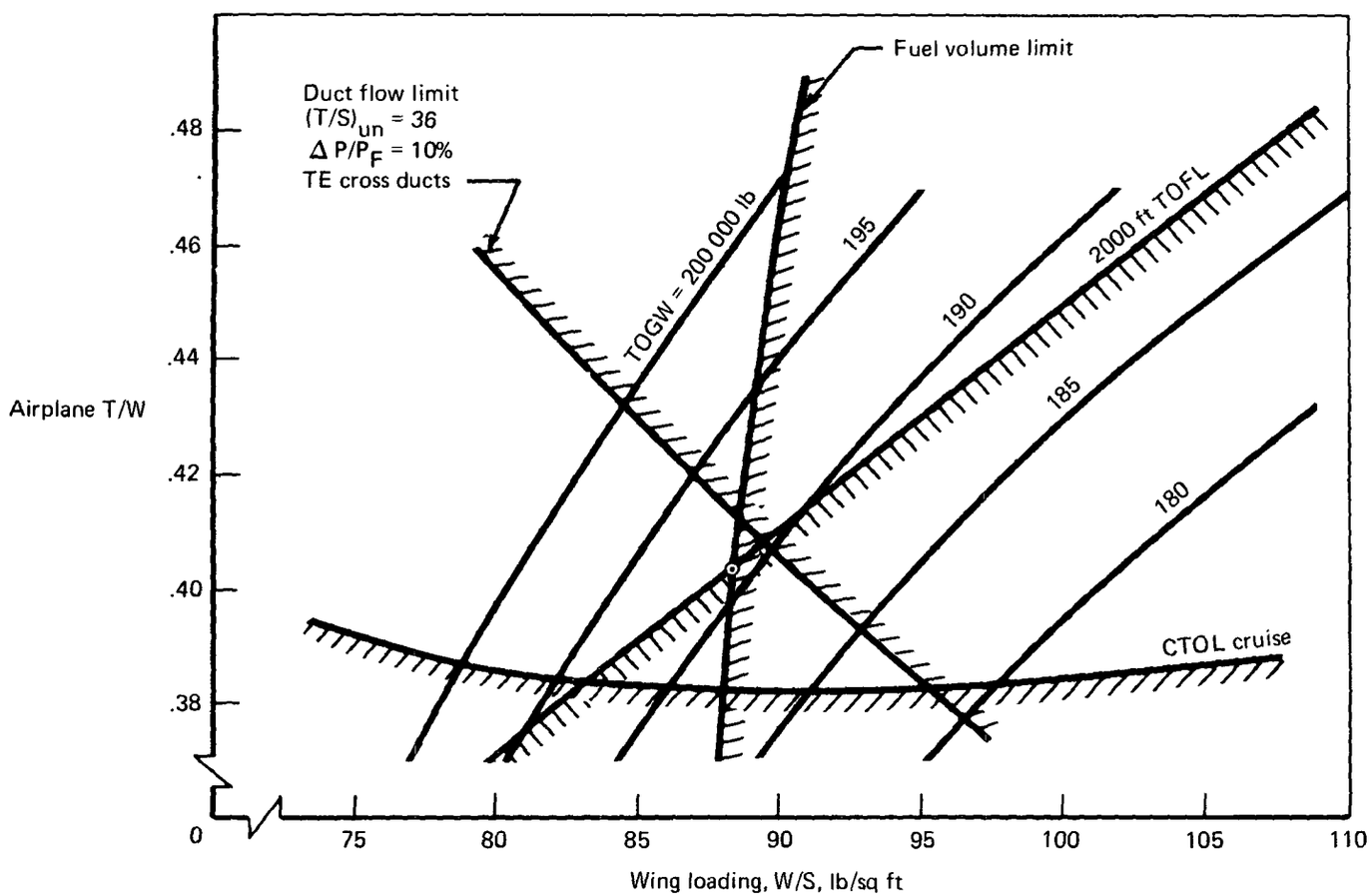

FIGURE 72.—AUGMENTOR WING CRUISE BLOWING SYSTEM AIRPLANE SIZING PARAMETERS, AR = 7.5, t/c = 0.132$_{inbd}$, 0.176$_{SOB}$, FPR = 3.2

4.6.2.2.2 Fan Pressure Ratio = 3.75: Figure 73 shows engine/airplane design relationships for the HP-1 (FPR = 3.75) engine cycle used with a 7.5 aspect ratio wing with $t/c = 0.157_{outbd}; 0.201_{SOB}$. This airplane is fuel volume limited to W/S = 96.7, with T/W = 0.427 and TOGW = 190 750 lb. The duct volume limit is above the W/S values on this plot, indicating that the airplane could be improved by decreasing wing t/c, increasing aspect ratio, or reducing duct Mach number (and therefore reducing installation losses).

Reducing wing t/c to $0.132_{outbd}; 0.176_{SOB}$ with this cycle rematches the parameters as shown in figure 74, giving W/S = 88.7, T/W = 0.396, and TOGW = 190 500 lb, or approximately 200 lb weight reduction. The reduced drag (lower fuel consumption) of the thinner wing is offset by the higher wing weight of the bigger, thinner wing while the engine size is reduced by 7%. The effect of higher wing aspect ratio is shown in figure 75 with 8.5 aspect ratio, t/c = 0.157; 0.201 and the HP-1 cycle. Because of the adverse effect of higher aspect ratio on duct volume limits, the thin (0.132; 0.176) wing could not be used with this duct system. The airplane size is defined by the intersection of the fuel volume limit and the takeoff thrust requirements at W/S - 89.6, T/W = 0.381, and TOGW = 186 700 lb.

While this airplane appears to provide significant gross weight and thrust size advantages, the technical risks inherent in the high aspect ratio (flutter) and extreme thickness (early drag rise) together with the development of the four-stage fan required in the HP-1 cycle rule out its selection as a basis for sizing the wind tunnel models.

4.6.3 Effects of Varying System Parameters

The variations of airplane characteristics may be displayed as a function of component parameters affecting the integrated systems used in the point designs of section 4.6.2. Those items of greatest significance are fan pressure ratio, wing aspect ratio, and wing thickness. Duct flow velocity (as measured by the index $\Delta P/P_F$) is also important in establishing the basic thrust capacity of the duct system and in its relation to blowing nozzle area, which is a key element in the performance of the augmentor.

4.6.3.1 Wing Aspect Ratio Relationships—The wing loading (W/S), airplane thrust loading (T/W) and takeoff gross weights of the airplanes described in section 4.6.2 are displayed in figure 76 in relation to wing aspect ratio. Included in the data are the major effects of fan pressure ratio, percentage of fan air directed to the wing, and wing thickness as well as the relative thrust capacity and weight effects of leading edge and trailing edge cross-duct systems. The trend toward lower wing loading with increasing aspect ratio is evident and is primarily the result of the duct volume constraint.

Airplanes with 1.7 FPR required the thicker wing section with leading edge cross ducts and 50% fan flow diverted through the nacelle nozzle. These airplane design points were at relatively low aspect ratios and had the highest gross weight and T/W ratios of the range studied.

At the other extreme, airplanes with 3.7 FPR permitted aspect ratios as high as 8.5 in the thicker wing with trailing edge cross ducts. Wing loading (W/S) of this point was 90 lb/sq ft while the TOGW and thrust loading (T/W) were 187 000 lb and 0.38, respectively, the lowest of the airplanes in the study.

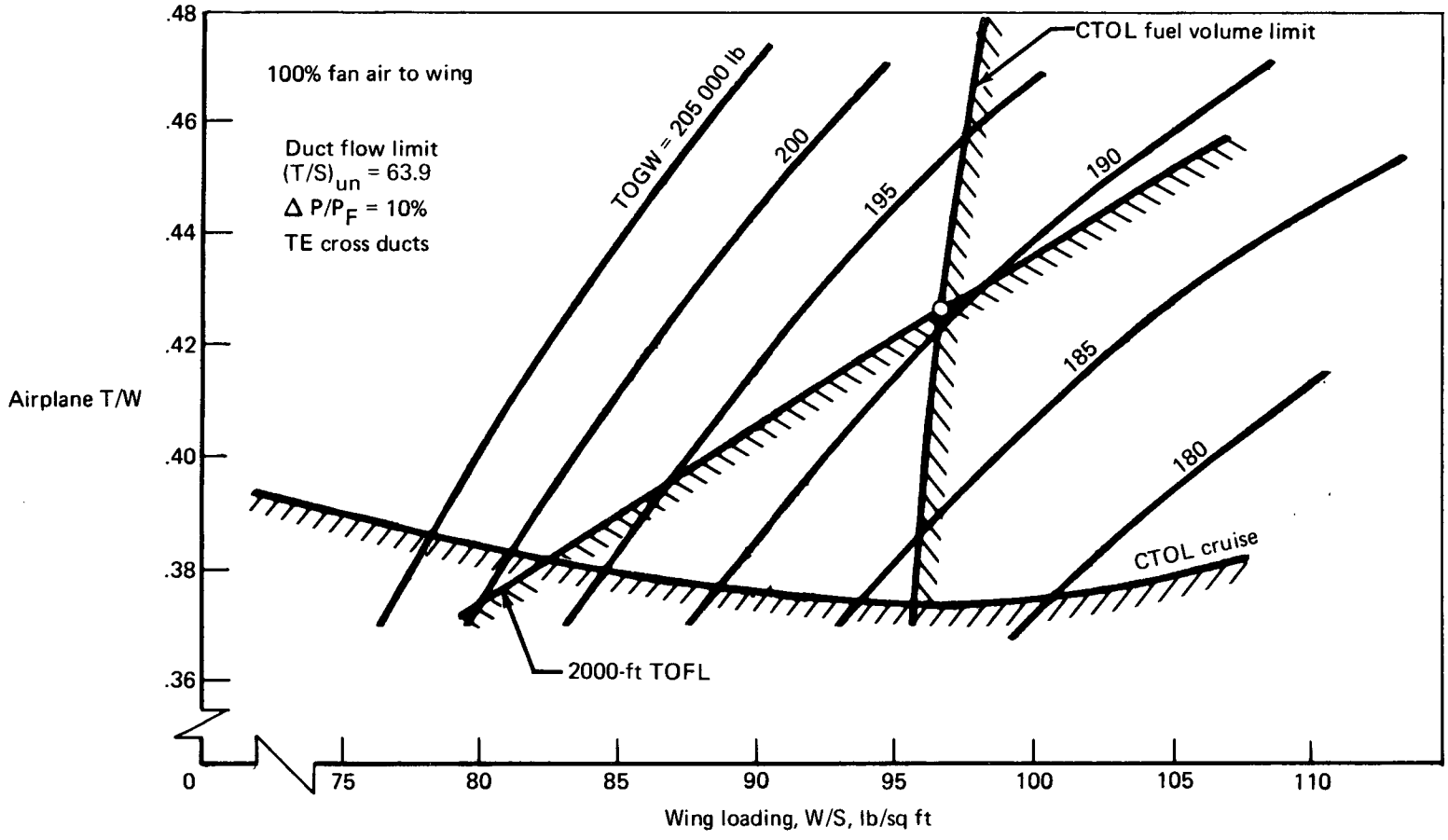

FIGURE 73.–AUGMENTOR WING CRUISE BLOWING SYSTEM AIRPLANE SIZING PARAMETERS, AR = 7.5, t/c = 0.157$_{outbd}$, 0.201$_{SOB}$, FPR = 3.75

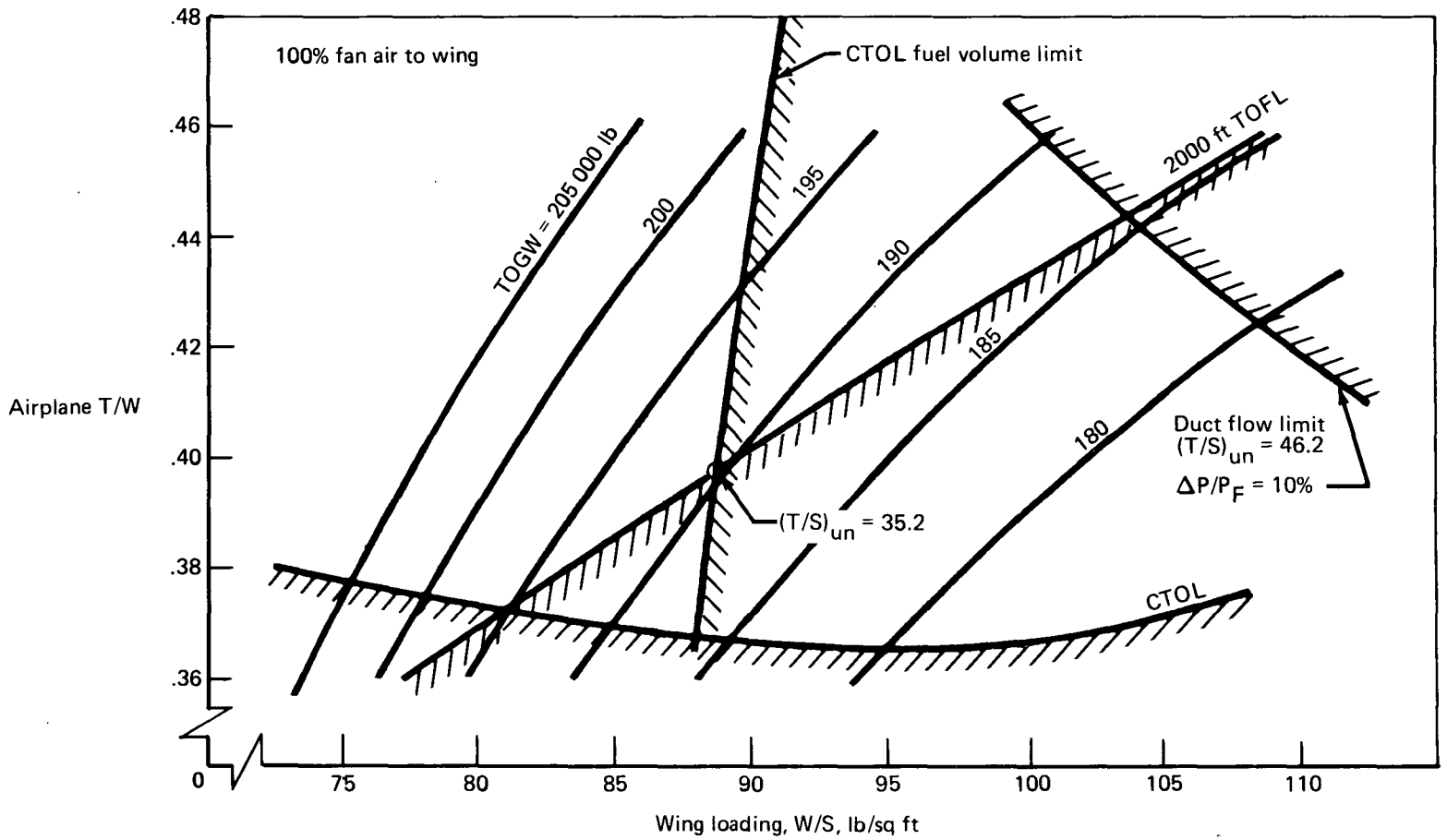

FIGURE 74.—AUGMENTOR WING CRUISE BLOWING SYSTEM AIRPLANE SIZING PARAMETERS, AR = 7.5, t/c = 0.132$_{outbd}$, 0.176$_{SOB}$, FPR = 3.75

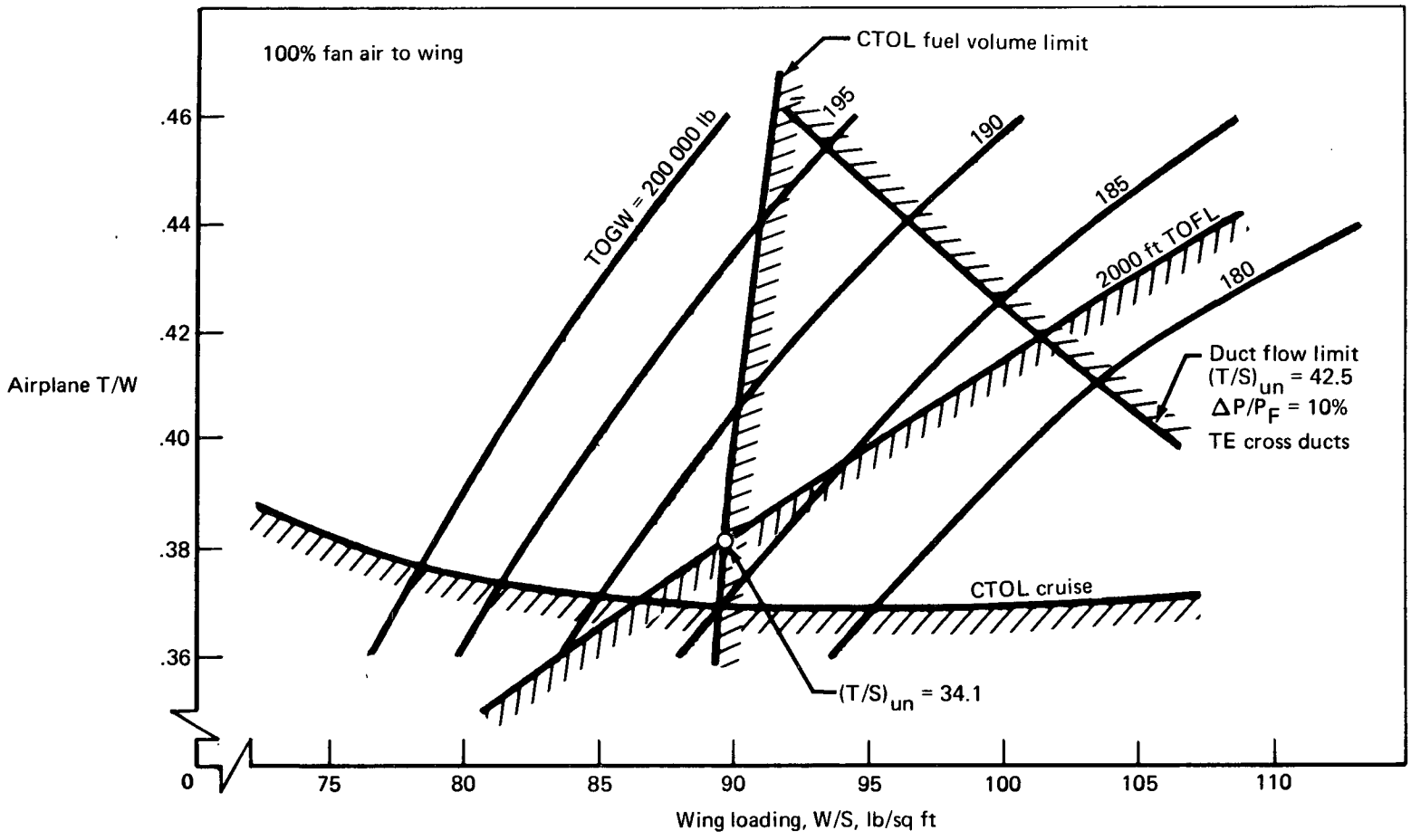

FIGURE 75.—AUGMENTOR WING CRUISE BLOWING SYSTEM AIRPLANE SIZING PARAMETERS, AR = 8.5, $t/c = 0.157_{outbd}$, 0.201_{SOB}, FPR = 3.75

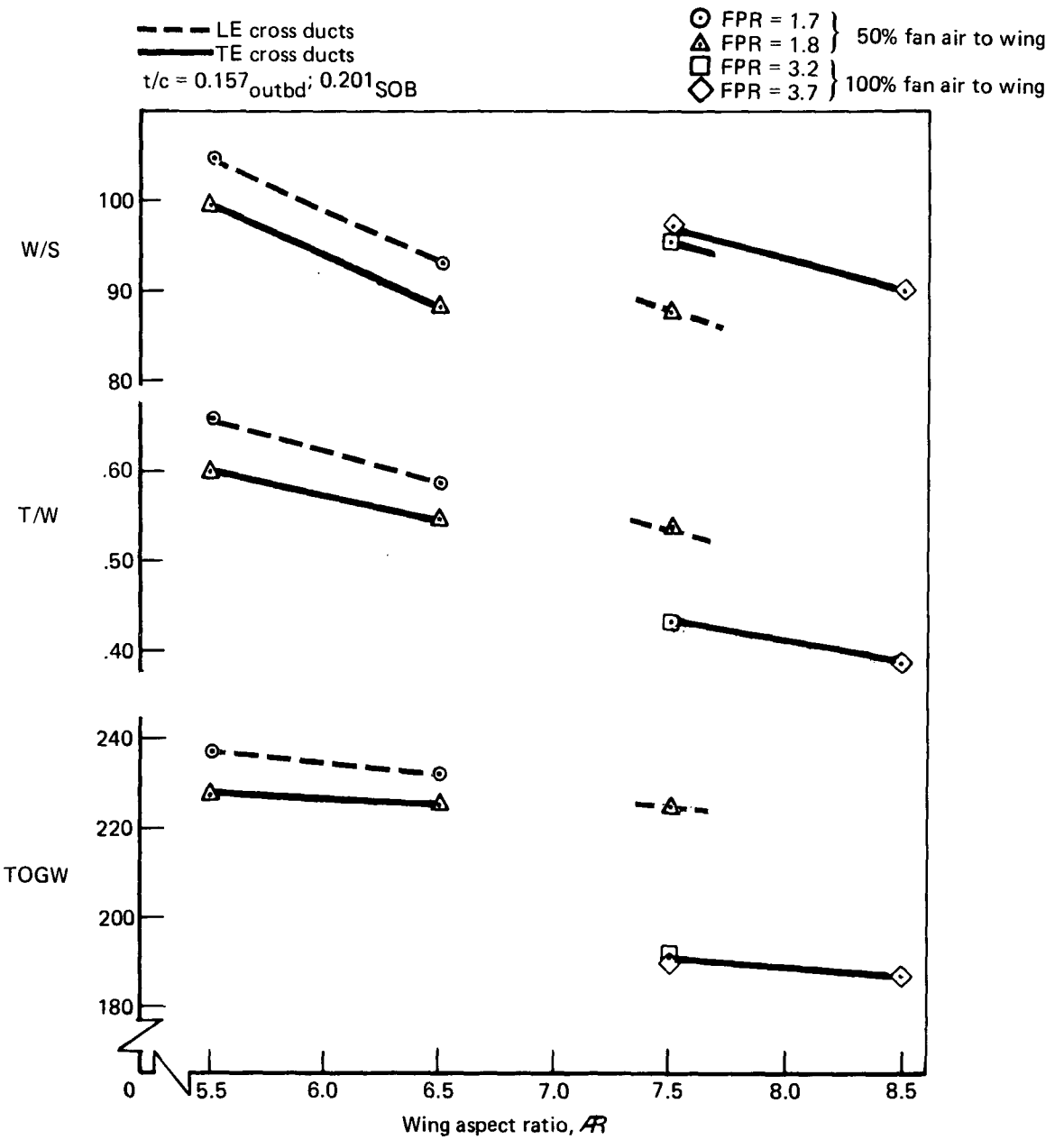

FIGURE 76.–EFFECT OF WING ASPECT RATIO ON MAJOR AIRPLANE CHARACTERISTICS, CRUISE BLOWING AUGMENTOR WING SYSTEM

The thinner wing (t/c_{outbd} = 0.137) at 7.5 aspect ratio provides acceptable wing loading of 89 lb/sq ft with small increases in TOGW and T/W. Compared with the 8.5 aspect ratio, $t/c = 0.157_{outbd}$, $\Delta P/P_F = 3.7$ design point, this represents substantially less technical risk from wing aeroelastic flutter and cruise drag rise problems while requiring an engine fan of three rather than four stages.

4.6.3.2 System Pressure Ratio Effects—System characteristics in the low- and high-pressure ratio ranges studied may be summarized comparatively in terms of the advantages of each as follows:

Low-Pressure System

- Better SFC
- Higher base engine thrust/weight

High-Pressure Systems

- Less duct volume required (At FPR above about 2.5, it is feasible to use all of the fan air in the wing blowing system, thus reducing the engine size needed to satisfy STOL thrust requirements.)
- Higher available cruise thrust because of low BPR and lower duct loss penalty on nozzle thrust
- Smaller installation penalty on engine thrust/weight
- Smaller engine ram drag effects during takeoff due to lower engine airflow
- Smaller nacelle size reduces drag
- Smaller thrust installation losses attributable to pressure drop in duct system
- Higher augmentation ratio because smaller nozzles improve augmentor flap geometry
- Lower cruise drag of the exposed nozzles used in the valveless concept

Figure 77 displays the combined effects of these several factors in STOL airplanes selected from the point designs of section 4.6.2. The curves are for the thicker of the two airfoils in the study ($t/c = 0.157_{outbd}$; 0.201_{SOB}), duct loss, $\Delta P/P_F$ = 10%, and with the aspect ratio for the lowest TOGW at each pressure level. The curves show that 6.5 aspect ratio gave lowest weight, 224 000 to 230 000 lb TOGW for the low pressures compared with the aspect ratio 8.5 at 189 000 lb TOGW match point with FPR = 3.75.

As indicated above, the high-pressure systems permit smaller nacelles, use of the trailing edge cross-duct configuration (eliminating external transfer ducts) and higher wing aspect ratio, all of which contribute to a moderate improvement in lift/drag compared with the low-pressure systems. The uninstalled thrust/weight advantage of the low-pressure engine is not

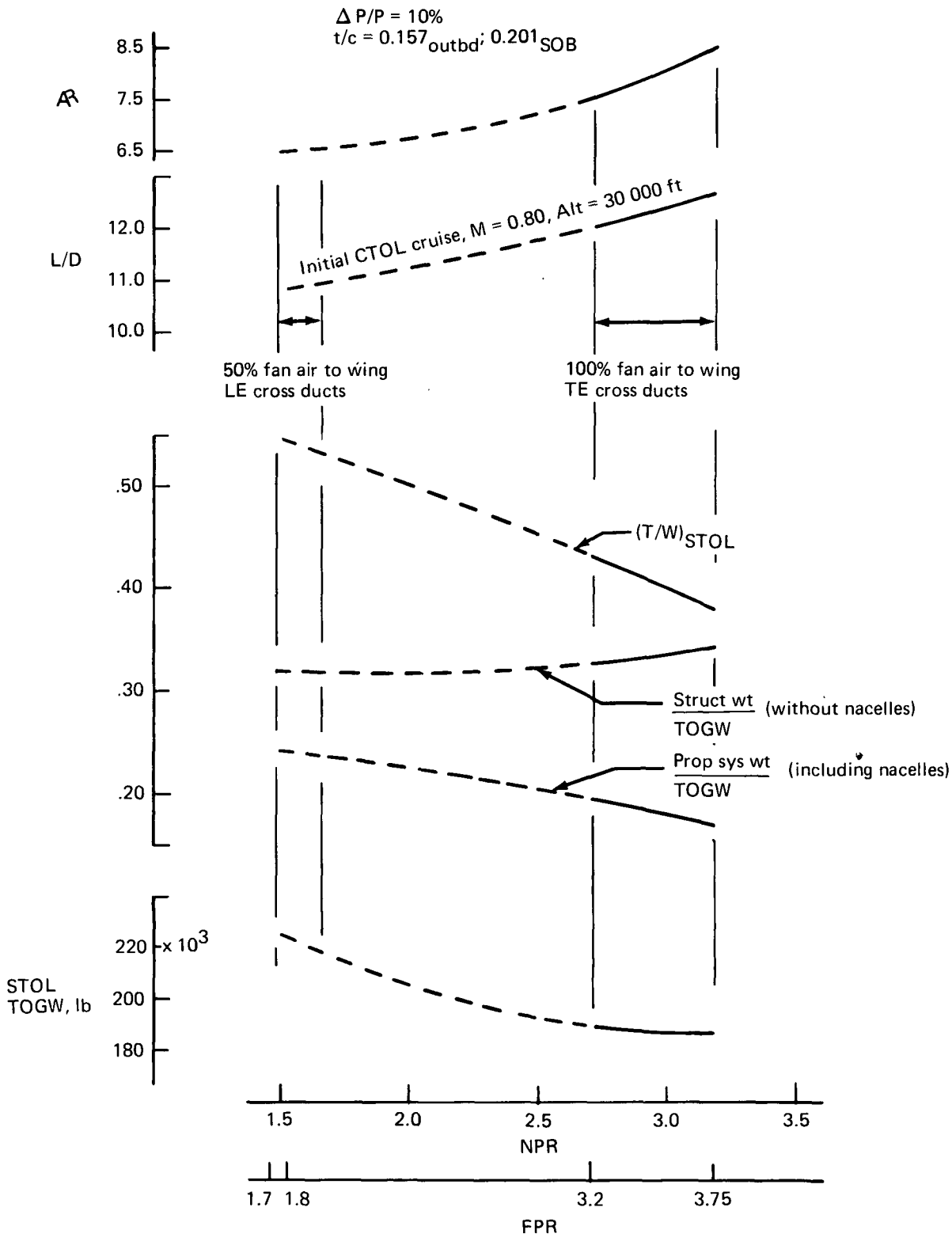

FIGURE 77.– EFFECT OF SYSTEM PRESSURE ON MAJOR AIRPLANE CHARACTERISTICS, CRUISE BLOWING AUGMENTOR WING SYSTEM

B

realized in the airplane because of thrust loss and weight in the installation, (fig. 59). At the same time, the installed cruise thrust fraction of the high-pressure engine is 35% to 40% higher (fig. 58).

The high-pressure systems thus show a substantial advantage in engine size, as indicated by relating the airplane thrust/weight ratios and takeoff gross weights of figure 77. The effect of this is further delineated by the structural weight/TOGW and propulsion-system-weight/TOGW fractions shown in which structural weight varies from 31% to 35% while propulsion weight varies from 25% to 17% for low-pressure versus high-pressure systems.

It should be reiterated that the low-pressure systems could be further optimized: (a) by increasing the cruise/takeoff turbine temperature ratio to reduce the thrust lapse, or (b) by reducing the portion of fan air directed to the wing.

A change in the assumed turbine temperature ratio would involve reassessment of the engine life characteristics of the STF-395D, which was the baseline engine used in the study. This was considered outside the scope of this program.

Reduction in the proportion of fan air to the wing, while reducing the effective cruise thrust lapse, adversly affects the powered lift and the augmented thrust in the takeoff mode, so that takeoff and cruise constraints rapidly converge to a match point with little improvement in airplane weight.

Preliminary assessment of these possible approaches showed that the maximum TOGW improvement to be realized would be about 1%. This would not substantially affect the basic comparison between the low- and high-pressure systems.

4.6.3.3 Wing Thickness Effects—The two wing thicknesses evaluated (t/c - 0.137_{outbd}; 0.176_{SOB} and 0.157; 0.201) are compared in figure 78 for 7.5 wing aspect ratio and 3.2 FPR. While the thicker wing provides about 0.5% advantage in takeoff gross weight with wing loading of 95 lb/sq ft and T/W = 0.43, only 75% of the available duct capacity (as measured by nozzle area per unit wing area (A_N/S) with $\Delta P/P_F$ = 10%) is utilized when adjustment is made for fuel volume requirements of the CTOL mission. By comparison, the thinner wing at W/S = 88 lb/sq ft yields 8.5% reduction in engine size with about 87% of the available duct capacity utilized. A portion of the engine size advantage is derived from the lower A_N/S with accompanying improved augmentor nozzle/flap relationship and resulting higher thrust augmentation. Further optimization is possible as discussed below to obtain a final match point with further reduction in engine size for this airplane.

4.6.3.4 Duct Flow Velocity Effects—The iteration process in which the relationship of the design constraints, duct capacity, takeoff thrust, cruise thrust, and fuel volume is changed by varying the duct flow velocity includes adjustment of the thrust augmentation ratio with the varying nozzle area. The relationships of the parameters involved in this adjustment are shown in figure 79 as a function of wing loading (W/S) and without the constraint of duct flow area limit.

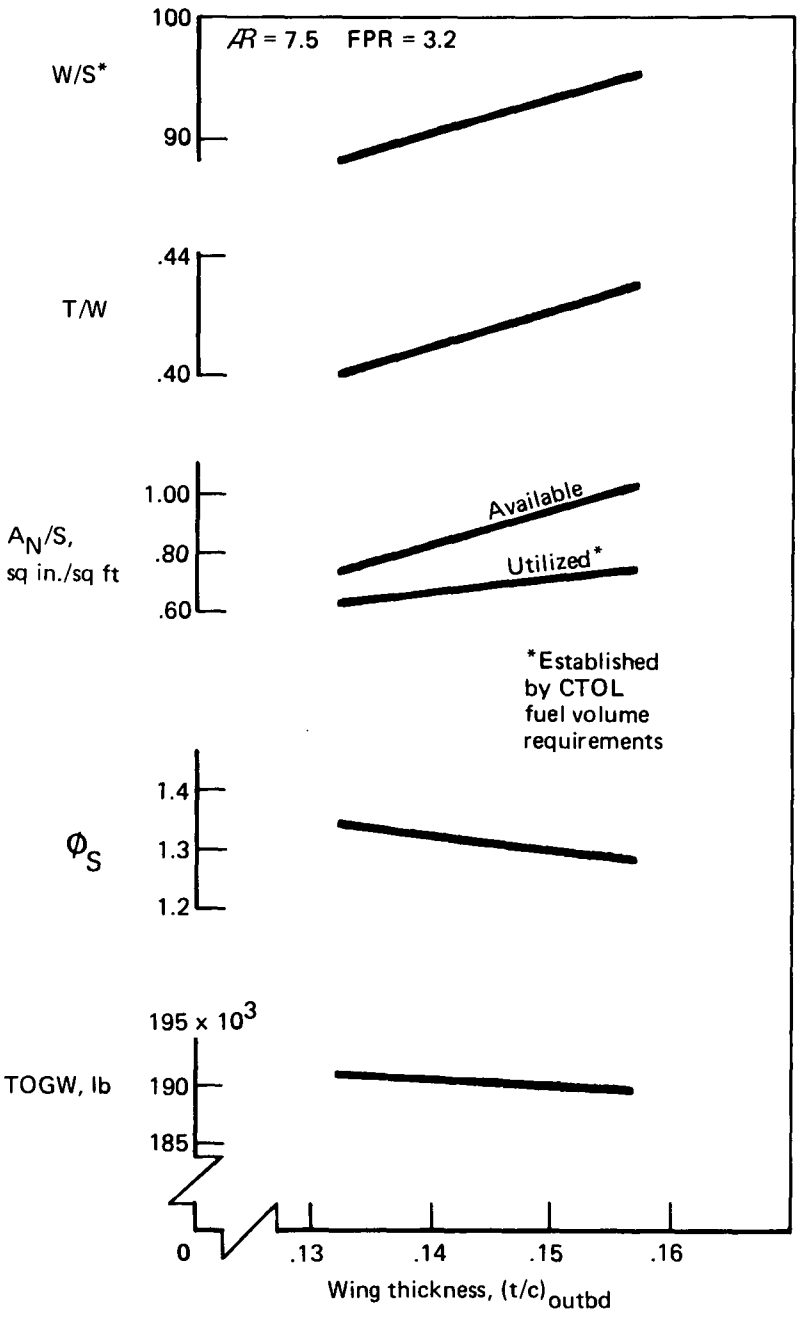

FIGURE 78.—EFFECT OF WING THICKNESS ON AIRPLANE DESIGN PARAMETERS

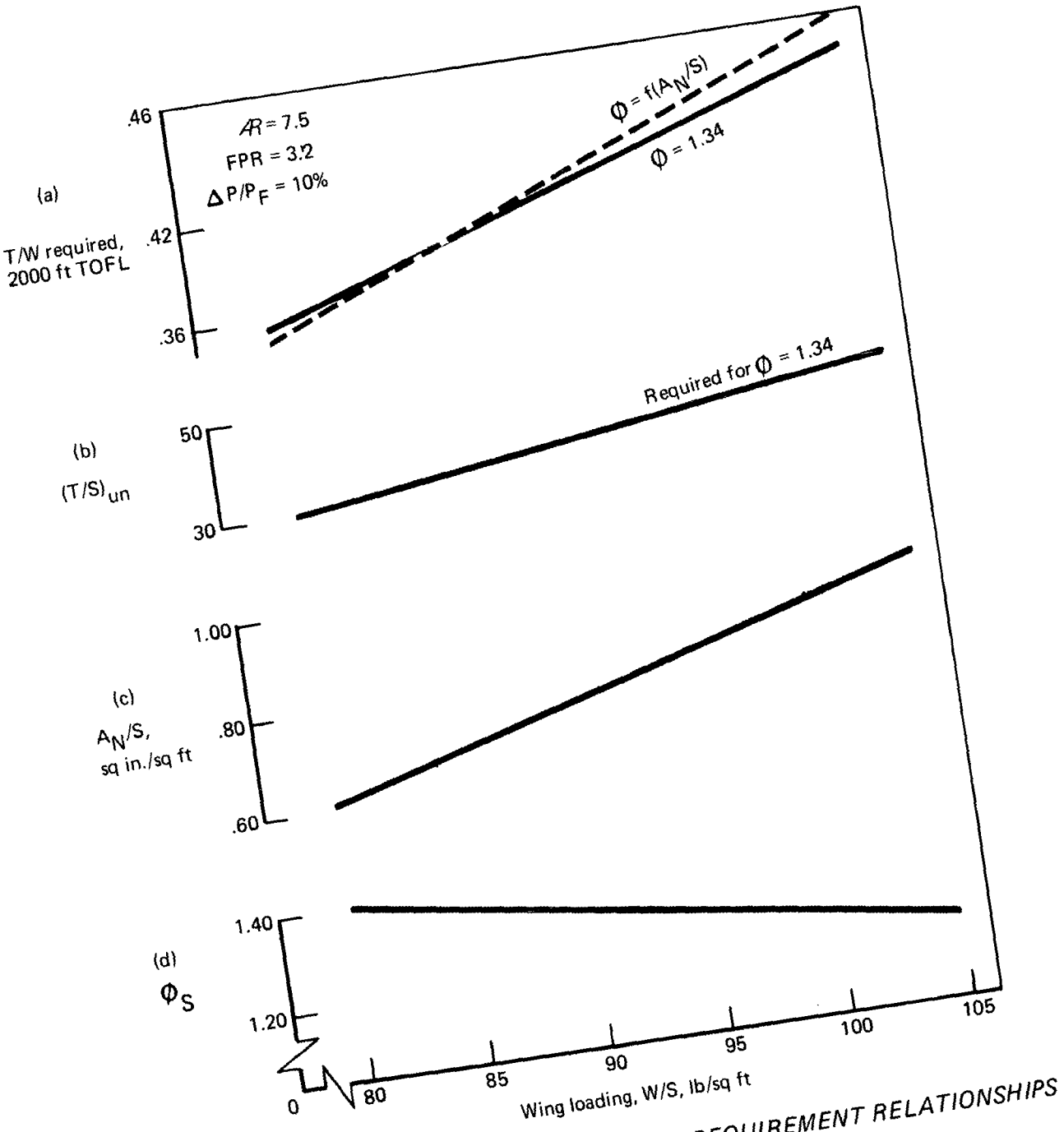

FIGURE 79.–AUGMENTATION AND THRUST REQUIREMENT RELATIONSHIPS AS FUNCTION OF WING LOADING

With a typical fixed augmentation ratio, the takeoff thrust/weight requirement increases with W/S, as indicated by the solid line of figure 79a. The corresponding increases in thrust loading (T/S) and relative nozzle area (A_N/S) are shown in figure 79b and c. However, such increase in nozzle area relative to flap chord (augmentor length) causes decreasing thrust augmentation, as indicated in figure 79d. The adjusted effect on thrust required with ϕ a function of the iterated A_N/S is represented by the dashed line in figure 79a.

This adjustment was applied in the parametric sizing curves of figures 80, 81, and 82, in which duct flow velocity was varied with the index $\Delta P/P_F$ = 11.5%, 9.6% and 8.2%, respectively.

Reviewing these figures, the 11.5% duct loss provides thrust in excess of the corresponding CTOL fuel volume limit and substantially higher than the engine size to meet the cruise requirement (fig. 80). As the duct velocity is reduced ($\Delta P/P_F$ = 9.6%, fig. 81), engine size to meet 2000-ft takeoff is also reduced due to the improving augmentation (ϕ). A match is achieved with reduced T/S (35.5), and the fuel volume limit, although at an engine size greater than needed for cruise. Further reduction in duct velocity to $\Delta P/P_F$ = 8.2% provides a match among T/S available, takeoff thrust, and cruise thrust, as shown in figure 82 at T/W = 0.38, W/S = 84 lb/sq ft, and TOGW = 191 500 lb. The fuel volume limit is not a factor. This design point was used for sizing the high-speed wind tunnel exploratory test model.

The pertinent parameters of these airplane design points are displayed in figure 83 as a function of duct velocity, using the index, $\Delta P/P_F$. The duct-flow-limited thrust per unit wing area (T/S) and maximum W/S are shown in figure 83a and b. The corresponding nozzle area (A_N/S) variation shown in figure 83c is caused primarily by nozzle area per unit thrust required to match the nozzle volume flow (NPR varying with duct $\Delta P/P_F$). This A_N/S changes more rapidly with W/S than if $\Delta P/P_F$ were constant. The resulting ϕ variations shown in figure 83d are therefore greater than would be the case if the duct volume limits on W/S were increased at constant $\Delta P/P_F$ by enlarging the duct.

Similarly, the changes in takeoff T/W shown in figure 83e are relatively larger for changes in W/S because of the additional effect of changes in nozzle thrust due to $\Delta P/P_F$ as well as changes in ϕ.

Although the blowing system weight for a constant wing area varies with duct $\Delta P/P_F$ due to the variations in A_N/S, this effect is offset in the actual case by the duct weight, which changes with wing area.

As the $\Delta P/P_F$ losses are increased, installed specific fuel consumption and fuel volume requirement also increase; however this is partially compensated by lower weight and drag of the smaller wing as W/S simultaneously increases. The resulting effect on airplane takeoff gross weight is 1000 lb or about 0.5% as $\Delta P/P_F$ varies from 8.2% to 11.5%.

This relative insensitivity of the airplane weight to duct velocity provides a useful avenue for the final engine/airframe matching process. Furthermore, by matching to the lower velocity ($\Delta P/P_F$ = 8.2%), a thrust growth capability of as much as 20% is available through increased fan flow accompanied by appropriate adjustment of nozzle area.

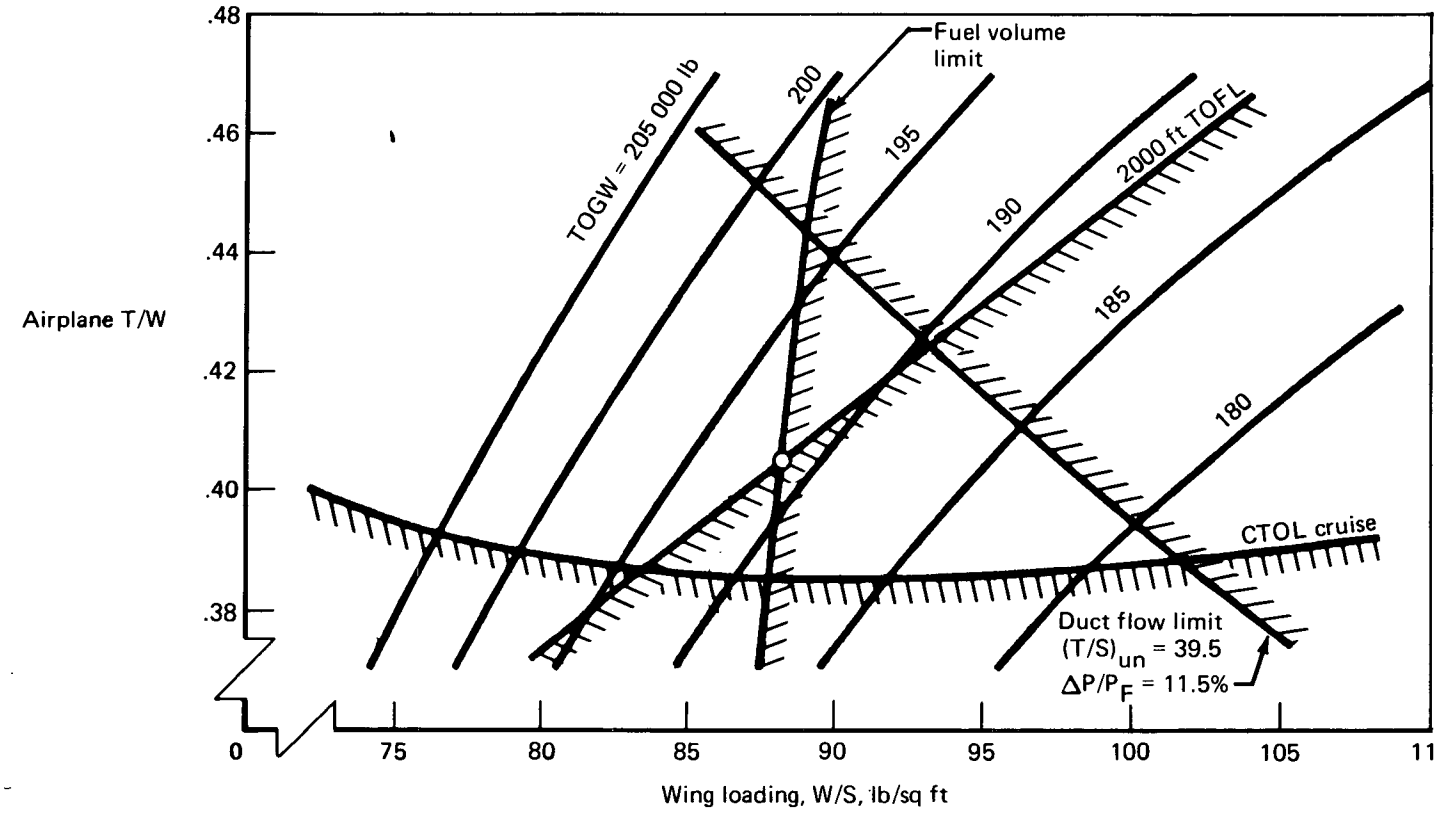

FIGURE 80.—AUGMENTOR WING CRUISE BLOWING SYSTEM AIRPLANE SIZING PARAMETERS, AR = 7.5, t/c = 0.132$_{outbd}$, 0.176$_{SOB}$, FPR = 3.2, $\Delta P/P_F$ = 11.5%

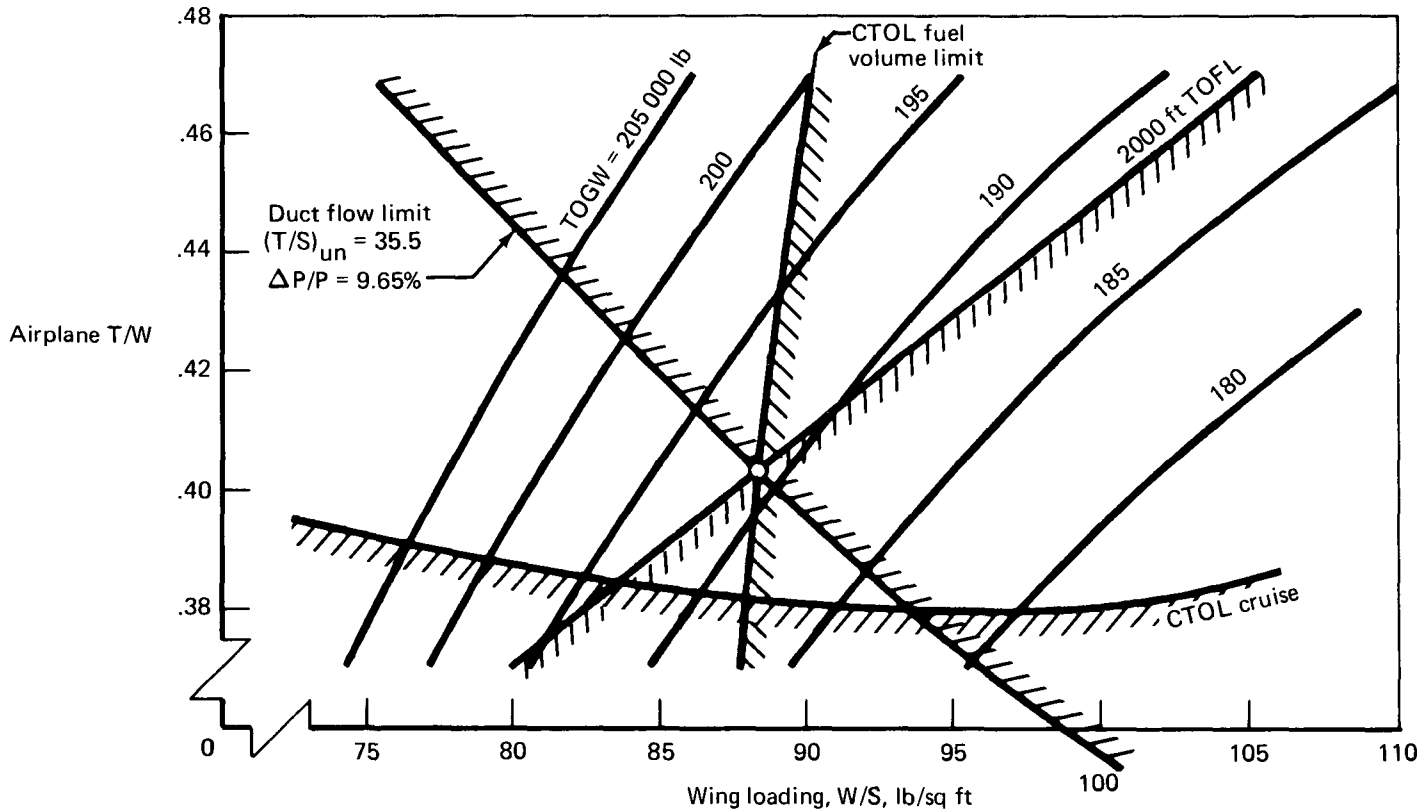

FIGURE 81.—AUGMENTOR WING CRUISE BLOWING SYSTEM AIRPLANE SIZING PARAMETERS, $AR = 7.5$, $t/c = 0.132_{outbd}$, 0.176_{SOB}, FPR = 3.2, $\Delta P/P_F = 9.65\%$

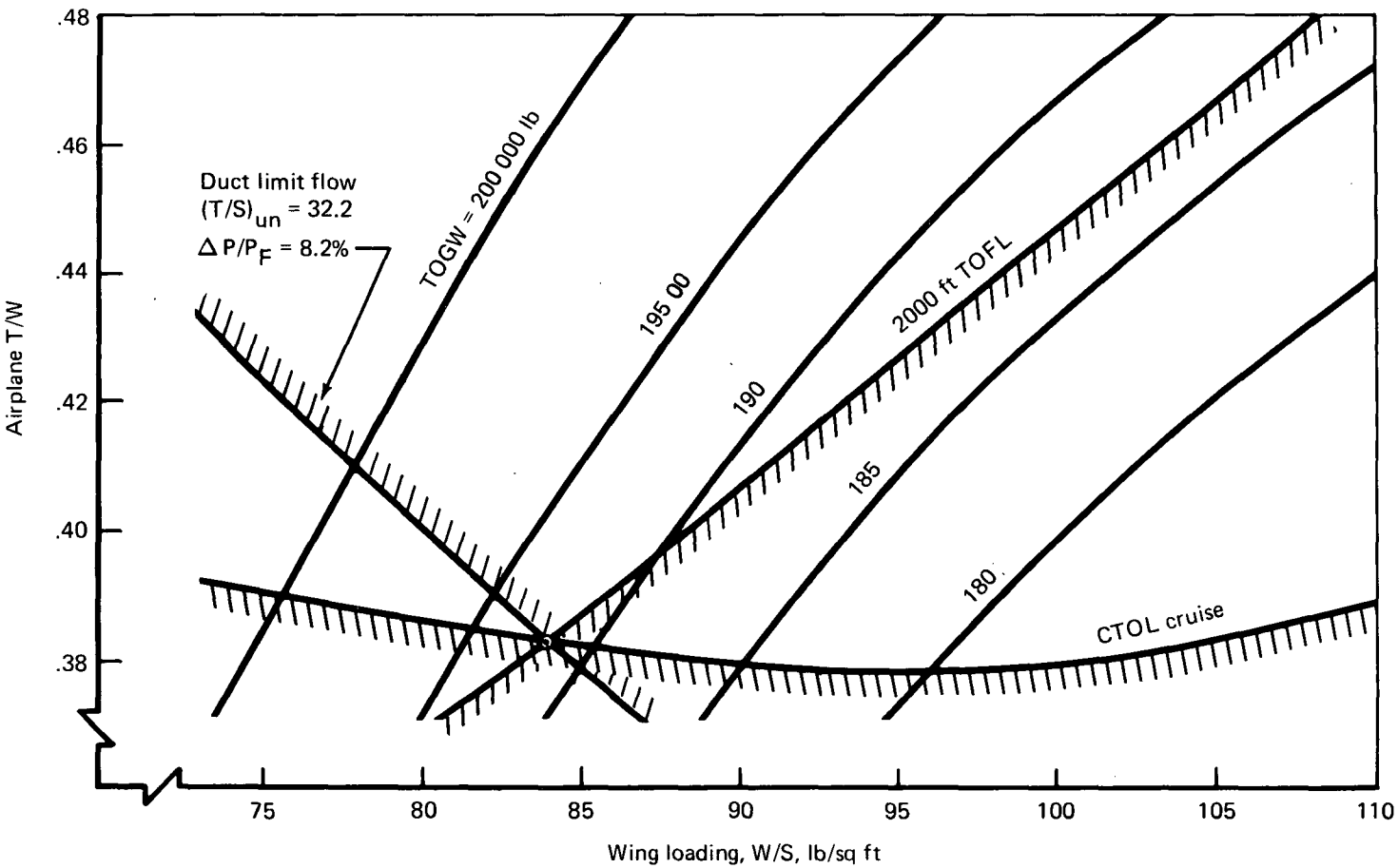

FIGURE 82.—AUGMENTOR WING CRUISE BLOWING SYSTEM AIRPLANE SIZING PARAMETERS, AR = 7.5, $t/c = 0.132_{outbd}$, 0.176_{SOB}, FPR = 3.2, P/P_F = 8.2%

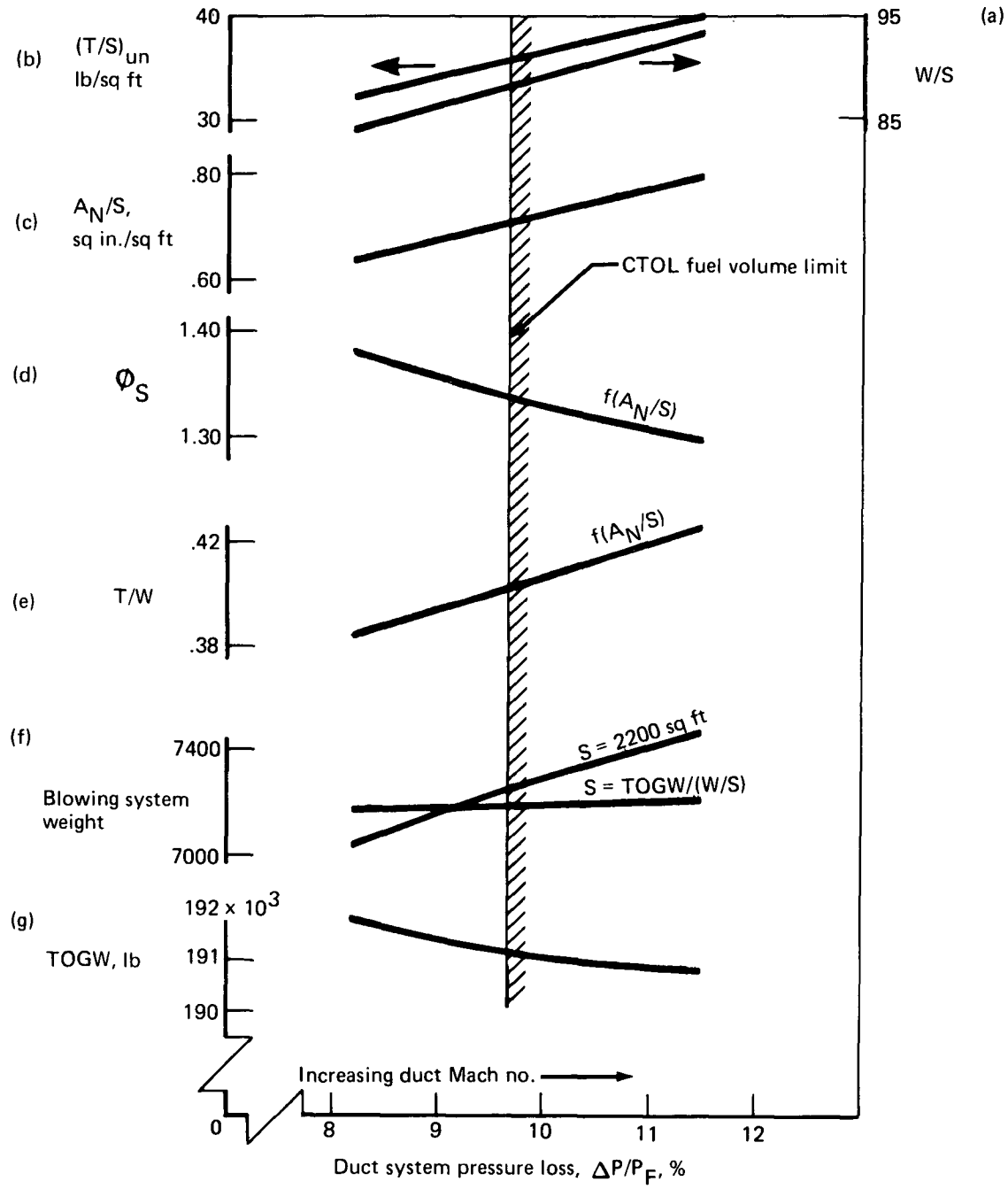

FIGURE 83.—EFFECT OF DUCT FLOW VELOCITY ON AIRPLANE DESIGN CHARACTERISTICS, AR = 7.5, FPR = 3.2, CONSTANT DUCT CONFIGURATION

4.6.4 Airplane Integration Summary and Definition of Selected Configuration

In assessing the range of system variables studied, the low and high pressures, combined with duct system, wing thickness, and aspect ratio appropriate to each, yield an airplane take-off gross weight advantage of about 20% for FPR = 3.75 compared with FPR = 1.7.

Several characteristics together cause this advantage in the high-pressure system, including:

- One half the thrust loss associated with duct flow loss
- Lower duct volume required permitting a more efficient, higher aspect ratio, thinner wing
- Superior cruise/takeoff engine thrust ratio
- Installed thrust and weight penalties which nullify the inherent thrust/weight advantage of the low-pressure, high-bypass engine in the augmentor wing application

A design point with FPR = 3.2 discussed in sections 4.6.2.2 and 4.6.3.4 was chosen for sizing test models to limit the engine fan to three stages.

Wing aspect ratio and thickness were also selected to minimize possible risk of flutter and cruise drag problems.

With these compromises, the selected configuration retains a 17% gross weight advantage and a 47% engine thrust-size advantage over the FPR = 1.7 configuration. Table 4 compares the low and high pressure with the selected system.

TABLE 4.–WEIGHT COMPARISON AT VARIOUS FAN PRESSURE RATIOS

FPR	Cross duct config	Fan air to wing, %	Wing aspect ratio	t/c outbd; SOB	Engine size, SLST, lb; location	TOGW, lb	Noise PNdB*
1.7	LE	50	6.5	0.157; 0.201	34 700 overwing	232 100	103
3.75	TE	100	8.5	0.157; 0.201	17 800 underwing	186 700	–
3.2 (Selected)	TE	100	7.5	0.132; 0.176	18 300 underwing	191 500	90

*500-ft sideline, takeoff

5.0 CONCLUSIONS

- Compared with the reference valved augmentor wing configuration, the cruise blowing configuration gives an increase in available duct volume through use of a 10% thicker wing section and by placing the nozzles outside the wing surface. This volume, together with the lower flow losses of the valveless arrangement, can be used to increase the wing aspect ratio of the high-pressure design.

- The system recommended for sizing the high-speed exploratory wind tunnel test model has the following characteristics:

TOGW	191 500 lb
Wing loading	84 lb/sq ft
Aspect ratio	7.5
Wing sweep angle (0.25c)	25°
Wing thickness	0.132_{outbd}, 0.176_{SOB}
SLST (uninstalled), four engines	18 300 lb
FPR	3.2
NPR	2.7

- There is insufficient wing duct volume for a two-stream, low-pressure (single-fan stage) configuration at moderate wing loadings. A split-flow system with part of the fan air discharging through a conventional nozzle in the nacelle is therefore required to match the available duct volume.

- Dispite use of the split fan flow, the large wing nozzle area required in the low-pressure system gives a low augmentor mixing length ratio ($L/h_{\bar{E}}$) resulting in relatively poor static augmentation of 1.14 compared with 1.30 estimated for the high-pressure system.

- The low-pressure augmentor is not advantageous for noise because of the large wing nozzle area, poor suppression characteristics of the low-pressure-ratio jet and short relative flap length for acoustic lining. However, the aft fan turbomachinery and nacelle jet on the split-flow system are the dominant noise sources and limit the system noise floor to 103 PNdB at the 500-ft sideline.

- An overwing nacelle is desirable to decrease nacelle-fuselage interference and to use wing shielding for noise suppression for the low-pressure system.

- Vectoring the engine thrust on the split-flow, low-pressure system would enhance the approach flight path control and provide a slight reduction in takeoff thrust/weight required. However, this reduction is of minimum value because the engine is sized by cruise thrust requirements. Furthermore, vectoring increases the noise of the nacelle nozzle stream.

- Due to the basic relationship of blowing nozzle thrust with pressure ratio and duct flow loss, a substantially higher loss in thrust (a factor of 2.5) is incurred for the

same percentage duct pressure loss in the low-pressure system compared with the selected high-pressure system.

- Because of unfavorable installed cruise thrust fraction, $T_{cruise}/T_{SLS_{un}}$, (thrust lapse) of the low-fan-pressure engines, these engines are sized by the cruise requirement rather than by takeoff. Compared with high-bypass engines tailored to long-range commercial jet aircraft requirements, the basic thrust of the augmentor wing STOL engine cycle is adjusted downward to account for frequency of duty cycle and for overextraction in the turbine to limit velocity of the primary jet so as to match the noise attenuation available in the augmentor.

- Installation weight and thrust loss negate the takeoff thrust/weight advantage inherent in the basic low-fan-pressure, high-bypass engine.

- The reduction in airplane gross weight to 186 700 lb by use of fan pressure ratio of 3.75 and wing aspect ratio of 8.5 with t/c_{outbd} of 0.157 is not judged sufficient to justify development of the four-stage engine fan together with the potential risk of drag rise and/or flutter problems with the thick, high-aspect-ratio wing.

- Expandable duct concepts explored as a means of increasing duct volume are not compatible with cruise blowing systems without introducing complexities such as diverter valves and variable nozzles or ducts-within-ducts, which are inconsistent with the objectives of simplifying the augmentor system.

APPENDIX

AUGMENTOR WING EXPANDABLE DUCT CONCEPT DRAWINGS

This appendix contains the following drawings.

Concept Number (Table 1)	Drawing Number	Title
4	LO-DNS-203	Retractable Lobe Nozzle, Expandable Ducts
5	LO-DNS-213	External Expandable Duct, In-Wing Lobe Nozzle
6	LO-DNS-211	Expandable Duct, Flap Drop Panel, Slot Nozzle
7	LO-DNS-204	Drop Panel, Lobe and Slot Nozzle
8	LO-DNS-210	Expandable Duct Underwing Drop Panel
9	LO-DNS-212	Valveless Augmentor and Cruise Slot Nozzle
9	LO-DNS-214	Slot Nozzle, Augmentor and Cruise
10	LO-DNS-217	Fixed Slot Nozzle, Augmentor and Cruise Mode

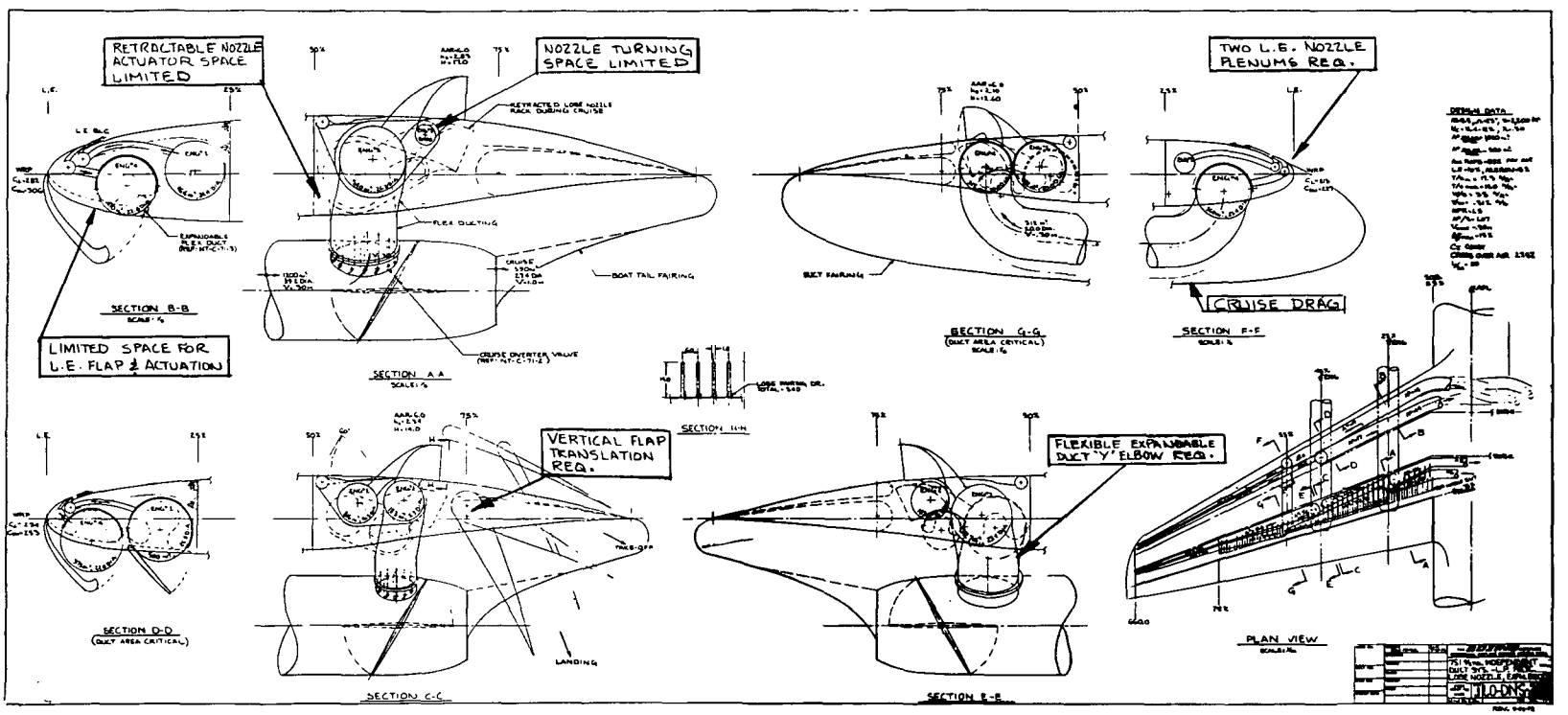

LO-DNS-203–RETRACTABLE LOBE NOZZLE, EXPANDABLE DUCTS

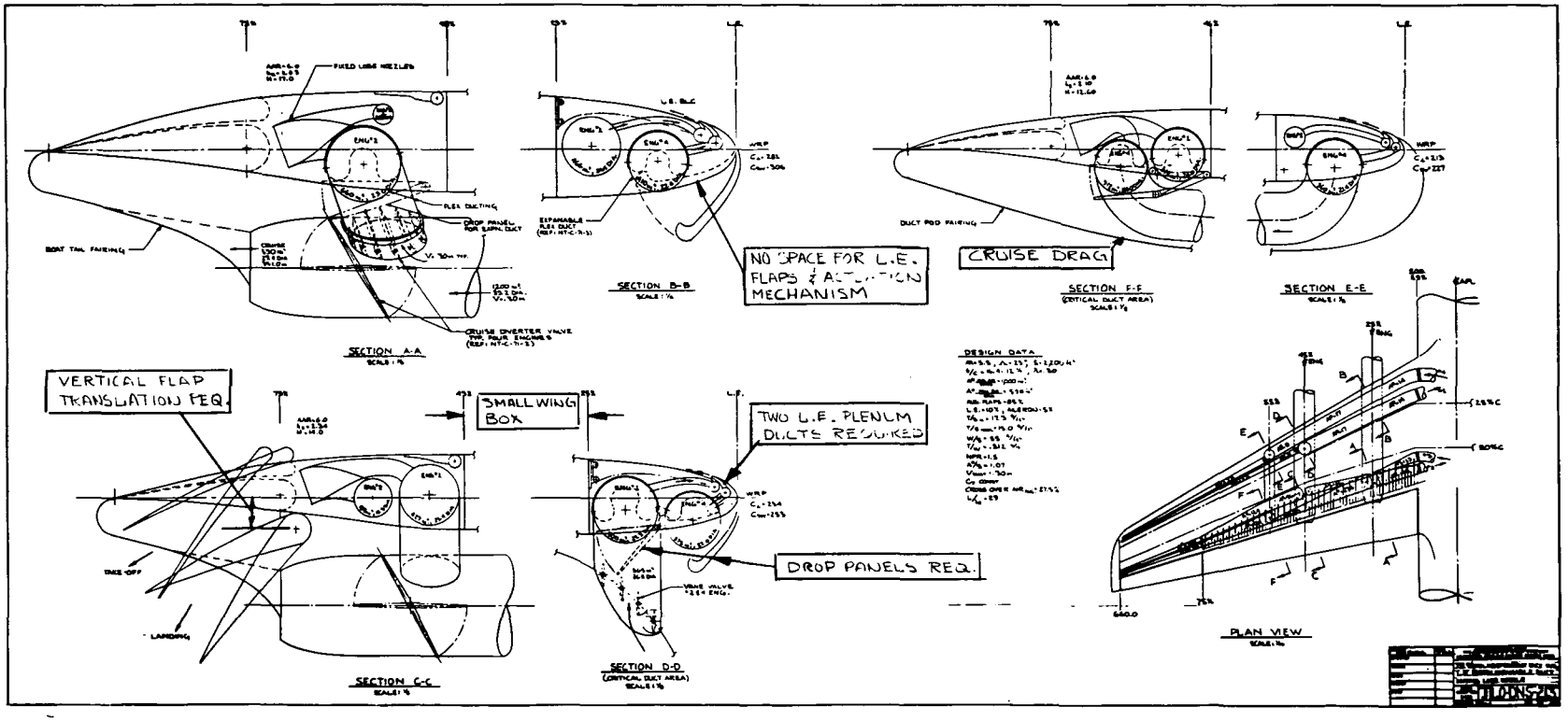

LO-DNS-213–EXTERNAL EXPANDABLE DUCT, IN-WING LOBE NOZZLE

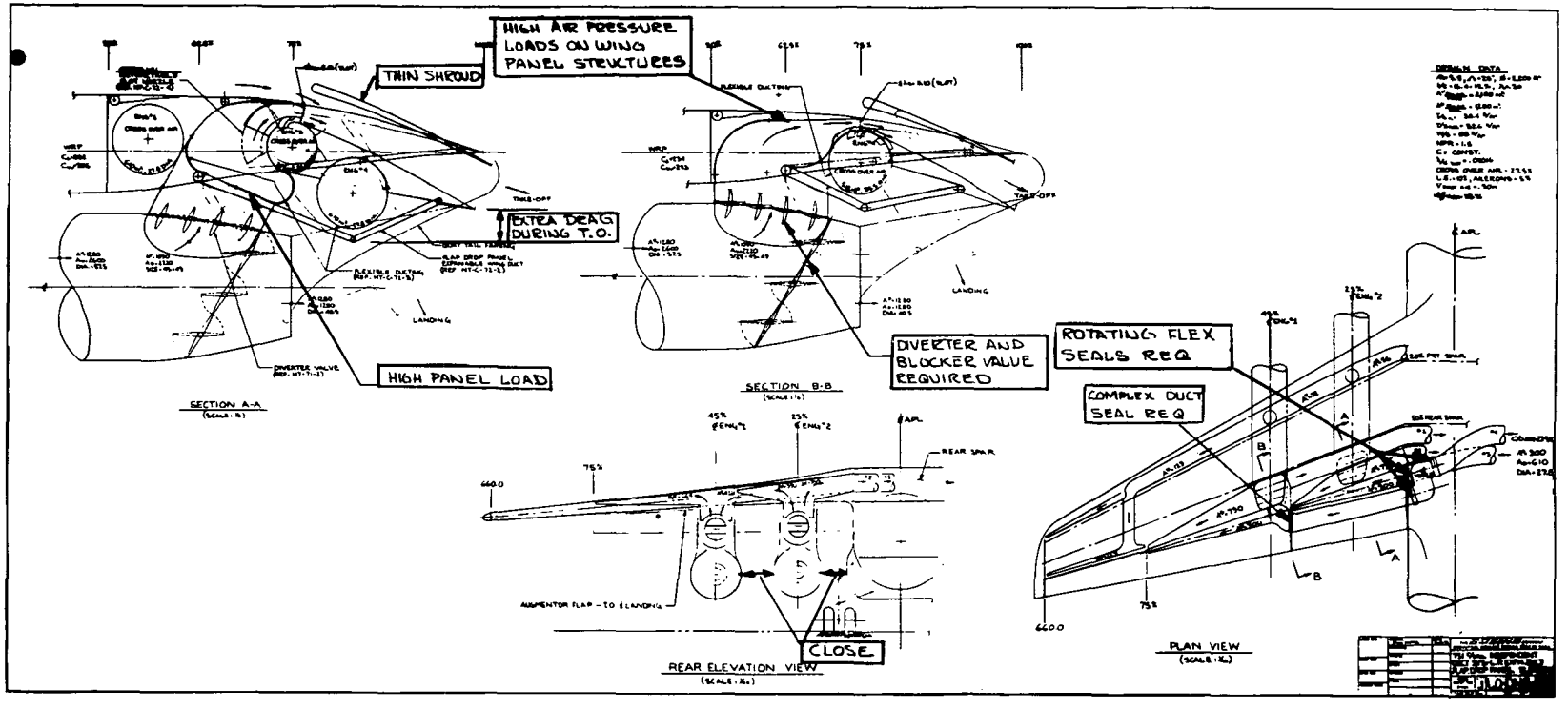

LO-DNS-211—EXPANDABLE DUCT, FLAP DROP PANEL, SLOT NOZZLE

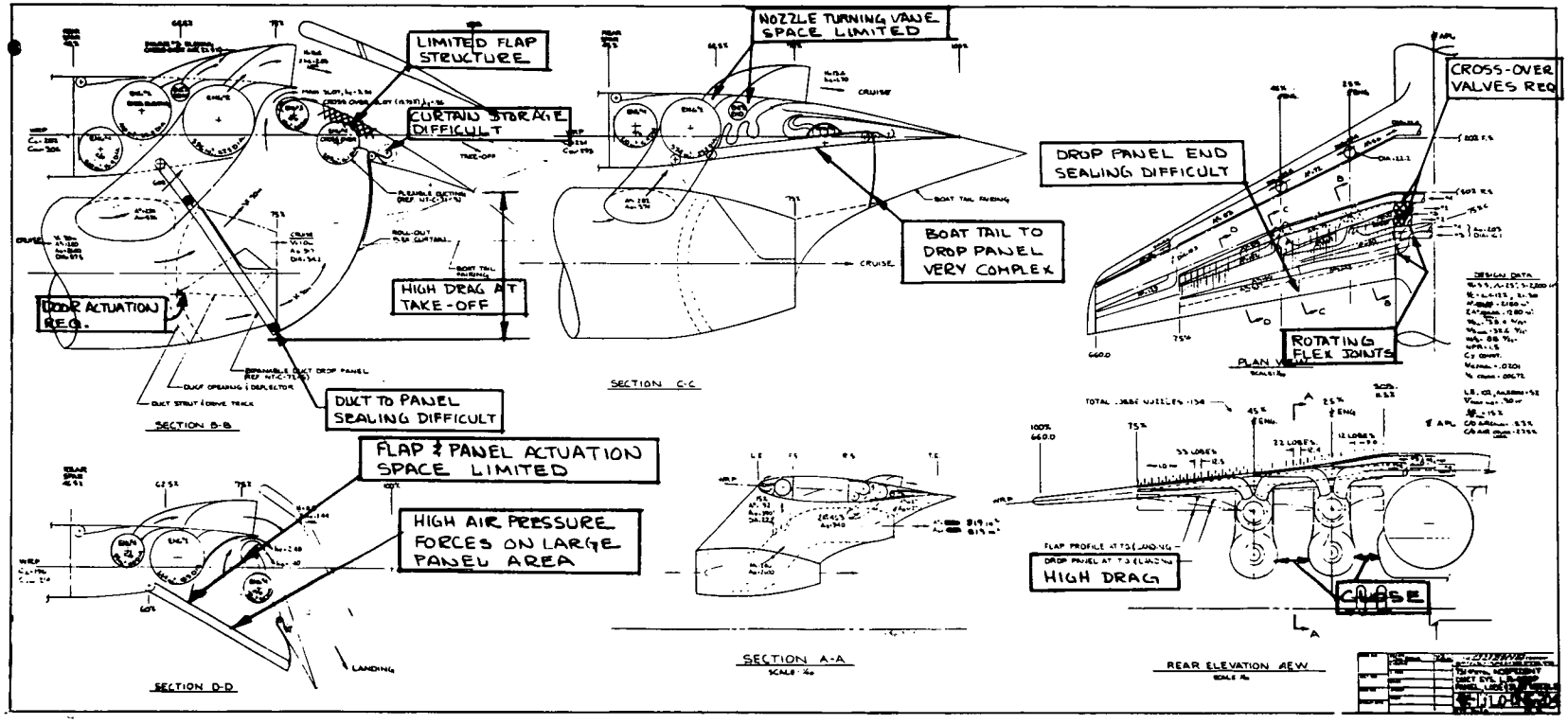

LO-DNS-204—DROP PANEL, LOBE AND SLOT NOZZLE

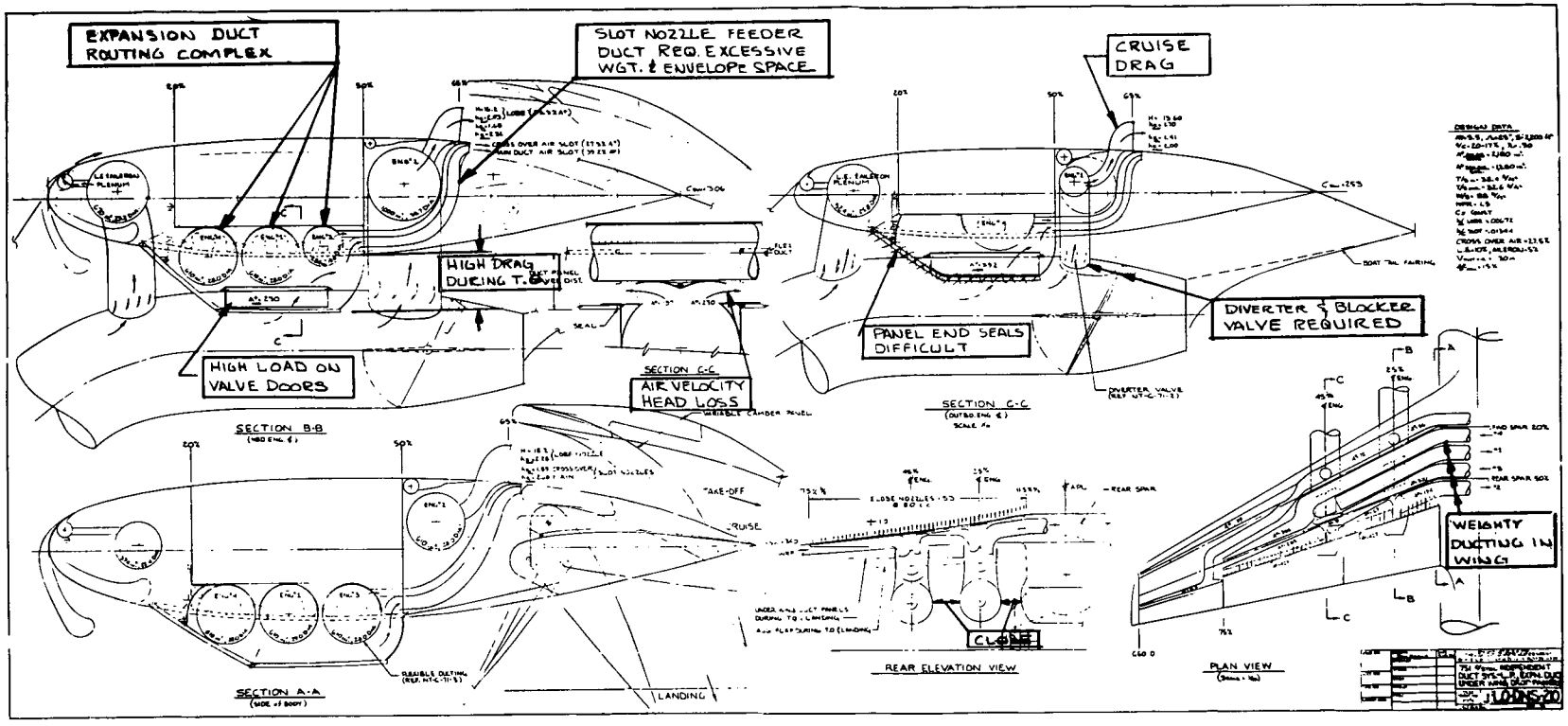

LO-DNS-210—EXPANDABLE DUCT UNDERWING DROP PANEL

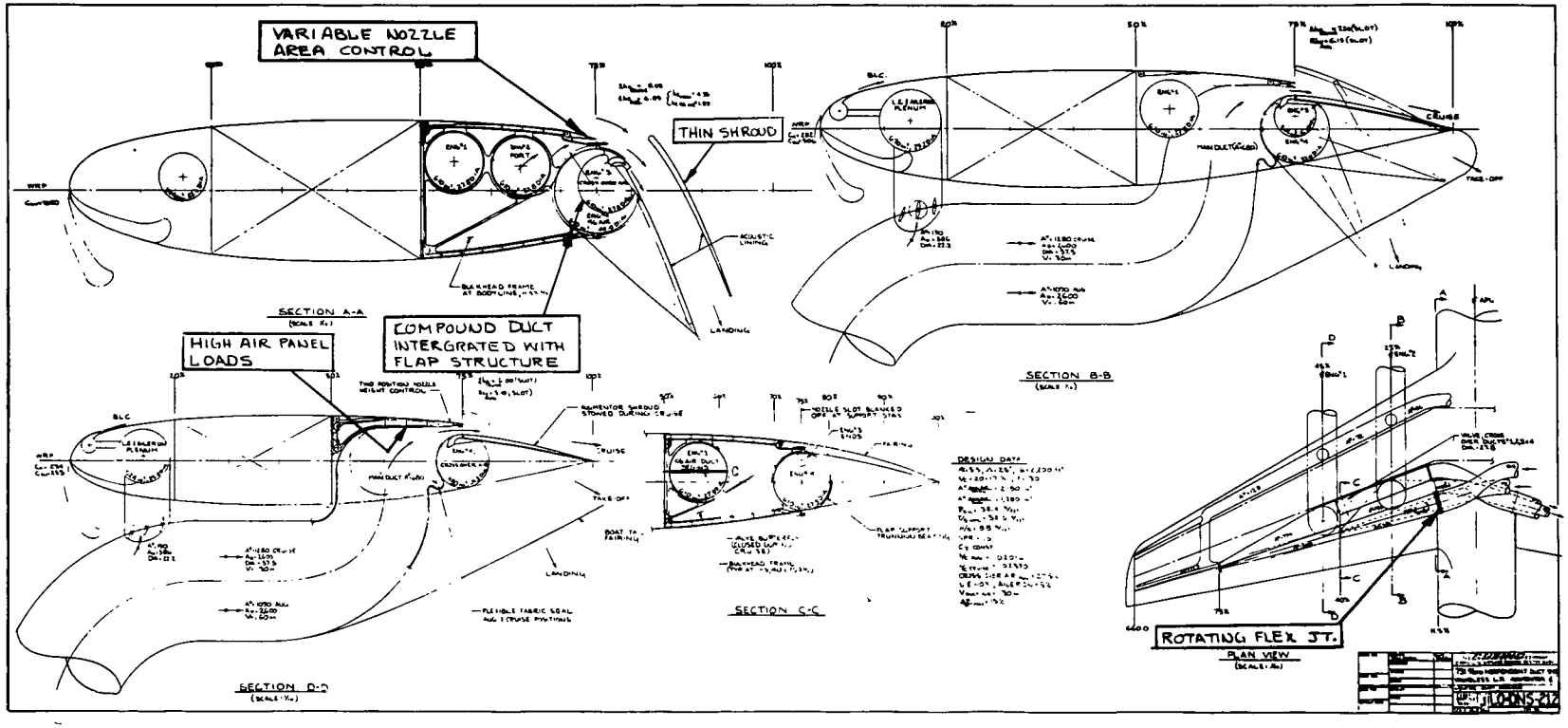

LO-DNS-212—VALVELESS AUGMENTOR AND CRUISE SLOT NOZZLE

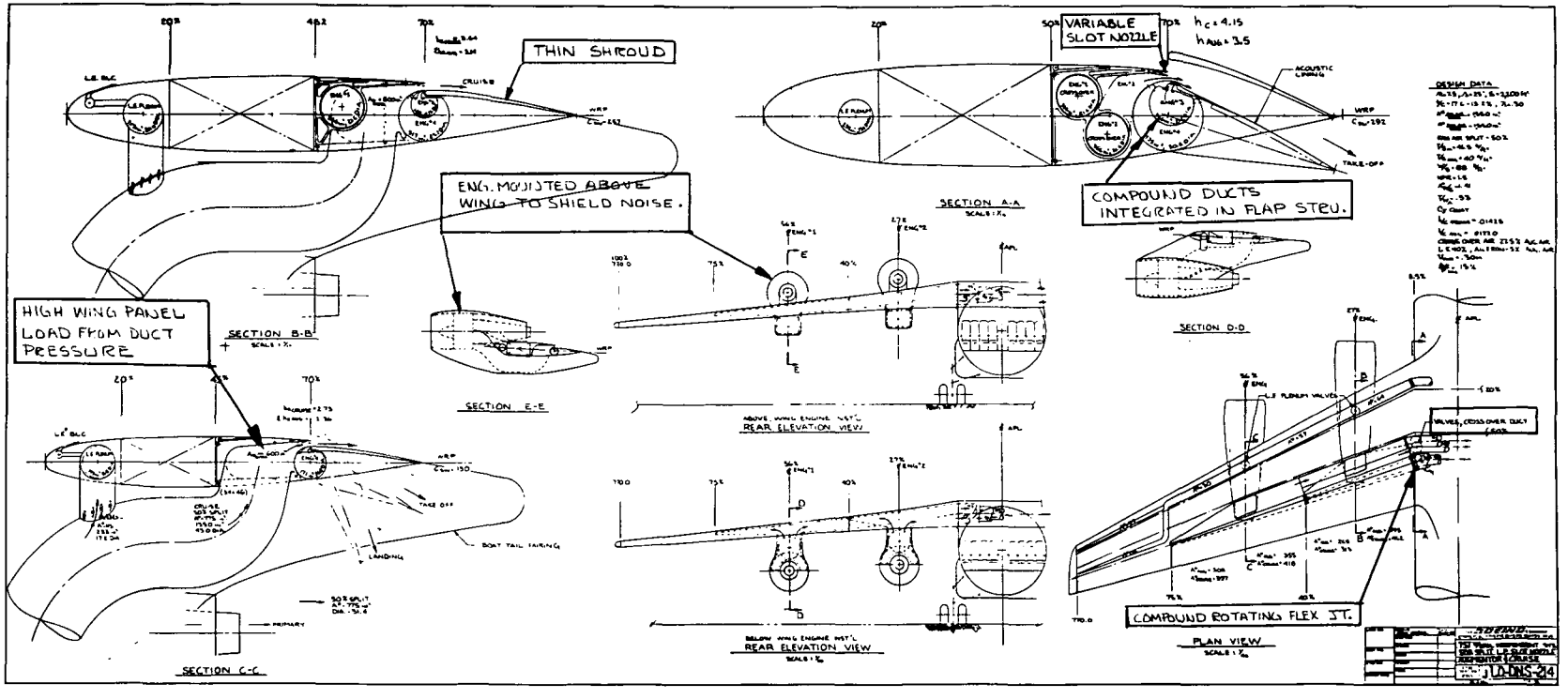

LO-DNS-214—SLOT NOZZLE, AUGMENTOR AND CRUISE

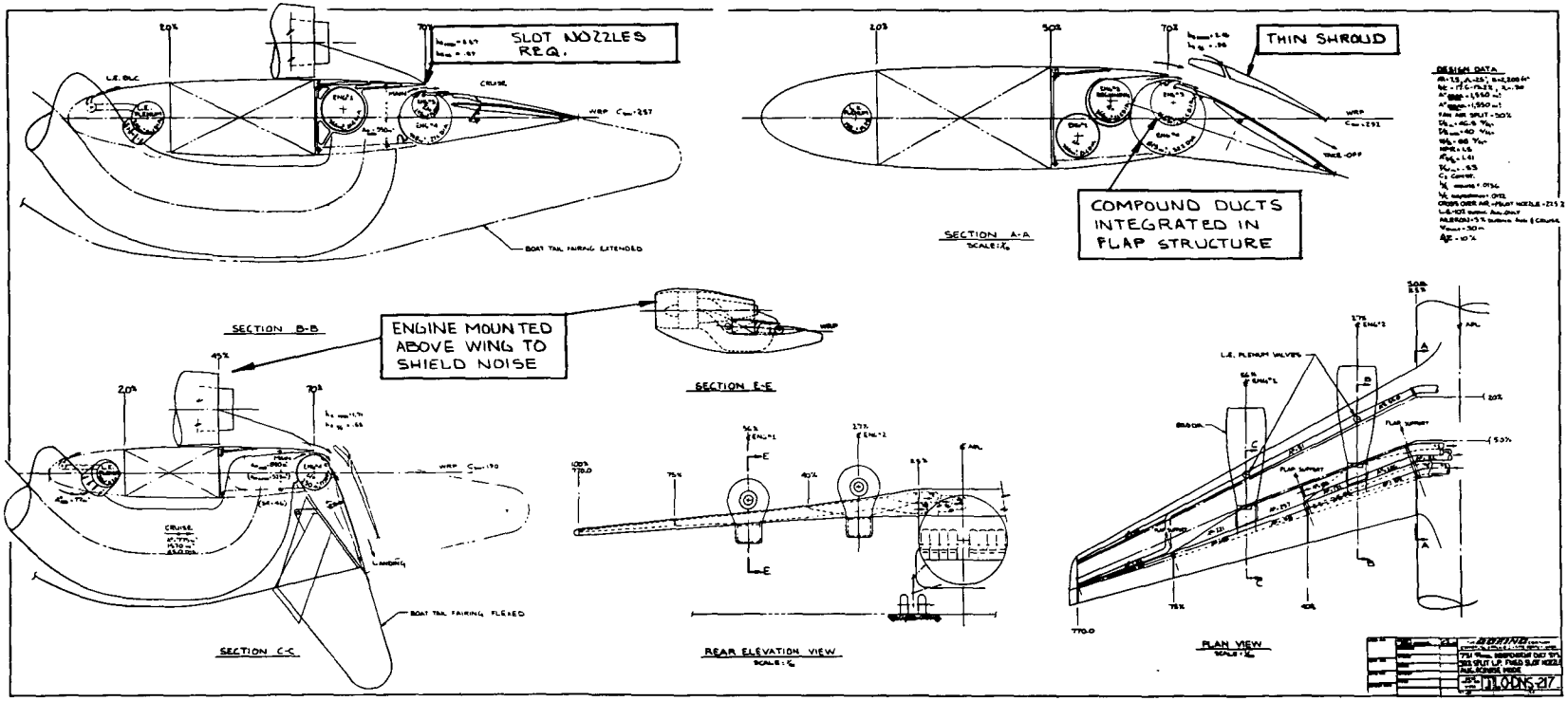

LO-DNS-217–FIXED SLOT NOZZLE, AUGMENTOR AND CRUISE MODE